THE EPHA2/EPHRIN-A1 AXIS REGULATES HOST-TUMOR INTERACTIONS

By
Eileen Fong Shiuan

Dissertation
Submitted to the Faculty of the
Graduate School of Vanderbilt University in
partial fulfillment of the requirements for the
degree of

DOCTOR OF PHILOSOPHY
in
Cancer Biology
May 31, 2020
Nashville, Tennessee

Approved:
Ann Richmond, Ph.D. (Chair)
Jin Chen, M.D., Ph.D. (Advisor)
Barbara Fingleton, Ph.D.
Pierre Massion, M.D.
Jeffrey Rathmell, Ph.D.

ORIGINAL PUBLICATIONS

1. **Shiuan E**, Song W, Wang S, Boothby M, and Chen J. Tumor-specific EphA2 receptor tyrosine kinase inhibits anti-tumor immunity by recruiting suppressive myeloid populations in NSCLC. (In preparation)
2. Wilson K, **Shiuan E**, and Brantley-Sieders DM. Targeting EphA2 in cancer therapeutics. (In preparation)
3. Wang S, Raybuck A*, **Shiuan E***, Cho SH, Wang QF, Brantley-Sieders DM, Allaman MM, Wilson KT, DeNardo D, Zhang S, Cook R, Boothby B, Chen J. Selective inhibition of mTORC1 in tumor blood vessels increases anti-tumor immunity. (Submitted)
4. **Shiuan E**, Inala A, Wang S, Song W, Youngblood VM, Chen J, Brantley-Sieders DM (2020). Host deficiency in ephrin-A1 inhibits breast cancer metastasis. *F1000Research*, 9, 217. https://doi.org/10.12688/f1000research.22689.1
5. Edwards DN, Ngwa VM, Wang S, **Shiuan E**, Brantley-Sieders DM, Kim LC, … Chen J (2017). The receptor tyrosine kinase EphA2 promotes glutamine metabolism in tumors by activating the transcriptional coactivators YAP and TAZ. *Science Signaling*, *10*(508). https://doi.org/10.1126/scisignal.aan4667
6. **Shiuan E**, & Chen J (2016, November 15). Eph receptor tyrosine kinases in tumor immunity. *Cancer Research*, Vol. 76, pp. 6452–6457. https://doi.org/10.1158/0008-5472.CAN-16-1521
7. Beckermann KE*, **Shiuan E***, Reddy A, Dudzinski S, Lim A, Sugiura A, … Rathmell WK. Clinical correlates and cross-platform molecular analysis of response to anti-PD-1/PD-L1 in renal cell carcinoma. (In preparation)
8. Iams WT, **Shiuan E**, Meador CB, Roth M, Bordeaux J, Vaupel C., … Lovly CM (2019). Improved Prognosis and Increased Tumor-Infiltrating Lymphocytes in Patients Who Have SCLC With Neurologic Paraneoplastic Syndromes. *Journal of Thoracic Oncology*, *14*(11), 1970–1981. https://doi.org/10.1016/j.jtho.2019.05.042
9. **Shiuan E***, Beckermann KE*, Ozgun A, Kelly C, McKean M, McQuade J, … Johnson DB (2017). Thrombocytopenia in patients with melanoma receiving immune checkpoint inhibitor therapy. *Journal for ImmunoTherapy of Cancer*, *5*(1). https://doi.org/10.1186/s40425-017-0210-0

This is dedicated to all the cancer patients who are fighting for their lives and the cancer survivors who give us all hope.

This is also dedicated to all those individuals and families battling against the COVID-19 pandemic, whether in the front lines of duty or in the flesh.

ACKNOWLEDGMENTS

There are countless individuals I must thank, without whom this work would not be possible. Family, friends, colleagues, mentors, and mentees – all have contributed in some shape or form to this thesis, whether it was a helping hand at the bench, a pair of fresh eyes on my grant and manuscripts, words of wisdom and advice, or a comforting shoulder to lean on and find solace. Below are the key individuals who have shaped my work and my journey as a graduate student.

First, I would like to thank my primary mentor Dr. Jin Chen, who gave me the opportunity to train in her laboratory and grow as a scientist. When I joined the lab in the fall of 2015, I expressed interest in studying tumor immunology, an area of research that was outside the expertise of the lab at the time. Though perhaps risky for a brand-new graduate student, Dr. Chen fully embraced this idea with enthusiasm and support. From then on, she has helped me navigate my many “firsts” as a scientist and inspired me to push boundaries, which has led to both successes that we have celebrated and failures that we have learned from. She has been my advocate, even through the many trials and tribulations we have experienced, and I am incredibly grateful for her mentorship for the past four and a half years.

Second, I must thank Dr. Dana Brantley-Sieders, who has become a secondary mentor over the past couple years. When I was struggling with my primary project in the lab, she offered me a new opportunity and has guided me through this project, all the way through the publication of the manuscript. As a breast cancer survivor and advocate with a feisty attitude and infectious optimism, she has inspired me and everyone else in the lab to continue our dedication and hard work towards the fight against cancer.

I would also like to thank my other mentors throughout this journey, both past and present. Before I joined the Vanderbilt MSTP, a great many individuals took a chance on an inexperienced undergraduate who had little clue about what to do in the research lab or in the clinic. I especially want to thank Dr. Michael Maitland who was my primary mentor at UChicago and gave me the first glimpse of what a career as a physician scientist was like. In addition, I am grateful for the mentorship of past and present committee members: Drs. Ann Richmond, Barbara Fingleton, Douglas Johnson, Jeff Rathmell, and Pierre Massion. Each of them has dedicated hours of their time to meet with me, offer advice, and push me to become a better scientist. I also would like to acknowledge my present and past clinical mentors: Drs. Katy Beckermann, Douglas Johnson, Jeff Sosman, and Wade Iams. Each of them has given me exciting opportunities in clinical research and further inspired me to become an oncologist.

Because science cannot happen in a bubble, I must absolutely thank everyone who has created and shared this environment with me. All current members of the Chen and Brantley-Sieders labs (Shan, Deanna, Yoonha, Laura, Verra, Kalin, Ashwin, Chris), as well as some former members (Wenqiang, Tim, Victoria, Kat) have impacted my work and time here as a graduate student. Special thanks to the following people: Shan, for sharing those miserable hours performing flow experiments and making sure I still remember my elementary school level of Mandarin; Wenqiang, for sharing technical expertise and ideas and being the last one to leave the lab almost every night; Laura, for commiserating in grad school life and strife and eating and drinking with me all things Asian and alcoholic, respectively. Ashwin, for taking a chance on research and on me as a mentor and diving into everything with enthusiasm no matter how challenging. They have all made tough days easier to bear. I would also like to thank our collaborators by marriage, members of the Boothby lab, particularly Dr. Mark Boothby, Sung Hoon, and Ariel, for their expertise in immunology and the many flow antibodies and reagents that have saved some experiments at the last minute. In addition, I must thank the Cancer Biology Graduate Program, VICC, and the VUMC and VU cores that made my work possible. My work would also not be possible without those who supported me financially during my graduate training, specifically the Vanderbilt MSTP training grant (T32 GM0734) and the National Cancer Institute for my pre-doctoral fellowship (F30 CA216891-01).

I am extremely lucky to be surrounded by a talented and classy group of MSTP classmates (Steph, Katherine, Gabby, Alex, Kevin, Sumeeth, Shawn, John, Josh, Joey), with whom I have endured the past many years with as guinea pigs for VMS curriculum 2.0 and become experienced wedding and baby shower party folk. They have made this crazy journey a bit more sane and a lot more fun. I thank the Vanderbilt MSTP for accepting me in the first place, particularly all the students that make it not just a program, but a family. In addition, I am very grateful for the MSTP leadership team, both past (Terry Dermody, Melissa Krasnove, Jim Bills, Larry Swift) and present (Chris Williams, Lourdes Estrada, Megan Williams, Sally York, Bryn Sierra, Ambra Pozzi, Danny Winder) for their support of all the MSTP students. Furthermore, I feel extremely lucky to be a part of the VMS community. I thank all my MD classmate residents and all other healthcare professionals who are currently fighting the COVID-19 pandemic, while I sit sheltered at home writing this thesis.

Last, but not least, my family and friends have been my rock throughout this entire journey. I thank my parents and my brother Jason for everything – for making me the person I am today – and my mom especially for instilling my fascination with science at a young age and being the strongest and most inspirational female role model I know. Furthermore, if it were not

for grad school, I would never have met Abhishek, my life partner for the last few years and likely many more. Although our career paths could not be more different, he always manages to be so patient and such a good listener. I also must thank my friends from VMS and Club Water Polo and especially my past and present roommates (Sarah, Haley, Tessa, Katherine) for all the emotional support, wine, and fond memories over the past several years. These wonderful humans have not only celebrated my achievements with me, but also reminded me that no matter how insurmountable an obstacle may seem, I am not alone in the world and we will get through it together.

TABLE OF CONTENTS

LIST OF TABLES

LIST OF FIGURES

LIST OF ABBREVIATIONS

AAALAC	Association for Assessment and Accreditation of Laboratory Animal Care
ACK	Ammonium-chloride-potassium
ADC	Antibody-drug conjugate
ANOVA	Analysis of variance
APC	Allophycocyanin
ARG1	Arginase 1
ATCC	American type culture collection
BCR-ABL	Breakpoint cluster region-Abelson kinase
BRCA	Breast cancer gene
CAR	Chimeric antigen receptor
CAS9	CRISPR-associated protein 9
CCL	C-C chemokine ligand
CCR2	C-C chemokine receptor type 2
cDNA	Complementary deoxyribonucleic acid
CM	Conditioned media
COX2	Cyclooxygenase-2
CRISPR	Clustered regularly interspaced short palindromic repeats
CSF1R	Colony-stimulating factor 1 receptor
CTC	Circulating tumor cell
CTL	Cytotoxic T lymphocyte
CTLA-4	Cytotoxic T lymphocyte antigen 4
DAPI	4’,6-diamidino-2-phenylindole
DC	Dendritic cell
DMEM	Dulbecco’s modified eagle’s medium
DNase	Deoxyribonuclease
EGFR	Epidermal growth factor receptor
EMT	Epithelial-mesenchymal transition
EpCAM	Epithelial cell adhesion molecule
EPH	Erythropoietin-producing hepatocellular receptor

ER	Estrogen receptor
FACS	Fluorescence-activated cell sorting
FBS	Fetal bovine serum
FFPE	Formalin-fixed paraffin-embedded
FGF	Fibroblast growth factor
FITC	Fluorescein isothiocyanate
FMO	Fluorescence minus one
FOX	Forkhead box protein
GEF	Guanine nucleotide exchange factor
GFP	Green fluorescence protein
GPI	Glycosylphosphatidylinositol
GZMB	Granzyme B
H&E	Hematoxylin and eosin
HER2	Human epidermal growth factor receptor 2
HSP70	Heat shock protein 70
ICAM-1	Intercellular adhesion molecule 1
ICI	Immune checkpoint inhibitor
IF	Immunofluorescence
IFN	Interferon
IHC	Immunohistochemistry
IL	Interleukin
ITGAM	Integrin alpha M
IVIS	*In Vivo* Imaging System
KO	Knockout
KPCY	KRAS G12D, TP53 R172H, YFP
KPL	KRAS G12D, TP53 KO, STK11/LKB1 KO
KRAS	Kirsten rat sarcoma viral oncogene
LKB1	Liver kinase B1
LLC	Lewis lung carcinoma
MAPK	Mitogen-activated protein kinase
MDSC	Myeloid-derived suppressor cell

MFI	Median fluorescence intensity
MHC	Major histocompatibility complex
mIF	Multiplexed immunofluorescence
MMTV-PyMT	Mouse mammary tumor virus-polyoma middle tumor-antigen
M.O.M.	Mouse-on-mouse
MRC1	Mannose receptor C type 1
MTT	Thiazolyl blue tetrazolium bromide
MV	Microvesicle
NIH	National Institutes of Health
NK	Natural killer
NP-40	Nonyl phenoxypolyethoxylethanol
NSCLC	Non-small cell lung cancer
OCT	Optimal cutting temperature
PBS	Phosphate buffered saline
PCNA	Proliferating cell nuclear antigen
PD-1	Programmed death 1
PD-L	Programmed death ligand
PDAC	Pancreatic ductal adenocarcinoma
PDGF	Platelet-derived growth factor
PDZ	PSD95/DIg/ZO1
PE	Phycoerythrin
PerCP	Peridinin chlorophyll protein
PFA	Paraformaldehyde
PI3K	Phosphoinositide 3-kinase
PR	Progesterone receptor
PRF1	Perforin-1
PTGS2	Prostaglandin-endoperoxide synthase 2
qRT-PCR	Quantitative real-time polymerase chain reaction
RAF	Rapidly accelerated fibrosarcoma
RAC	Ras-related C3 botulinum toxin substrate
RCC	Renal cell carcinoma

RHO	Ras homolog family member
RIPA	Radioimmunoprecipitation assay
RNAi	RNA interference
RNAse	Ribonuclease
RNAseq	RNA-sequencing
RPMI	Roswell Park Memorial Institute
RTK	Receptor tyrosine kinase
SAM	Sterile alpha motif
SCLC	Small cell lung cancer
SD	Standard deviation
SDS	Sodium dodecyl sulfate
SH2	SRC homology 2
shRNA	Short hairpin RNA
siRNA	Small interfering RNA
SMA	Smooth muscle actin
STK11	Serine/threonine kinase 11
TAA	Tumor-associated antigen
TAM	Tumor-associated macrophage
TBS-T	Tris-buffered saline-Tween 20
TCGA	The Cancer Genome Atlas
TCR	T cell receptor
TGF	Transforming growth factor
TIL	Tumor-infiltrating lymphocyte
TKI	Tyrosine kinase inhibitor
TNF	Tumor necrosis factor
TEM	Transendothelial migration
TNBC	Triple-negative breast cancer
TP53	Tumor protein 53
Treg	Regulatory T cell
UC-Exos	Ultracentrifuged exosomes
VCAM-1	Vascular cell adhesion molecule 1

VEGF	Vascular endothelial growth factor
VEGFR2	Vascular endothelial growth factor receptor 2
WCL	Whole cell lysate
WT	Wild-type
YFP	Yellow fluorescence protein

CHAPTER I

INTRODUCTION

Overview

Cancer is the second leading cause of mortality in the United States and worldwide and is growing in prevalence despite significant advancements in prevention and treatment. At the turn of the last century, six “hallmarks of cancer” were highlighted: resisting cell death, sustaining proliferative signaling, enabling replicative immortality, evading growth suppressors, inducing angiogenesis, and activating invasion and metastasis[1]. These characteristics were regarded as critical to the initiation and progression of cancer growth. However, over the past two decades, the scientific field has advanced far beyond these six hallmarks and increasingly realized the contribution of dysregulated host systems towards the evolution of cancer. There are now ten putative hallmarks of cancer, several of which attribute host-tumor interactions (Figure 1.1).

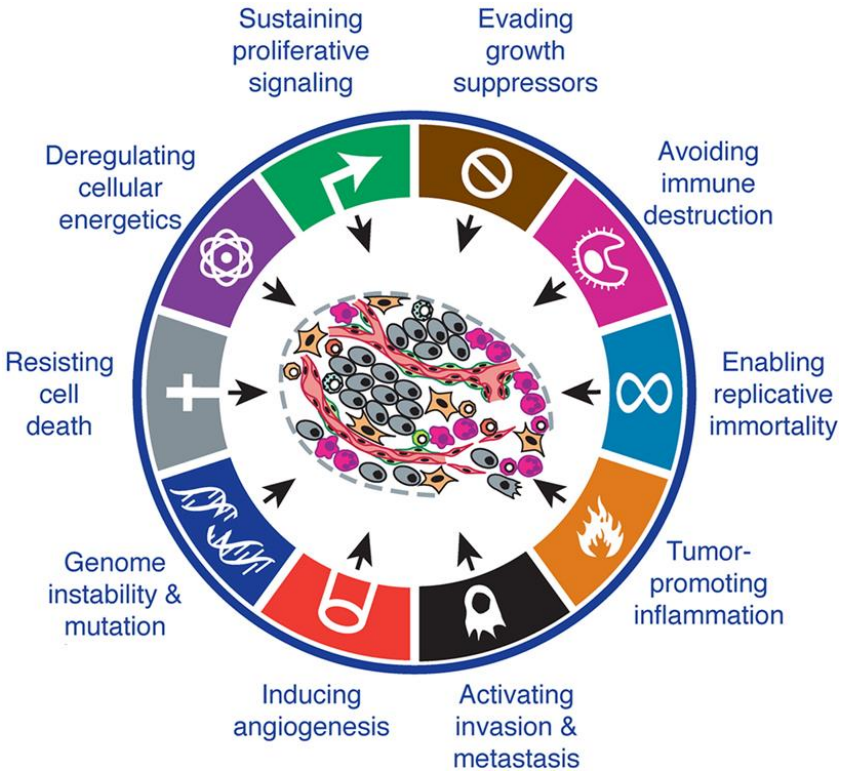

Figure 1.1. The ten hallmarks of cancer. (Adapted from (2))

Among the many players that have been implicated in the progression of cancer are EphA2 receptor tyrosine kinase (RTK) and its primary ligand ephrin-A1. Under normal physiological conditions, the EphA2/ephrin-A1 signaling axis maintains a homeostatic balance between cell-to-cell adhesion, migration, and proliferation. However, in cancer, this axis is commonly dysregulated, and balance is disrupted. This balance is not only disrupted within tumor cells that have altered expression of EphA2 and/or ephrin-A1, but also between tumor cells and host cells that express EphA2 and ephrin-A1. Herein, we investigate EphA2/ephrin-A1 axis-mediated host-tumor interactions, specifically interactions with the host immune system and endothelium, and how they contribute to progression of cancer *in vivo*. We discover that EphA2 overexpression in the cancer cell leads to the recruitment of immunosuppressive myeloid populations, which dampen the anti-tumor immune response and allow for tumor immune escape. Conversely, we demonstrate that host deficiency of ephrin-A1 provides a less favorable metastatic niche that inhibits development of metastatic disease. Overall, these studies suggest that EphA2 on the tumor cell and ephrin-A1 in host tissues both impact the development of cancer, and further investigations evaluating how to best target this signaling axis may provide novel therapeutic strategies.

Lung and Breast Cancer

Lung and breast cancer are the top two most commonly diagnosed cancers in the United States and worldwide and together make up almost a quarter of all new cases each year[3]. For the year 2020, an estimated 228,000 and 271,000 new cases and 143,000 and 42,000 cancer-related deaths in the United States will be attributed to lung and breast cancer, respectively. Many of the environmental factors that contribute to these cancers are well-known, such as smoking and exposure to asbestos related to lung cancer and body mass and hormone replacement therapy related to breast cancer. In addition, certain genetic mutations are proven risk factors for cancers, such as germline mutations in *BRCA1* and *BRCA2*, which predispose some women to breast and ovarian cancer. These insights have led to modern prevention and anti-cancer treatment strategies.

Back in the early 1900s, the cornerstones of anti-cancer therapy were surgery, radiotherapy, and chemotherapy, and all solid tumors were treated largely in similar fashion[4]. However, during the second half of the 1900s, advancements in molecular biology led to the discovery that cancer was not just one disease but included many different types and subtypes

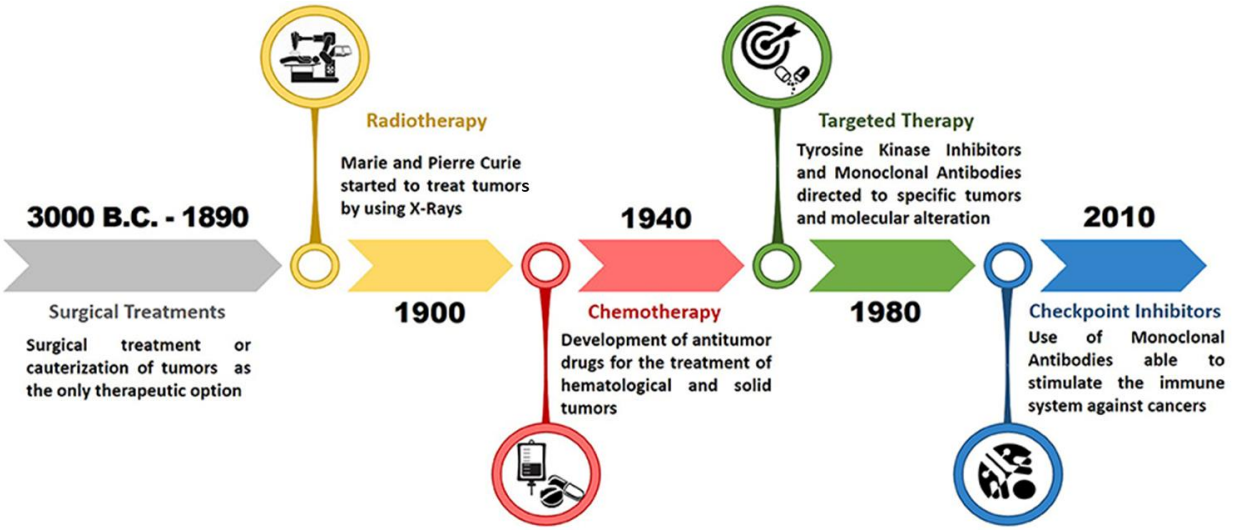

Figure 1.2. The evolution of anti-cancer therapy. (Adapted from (4))

that each had its own complex network of molecular drivers and enablers. These discoveries eventually led to the development of targeted therapies and immunotherapies, which ushered in the era of precision medicine (Figure 1.2). Precision medicine incorporates a cancer's histological and molecular subtype to tailor individualized treatments.

Histological and molecular classification

Both lung and breast cancer are categorized by histological and molecular subtypes. Lung cancer is histologically divided into small cell lung cancer (SCLC), which comprise 15% of lung cancers, and non-small cell lung cancer (NSCLC), which make up the majority of cases[5]. SCLC is neuroendocrine in origin and typically responds well to chemotherapy regimens. NSCLC can be further categorized based on cell of origin, for example, squamous cell carcinoma, adenocarcinoma, and large cell carcinoma, which are identified by morphological features and immunohistochemistry (IHC) staining. Historically, treatment regimens for NSCLC were selected based on histological subtype. However, with advances in genome sequencing and the advent of the precision medicine era, NSCLC is now more practically categorized into molecular subtypes. This molecular classification is based on the concept that tumors often harbor recurring genetic aberrations, such as mutations, amplifications, and deletions, that drive the proliferation and survival of the cancer cells. These aberrations can be targeted more specifically by drugs designed to inhibit the resultant mutant protein or downstream pathways, compared to chemotherapy agents, which eliminate all rapidly dividing cells including normal host cells[6]. For example, over half of all metastatic lung adenocarcinomas are driven by either *EGFR* or *KRAS* aberrations (Figure 1.3). Monoclonal antibodies and small molecule inhibitors

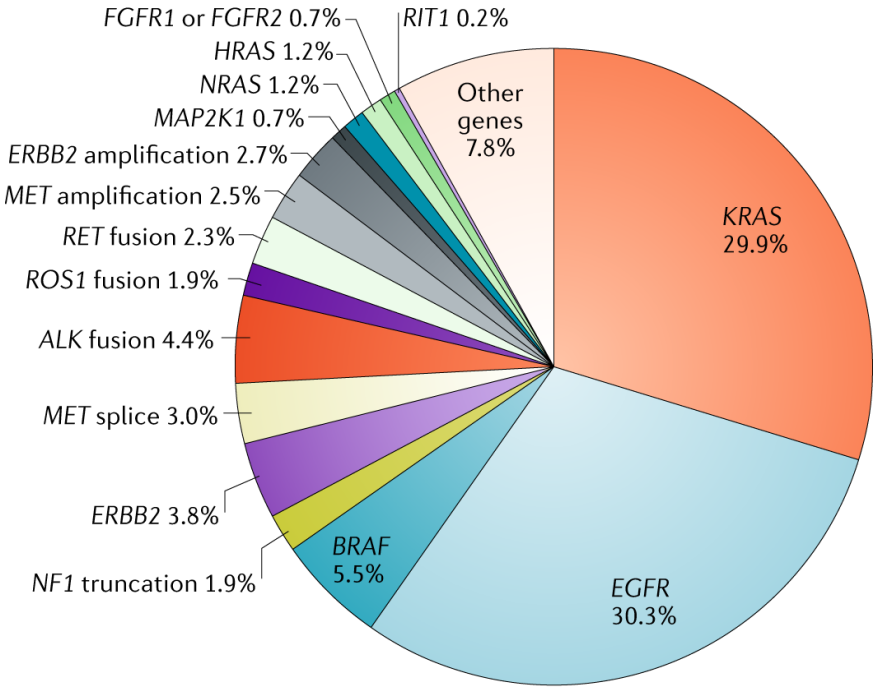

Figure 1.3. Oncogenic driver alterations in metastatic lung adenocarcinoma. (Adapted from ([7]))

against epidermal growth factor receptor (EGFR), the protein encoded by *EGFR*, have shown superior therapeutic benefit in patients with mutations in this gene, compared to chemotherapy agents[8]. *KRAS* mutant lung cancer has been notably more difficult to target. Despite the development of a specific inhibitor against the *KRAS K12C* mutation[9], there is still no effective targeted therapy for a majority of *KRAS* mutant cancers.

Similarly, breast cancer can be classified based on histological and molecular characteristics. The vast majority of breast cancers arise in the epithelium of the mammary gland and are thus categorized as carcinomas. Mammary carcinomas can further be divided into subtypes based on cell of origin[10]. For example, ductal carcinomas arise from epithelial cells that line the mammary ducts and make up 60-80% of all mammary carcinomas. More recently, IHC and gene expression profiling has led to two distinct but parallel molecular classification systems. IHC-based profiling evaluates the protein expression of estrogen (ER), progesterone (PR), and human epidermal growth factor receptor 2 (HER2) receptors and identifies categories based on high and low expression of these biomarkers. For example, hormone receptor positive cancers are generally ER+ and/or PR+, while triple-negative breast cancers (TNBC) have low or negative expression of all three biomarkers. In contrast, global gene expression profiling classifies breast cancers into luminal A, luminal B, basal-like, HER2-enriched, claudin-low, and normal breast-like groups[11]. While certain groups correspond with IHC-profiled categories, this classification system is not exactly aligned with receptor biomarker

Molecular subtype	Overall prevalence	% ER+	% PR+	% HER2+	% TNBC
Luminal A	28-31%	91-100%	70-74%	8-11%	3-4%
Luminal B	19-20%	91-100%	41-53%	15-24%	4-9%
HER2-enriched	12-21%	29-59%	25-30%	66-71%	14-22%
Basal-like	11-23%	0-19%	6-13%	9-13%	73-80%
Claudin-low	7-14%	12-33%	22-23%	6-22%	61-71%

Table 1.1. Overall prevalence of molecular subtypes of breast cancer and expression of biomarker receptors. (Summarized from (11))

expression (Table 1.1). TNBC, which makes up a high percentage of basal-like and claudin-low tumors, is an aggressive subtype of breast cancer that lacks effective therapeutic options[11]. In addition, the invasive phenotype of this subtype confers a higher chance of metastasis and diagnosis at a later stage compared to other subtypes of breast cancer.

Metastasis

Cancer metastasis is the dissemination of cancer cells from a primary tumor to a distant site and is ultimately responsible for most cancer-related deaths. Patients diagnosed with stage IV metastatic disease have a worse prognosis compared to those with lower stages of disease. For example, the five-year survival for lung cancer patients diagnosed with localized disease and regional spread is 57.4% and 30.8%, respectively; however, the five-year survival for patients with distant metastases is 5.2%[12]. Similarly, among women with breast cancer, the five-year survival for localized disease and regional spread is 98.8% and 85.5%, respectively, compared to 27.4% for patients with distant spread[13]. Interestingly, both lung and breast cancers preferentially spread to the brain, bone, liver, and lung, but how and why these cells travel to and colonize these particular organs is still largely unknown[14–16].

Metastasis is a dynamic and complex process that requires tumor cells to undergo many steps, including adopting invasive properties, intravasating into proximal vasculature, surviving in circulation, evading immunosurveillance, extravasating from distant vasculature, and finally adapting to selective pressures of a new environment[17–19]. Each of these steps involves multiple interactions among cancer cells themselves and between cancer cells and different types of host stromal cells. First, tumor cells in the primary tumor gain migratory and invasive qualities that allow them to break away from neighboring cells. They migrate through the stroma and pass through basement membranes, while simultaneously evading destruction by local immune cells, including macrophages. Second, they enter local vessels, either the blood or lymphatic vasculature, through junctions between endothelial cells lining vessel walls. While in the blood or lymph, these circulating tumor cells (CTCs) must survive the shear-stress of circulation and escape peripheral immunosurveillance from circulating leukocytes. Those CTCs that survive

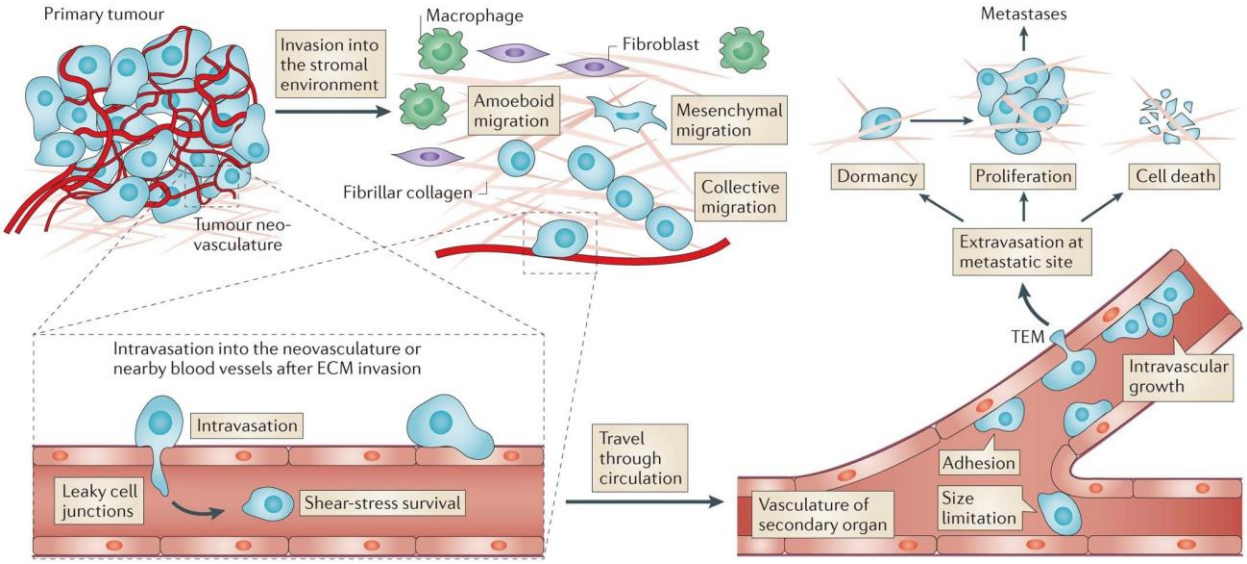

Figure 1.4. The journey of a cancer cell from the primary tumor to a distant metastatic site. (Adapted from (19))

circulation eventually adhere to the endothelium of another organ, typically within the capillaries where size restriction of the vessel lumen limits CTC movement. Next, CTCs extravasate from the vessel into a new metastatic niche. The tumor cells must overcome the new stressors imposed by this new environment, which could include a novel immune response or restricted nutrient or oxygen availability, in order to survive. The surviving tumor cells may become senescent, in which case detectable metastases may never develop, or they may adapt in a manner that promotes their proliferation in the new organ, forming observable metastases.

The journey that a cancer cell takes from a primary tumor to a metastatic lesion requires molecular reprogramming within the cancer cell, as well as changes in host tissues that can be co-opted by the cancer. While many studies have identified key mutations or shifts in gene expression that enable metastatic processes, such as cancer cell epithelial-mesenchymal transition (EMT) and transendothelial migration (TEM), the mechanisms by which tumor and host cell interactions lead to cancer and metastasis require much more investigation. One group of proteins that deserve greater investigation in this field of study is the Eph family of receptor tyrosine kinases and their ephrin ligands.

Eph Receptors and Ephrin Ligands

The Eph RTK family comprises the largest group of surface receptors and are categorized into EphA or EphB subclasses based on sequence homology and preferential

binding to their ephrin-A and ephrin-B ligands, respectively[20]. In humans, nine EphA (EphA1-8,10) and five EphB (EphB1-4,6) receptors are expressed, along with five ephrin-A and three ephrin-B ligands, all of which display promiscuous but preferential binding (Table 1.2). For example, EphA2 RTK can bind to all five ephrin-A ligands but has the highest affinity for ephrin-A1. Unlike most RTKs, Eph receptors can interact with ligands that are either soluble or membrane-bound or even signal in the absence of ligand. With the many complex ways that Eph receptors and ephrin ligands can initiate or relay signaling, there is no surprise that these proteins are involved in a wide range of physiological and pathological processes.

Structure and signaling

EphA and EphB RTKs are similar in structure and contain an extracellular domain with an ephrin-binding domain and fibronectin III repeats, a transmembrane domain, and an intracellular domain that contains the juxtamembrane region, a kinase domain, a sterile alpha motif (SAM) domain, and a PSD95/Dlg/ZO1 (PDZ)-binding motif (Figure 1.5). Conversely, ephrin-A and ephrin-B ligands have differing structures. Ephrin-A ligands have an extracellular Eph receptor-binding domain and a glycosylphosphatidylinositol (GPI) anchor without an intracellular region, while ephrin-B ligands have an additional transmembrane domain and an intracellular PDZ-binding motif (Figure 1.5).

Canonical Eph receptor and ephrin ligand (Eph/ephrin) signaling initiates upon binding of the ligand on one cell to the receptor on a neighboring cell *in trans*[21,22]. This binding induces a conformational change in both receptor and ligand that allows for oligomerization with

Eph receptor	Preferential ephrin ligand binding
EphA1	ephrin-A4 > A1 > A3 > A2 > A5
EphA2	ephrin-A1 > A5 > A4 > A3 > A2
EphA3	ephrin-A5 > A4 > A2 > A3 > A1
EphA4	ephrin-A4 > A5 > A1 > A2 > A3 > B1-3
EphA5	ephrin-A1 > A3 > A4 > A2 > A1
EphA6	ephrin-A1 > A4 > A2 > A1 > A3
EphA7	ephrin-A5 > A3 > A4 > A1 > A2
EphA8	ephrin-A4,A5 > A1 > A3 > A2
EphA10*	ephrin-A1-5**
EphB1	ephrin-B2 > B1 > B3 > A4
EphB2	ephrin-B2 > B1 > B3 > A1-5
EphB3	ephrin-B2 > B1 > B3 > A4
EphB4	ephrin-B2 > B1 > B3 > A4
EphB6*	ephrin-B2 > B1 > B3 > A4

Table 1.2. Eph receptors expressed in humans and their ephrin ligand binding preferences. (Adapted from (23)) *inactive kinase; **binding affinities undetermined

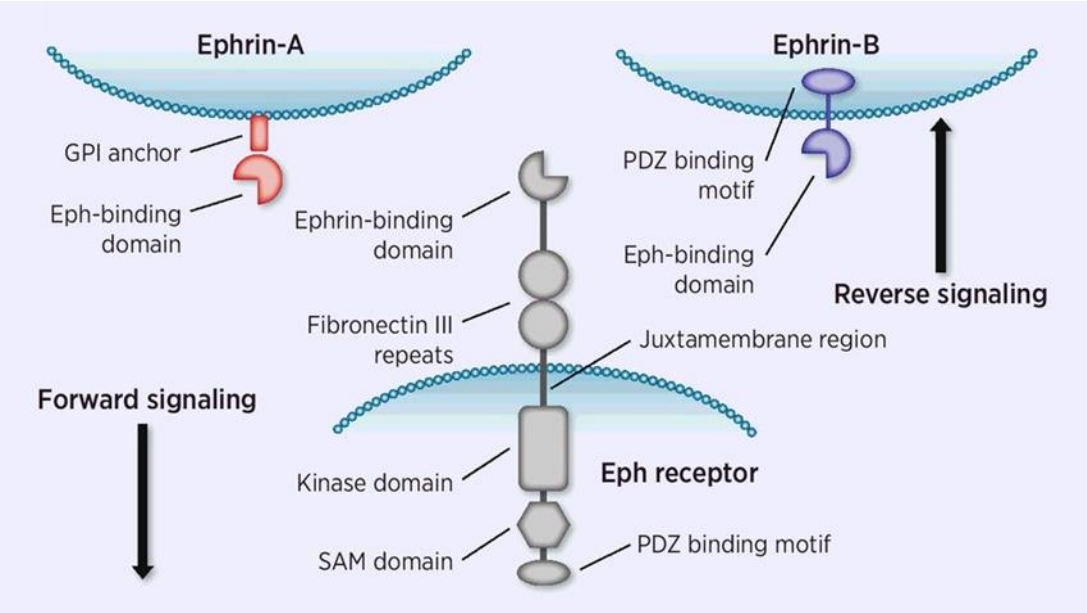

Figure 1.5. The structural elements of an Eph receptor and ephrin ligands. (Adapted from (24))

neighboring Eph/ephrin complexes and autophosphorylation of conserved tyrosine residues in the juxtamembrane region[25,26]. This then exposes the kinase domain, rendering it into its active form, and initiates a phosphorylation cascade along the intracellular region that allows for recruitment and docking of downstream effector molecules with SRC homology 2 (SH2) domains[26–28]. Because both Eph receptors and ephrin ligands are membrane-bound in this canonical pathway, this leads to a unique bidirectional signaling – “forward signaling” in the receptor-bound cell and “reverse signaling” in the ephrin-bound cell (Figure 1.5). Forward signaling of Eph receptors can regulate a diverse array of pathways. For example, EphA2 forward signaling has been shown to downregulate the RAS/PI3K/AKT and RAS/RAF/MAPK pathways[29,30] and upregulate the RHO/RAC pathway[31,32]. Reverse signaling through ephrin-B ligands via interactions with SRC family proteins has been well-studied[26,33]; however reverse signaling through ephrin-A ligands has been more difficult to investigate primarily due to an absence of an intracellular domain.

There are various other ways that noncanonical signaling may occur through Eph receptors. Instead of binding to ephrin ligands *in trans*, interactions can also occur *in cis*, which attenuate traditional forward signaling[34–36]. Ephrin ligands can also be cleaved from the cell membrane and bind and activate Eph receptors in a soluble form[37,38]. In addition, both ephrin and Eph receptors have also been found in extracellular vesicles, including exosomes, and these vesicular Eph RTKs and ephrins have been shown to bind to and activate signaling in target cells[39–41]. Hence, these proteins in soluble form or packaged in vesicles may induce

distant changes far from the cell of origin. To make things even more complicated, Eph receptors can also signal in the absence of ligand binding and kinase activation through crosstalk with other surface receptors. For example, EphA2 has been shown to dimerize with E-Cadherin, EGFR, HER2, and integrins and alter downstream signaling[32,42–45]. Thus, deciphering the many different mechanisms by which Eph receptors and ephrin ligands can contribute to physiological and pathological processes remains a challenge.

Roles in the cancer cell

The connection between Eph RTKs and cancer dates back to the discovery of the first Eph receptor from a screen of a cancer cell line in 1987, coined erythropoietin-producing hepatocellular receptor A1 (EphA1)[46]. Since then, almost every Eph receptor has been shown to play a role in some form of cancer, whether it is tumor-promoting or tumor-suppressing or sometimes both. Overexpression of Eph RTKs, especially EphA2, EphB2, and EphB4, have been observed in a variety of solid tumors, including lung and breast cancer, and expression levels of some Eph receptors are correlated with more malignant disease and worse prognosis[47,48]. Additionally, somatic mutations have been detected in Eph RTKs, such as EphA3, EphA5, and EphB2[47,49–55]. However, Eph RTKs are not necessarily considered strictly oncogenic. Expression of some Eph RTKs can also be lost or downregulated in cancers, suggesting a more tumor-suppressive role[47].

These seemingly conflicting conclusions that imply Eph RTKs can play both tumor-promoting and suppressing roles may be explained in part by the different signaling modalities. Under most conditions in normal or cancer cells, ligand-dependent forward signaling promotes an epithelial phenotype and suppresses migration, invasion, and growth. Thus, when ephrin ligand and Eph receptor interactions are intact and the canonical forward and reverse signaling pathways predominate, Eph RTKs produce more of a tumor-suppressive effect (Figure 1.6). Conversely, in the absence or downregulation of ephrin expression relative to Eph RTK expression or loss of key events in forward signaling, for example caused by mutations rendering an inactive kinase, Eph RTKs participate more in ligand-independent signaling and therefore play a more oncogenic role (Figure 1.6). These dual roles have been demonstrated in many Eph RTKs, including EphA2[20,47].

EphA2/ephrin-A1 axis in the cancer cell

Most studies evaluating the relationship between EphA2 and ephrin-A1 have been in the context of the cancer cell. First, EphA2 has been shown to be intrinsically overexpressed in

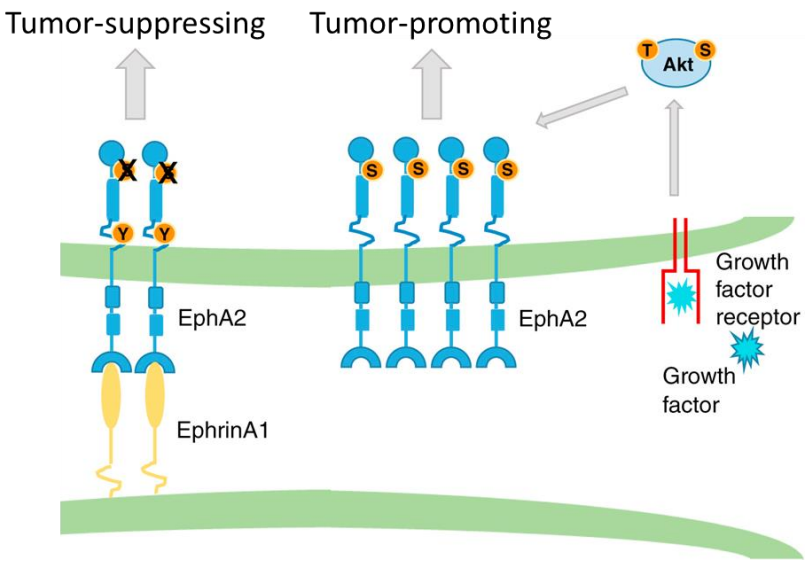

Figure 1.6. EphA2 ligand-dependent and independent signaling modalities in the cancer cell. (Adapted from (56))

tumor specimens, including lung, breast, ovarian, prostate, urinary bladder, colorectal, melanoma, and glioma tumors, compared to adjacent normal tissue[20,47,48,57–60], as well as in drug-resistant cells[61–64]. EphA2 overexpression has also been shown to transform normal cells and promote growth and invasion[65–67]. Second, EphA2 is able to engage in crosstalk with oncogenic RTKs and enhance downstream oncogenic signaling in a ligand-independent fashion. For example, EphA2 engages in cross-talk with EGFR in EGFR mutant lung cancer[45,64], as well as HER2 in HER2 amplified breast cancer[32]. These oncogenic growth factor receptors activate several signaling cascades, including PI3K/AKT signaling, which leads to AKT-mediated phosphorylation of S897 near the N-terminus of EphA2 and subsequent increased signaling through cell proliferation and survival pathways (Figure 1.6). Furthermore, the relative overexpression of EphA2 in tumor tissue likely contributes to the greater amount of ligand-independent forward signaling in cancer compared to normal tissues. Third, various methods used to knockdown EphA2 expression in cancer cells, including RNA interference (RNAi)-mediated silencing, have shown to decrease cell proliferation *in vitro* and tumor growth *in vivo*[32,64,65,68–71]. Thus, all these studies suggest EphA2 plays a strong tumor-promoting role. Interestingly, there are a few studies that highlight EphA2 as a tumor suppressor[72,73]. One study demonstrated that while EphA2 suppresses cell growth signaling when ephrin ligand binding occurs, proteolytic cleavage of the ligand binding domain can transform EphA2 from a tumor-suppressing receptor to an oncogenic one. While much of the published literature highlights EphA2's oncogenic potential, it is critical to keep in mind that under some circumstances, it may

play a tumor suppressive role.

Contrary to EphA2, ephrin-A1 is often downregulated in tumor tissue compared to adjacent normal[20,47,48,57–60]. In some studies, the oncogenic effects of EphA2 in cancer cells can be attenuated by stimulation with ephrin-A1 ligand, which leads to internalization of the EphA2 RTK, decreased EphA2 S897 phosphorylation, and subsequently decreased cell proliferation and invasion[37,44,67,74–78]. Therefore, under most circumstances, ephrin-A1 expression within the cancer cell can be appreciated as a tumor suppressor. However, like EphA2, ephrin-A1's overall role in cancer can be paradoxical. While ephrin-A1 stimulation of cancer cells has tumor suppressive effects, its impact on host tissues, particularly the endothelium, can become tumor-promoting. Thus, understanding of the EphA2/ephrin-A1 axis within cancer cells must be complemented with studies of the EphA2/ephrin-A1 axis in host-tumor interactions in order to make sense of the paradoxes that arise and refine our overall understanding of the EphA2/ephrin-A1 axis in cancer.

Host-Tumor Interactions

Over the past several decades, the paradigm of cancer research and anticancer therapy has shifted from a focus on solely targeting tumor cells to a broader approach of understanding and remodeling the tumor microenvironment. The tumor microenvironment contains a diverse population of host cells, among which include immune cells, endothelial cells, and fibroblasts that are often hijacked by cancer cells to fulfill the tumor's agenda for growth and metastasis. While there are an infinite number of different host-tumor interactions that enable the initiation and progression of cancer, we focus on two main fields of study that have led to breakthroughs in anti-cancer therapies, investigations of tumor vasculature that have led to anti-angiogenic agents and investigations of tumor immune evasion that have led to the development of immune checkpoint inhibitors (ICIs).

Cancer and the vasculature

The blood and lymphatic vessels of the host play critical roles in sustaining cancer growth and promoting cancer progression. Here, we focus on blood vessels and the vascular endothelial cells that line the inner walls of these vessels. Cancer cells in a small, developing solid tumor initially draw nutrients from its immediate surroundings and pre-existing blood vessels. However, as the solid tumor grows larger and its demand for nutrients and oxygen

increases, it must co-opt the existing vasculature and induce angiogenesis, the formation of new blood vessels from established vasculature. In order to sustain growth, tumor cells turn on the "angiogenic switch" and secrete stimulatory angiogenic factors, including vascular endothelial growth factor (VEGF), fibroblast growth factor (FGF), platelet-derived growth factor (PDGF), transforming growth factor (TGF), and tumor necrosis factor (TNF)[2,79–81]. These factors bind to receptors on endothelial cells such as VEGF receptor 2 (VEGFR2) and initiate signaling cascades within endothelial cells that promote cell proliferation, migration, and assembly. Thus, endothelial cells that were once senescent are now activated and recruited for tumor angiogenesis.

The new tumor vessels serve the needs of the growing tumor in various ways. First, they continue to provide nutrients and oxygen needed for cell survival and proliferation. However, these new vessels are typically hastily constructed due to the surge of pro-angiogenic signals from cancer cells and are thus abnormally tortuous, leaky, and poorly supported by pericytes[81–83]. These abnormal tumor vessels not only are inefficient at nutrient, oxygen, and drug delivery, but also allow increased opportunity for hematologic dissemination, particularly through gaps between neighboring endothelial cells.

These discoveries regarding tumor angiogenesis and the critical role of VEGFR led to the development and testing of anti-angiogenic agents targeting VEGFR. Despite the promise of this novel therapeutic strategy, anti-angiogenic agents were largely a failure in most cancer types except for renal cell carcinoma[84]. Despite reducing tumor size, anti-angiogenic monotherapy failed to control metastasis and improve overall survival and were plagued with unacceptable toxicities. Thus, an emerging concept to improve targeting of tumor endothelium is "vessel normalization". This strategy proposes to reshape the abnormal tumor vasculature into structures that are better supported by pericytes, have improved perfusion and drug delivery, and limit extravasation and metastasis of cancer cells[85].

EPHA2/ephrin-A1 axis in tumor endothelium

Both EphA2 and ephrin-A1 can be expressed in endothelial cells, in addition to cancer cells. Ephrin-A1 can be expressed in both developing and tumor vessels, and its soluble or cleaved forms have been shown to promote angiogenesis *in vitro* and neovascularization *in vivo*[86–89]. However, the ephrin-A1 that stimulates tumor angiogenesis *in vivo* appears to originate from cancer cells in a cleaved or secreted form, rather than ephrin-A1 expressed intrinsically in the endothelium[88,90]. Thus, EphA2 forward signaling in endothelial cells, rather than ephrin-A1 reverse signaling, contributes more towards the angiogenic phenotype. Although

EphA2 is not highly expressed in the developing or adult quiescent vasculature, interestingly, it is highly expressed in tumor vessels[88,91]. This has been shown to occur through ephrin-A1-dependent signaling of EphA2 in the endothelial cell, leading to downstream activation of RAC via interaction with guanine nucleotide exchange factors (GEFs) VAV2 and VAV3[28,92,93]. However, when EphA2 forward signaling is blocked either by EphA2 knockdown or with the addition of decoy EphA2-Fc recombinant protein, VEGF-induced endothelial cell survival, migration, sprouting, and angiogenesis were reduced[94]. EphA2's essential role in endothelial cell migration and assembly is further evident from studies using EphA2 knockout mice or treatment with EphA2-Fc fusion proteins as decoy receptors, which have shown significantly decreased angiogenesis *in vivo*[95–99]. Thus, ephrin-A1 from tumor cells and EphA2 on endothelial cells form an important signaling axis that promotes tumor angiogenesis. Conversely, the impact of endothelial ephrin-A1 on tumor vasculature is less clear.

Cancer and the immune system

A relationship between cancer and the immune system has been evident since before the 1900s, but its potential as a weapon against cancer was not fully realized until the past recent decades[100]. The rebirth of cancer immunotherapy began with cytokine therapy, including interferon (IFN) and high-dose interleukin-2 (IL-2), and cancer vaccines, and it has now grown to include adoptive T cell transfer such as chimeric antigen receptor (CAR)-T cells and ICIs. The introduction of these novel classes of drugs as a mainstay of cancer treatment has revolutionized the practice of oncology but has also revealed a greater need for basic research in order to develop improved predictive biomarkers of response and increase the efficacy of immunotherapies.

In 2013, Chen and Mellman proposed a model of the "cancer-immunity cycle," a multi-step process that includes the release of cancer cell antigens, antigen presentation by dendritic cells (DCs), priming and activation of T cells, trafficking of T cells to tumors, and recognition and killing of cancer cells by cytotoxic T lymphocytes (CTLs)[101]. This model, though simplified, provides an organized approach to identifying key players needed for an effective anti-tumor response and the vulnerabilities that can be capitalized by cancer cells (Figure 1.7). First, antigens released from cancer cell death are detected and processed by professional antigen-presenting cells, typically DCs. These antigens may contain normal self-antigens and tumor-associated antigens (TAAs), which can include antigens processed from overexpressed proteins or neoantigens from mutated proteins from cancer cells. These DCs then traffic to the draining lymph node where they present these antigens to naïve T cells using their major

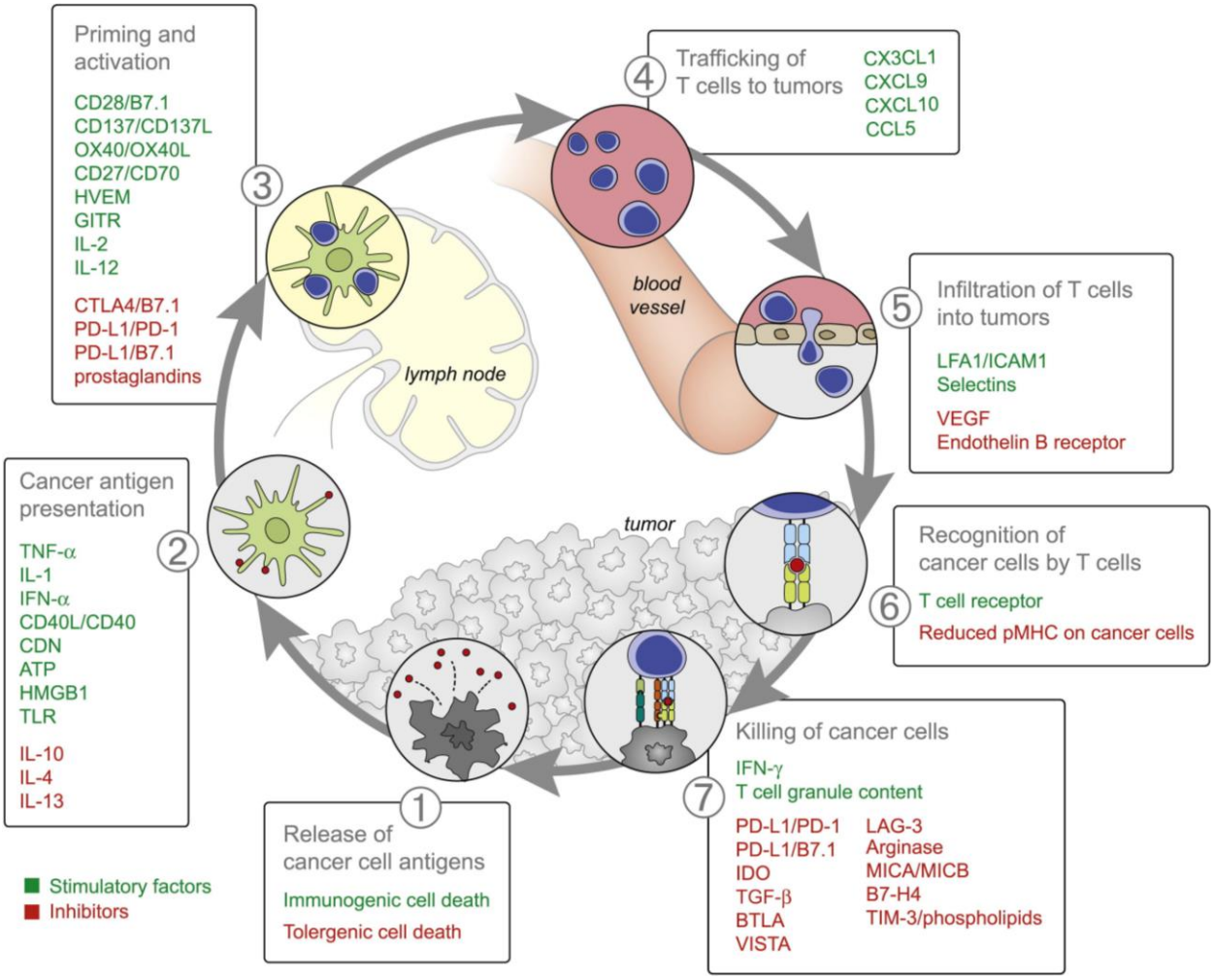

Figure 1.7. Stimulatory and inhibitory factors that contribute to the anti-tumor adaptive immune response. (Adapted from (101))

histocompatibility complex class II (MHCII) molecules, as well as MHCI molecules for cross-presenting DCs. If the antigen is recognized by a T cell receptor (TCR) and a secondary co-stimulatory signal is present, the T cell becomes primed and activated against this antigen. The activated T cell can then travel through the circulation and be recruited to the site of the tumor with help of chemokines. Once T cells infiltrate the tumor, they can recognize the tumor cells and, in the case of a cytotoxic CD8 T cells, selectively kill cancer cells by releasing granules filled with cytotoxic enzymes. The death of these cancer cells provides additional antigens that can fuel the cancer immunity cycle.

There are various ways that the tumor can escape this immunologic response (Figure 1.7). The best-studied examples thus far include inhibition of T cell activation through cytotoxic T-lymphocyte antigen 4 (CTLA-4) signaling and exhaustion of T cell effector function through programmed death 1 (PD-1) receptor signaling. Therapeutic anti-CTLA-4 (ipilimumab), anti-PD-

1 (nivolumab, pembrolizumab), and anti-programmed death ligand 1 (PD-L1) monoclonal antibodies (atezolizumab, avelumab, durvalumab) collectively make up the ICIs that have proven successful in the clinic. In addition to upregulation of immune checkpoint proteins, T cells can become suppressed in other ways. For example, regulatory T cells (Tregs) and myeloid-derived suppressor cells (MDSCs) are other immune cell types that are able to inhibit effector T cell function[102–104]. In addition, activated T cells may not be able to effectively traffic to and infiltrate tumors due to lack of chemokine signals or presence of physical barriers from extensive extracellular matrix production by the tumor. Despite the success of CAR-T cells and ICIs, there are still many ways that tumors evade immune detection and attack.

EphA2/ephrin-A1 axis in anti-tumor immunity

Relatively little is known about EphA2 and ephrin-A1's impact on the tumor immune microenvironment, but the literature suggests that the EphA2/ephrin-A1 axis may play a greater role than what is currently known. Because EphA2 is commonly overexpressed in cancer, human EphA2-derived epitopes have been recognized as tumor-associated antigens by CD4 and CD8 T cells, particularly epitope $EphA2_{883\text{-}891}$, which induces immunoreactivity in CD8+ T-cells via MHC I-restricted presentation in renal cell carcinoma (RCC) and glioma cells *in vitro*[105–108]. Several preclinical investigations have tested vaccinations with EphA2 peptide-pulsed DCs in mouse tumor models[109,110]. Together, these studies have provided rationale for early phase clinical trials to test the safety and efficacy of combination peptide vaccines with $EphA2_{883\text{-}891}$ plus other TAAs, as well as CAR-T cells targeting EphA2, in patients with gliomas, including glioblastomas[111–115].

Besides inducing immunologic responses, EphA2 and ephrin-A1 may also regulate immune cell trafficking, though this has not been studied in the context of cancer. Stimulation of ephrin-A1-mediated EphA2 signaling in endothelial cells leads to increased expression of adhesion proteins, such as E-selectin and vascular cell adhesion molecule 1 (VCAM-1), that bind to leukocyte integrins[116]. In parallel, EphA2 binding to ephrin-A1 expressed on T cells results in reverse signaling that promotes T cell adhesion to VCAM-1 and another vascular adhesion protein intercellular adhesion molecule 1 (ICAM-1)[117]. These results suggest that EphA2 on the endothelium and ephrin-A1 on T cells may regulate adhesion and transendothelial migration of T cells. Alternatively, ephrin-A1 can bind to EphA1 and EphA4 expressed in T cells and mediate chemotaxis *in vitro*[118–120]. In addition to *in vitro* investigations, the impact of EphA2 on immune cell trafficking has been studied in lung injury and inflammation mouse models; however, their effects remain equivocal and are likely model-dependent. For

	Monocytes / macrophages	DCs	B cells	T cells
EphA2 receptor expression	+	+	+	-
EphA2 cell-type specific function	Cell spreading and adhesion	Cell adhesion, entry receptor for herpesvirus	unknown	
Ephrin-A1 ligand expression	+	unknown	+	+
Ephrin-A1 cell-type specific function	Cell adhesion		unknown	Cell adhesion, migration, and activation

Table 1.3. EphA2 and ephrin-A1 expression and roles in immune cells. "+" indicates confirmed expression in indicated cell type, while "-" indicates no expression in indicated cell type (adapted from (23)).

example, Carpenter et al. report that EphA2 knockout mice have reduced vascular permeability, immune cell infiltration, and chemokine production in a bleomycin-induced lung injury model[121], while Okazaki et al. conclude that the same knockout mice have increased immune cell infiltration and inflammatory cytokine production in *Mycoplasma* and ovalbumin-induced inflammatory lung models[122]. Further *in vivo* studies are needed to clarify the effect of EphA2 in the lung vasculature and immune environment.

Although EphA2 and ephrin-A1 are both expressed in various subsets of immune cells, little is known about their functions, particularly in the context of cancer (Table 1.3). However, one recent study by Markosyan, et al. focused on the effect of EphA2 expressed in pancreatic tumor cells on the anti-tumor response[123]. They found that EphA2 expression in pancreatic ductal adenocarcinoma (PDAC) was inversely correlated with CD8 T cell infiltration. Using a murine PDAC model, they discovered that CRISPR/Cas9-engineered knockout of EphA2 in tumor cells increased tumor-infiltrating lymphocytes (TILs) and decreased granulocytic MDSCs, indicating an overall shift in an enhanced anti-tumor response. Thus, although EphA2 may be a source of immunogenic TAAs that can be leveraged to promote an anti-tumor response, as mentioned in earlier studies, it may also have other effects that can inhibit an effective response. Whether the EphA2/ephrin-A1 axis promotes or inhibits anti-tumor immunity is likely context and cell type dependent. These conflicting narratives mirror the paradoxes posed by the same signaling axis in the context of the cancer cells, which propose both tumor-promoting and tumor-suppressive roles. With these concepts in mind, the goal of future endeavors should include refining the roles of EphA2 and ephrin-A1, not just within the microcosm of the cancer cell, but also among the many complex interactions between host and tumor cells.

Thesis Projects

Despite significant advancements in cancer research, prevention, and therapeutics, cancer remains a major public health problem. Lung and breast cancer together make up a significant proportion of overall cancer incidence and mortality. The EphA2 RTK and ephrin-A1 ligand signaling axis has long been implicated in solid cancers, including lung and breast cancer, as well as other pathological processes, such as inflammation. The majority of research on EphA2 has focused on its tumor-promoting effects in the cancer cells. However, some of these studies have parsed out the differences between ephrin-dependent and independent EphA2 signaling and hinted at EphA2's dual role as a tumor-promoter and suppressor. In addition, the EphA2/ephrin-A1 signaling axis not only exists within tumor cells, but also in many other cell types, such as endothelial and immune cells, and facilitates communication between different cell types. Together, the many different mechanisms of signaling, expression across a multitude of cell types, and various physiological contexts make the EphA2/ephrin-A1 axis a very challenging but intriguing topic of study.

This dissertation dives into this complex challenge and examines the role of EphA2/ephrin-A1 axis among host-tumor interactions. In the first half of this dissertation, we concentrate on the role of tumor-specific EphA2 on the host immune response. We discovered that EphA2 overexpression in murine NSCLC cells increased tumor burden *in vivo* but not *in vitro*, due to suppression of the host T cell immune response. Further investigation into the mechanism of immune evasion revealed that EphA2-overexpressing tumors released more monocyte-attracting chemokines that likely contributed to the increased recruitment of macrophages and potential MDSCs observed in the EphA2-overexpressing tumors. This suggests that these immunosuppressive populations are responsible for the decreased CD8 T cell infiltration and activity found in EphA2-overexpressing tumors.

In the second half of this dissertation, we evaluate the impact of host deficiency of ephrin-A1 on cancer growth and metastasis. Using ephrin-A1 knockout mice, we discovered that ephrin-A1 deficiency in host tissues decreased lung metastasis of breast cancer cells, despite not affecting primary mammary tumor growth. Assessment of primary tumor endothelium and immune infiltrate did not reveal insightful differences between knockout and wild-type mice. However, analyses of the secondary metastatic site demonstrated that ephrin-A1-deficient lungs provide a less favorable metastatic niche for breast cancer cells. Together these two parallel works consistently demonstrate that EphA2 and ephrin-A1 play important roles in modulating host-tumor interactions. Tumor-specific EphA2 can evoke a tumor-promoting

effect through suppression of the host immune response, while ephrin-A1 expressed in host tissues can promote metastasis through facilitating cancer cell extravasation and adaptation to the lung metastatic niche. These studies provide additional insight into the many complex interactions that the EphA2/ephrin-A1 axis regulates in the tumor microenvironment.

CHAPTER II

Tumor-specific EphA2 receptor tyrosine kinase inhibits anti-tumor immunity by recruiting suppressive myeloid populations in NSCLC

Abstract

Given the success of both targeted and immunotherapies against cancer, there is increasing utility for identifying targeted agents that also promote anti-tumor immunity. EphA2 is a receptor tyrosine kinase that contributes to tumor growth and metastasis and has been identified as a viable target for many solid cancers. Investigating EphA2's impact on the host immune system may advance our understanding of tumor immune evasion and the consequences of targeting EphA2 on the tumor microenvironment. Here, we examine how tumor-specific EphA2 affects the activation and infiltration of immune cell populations and the cytokine and chemokine milieu in non-small cell lung cancer (NSCLC). Effects of EphA2 overexpression in murine NSCLC cells were evaluated in both *in vitro* cell viability assays and *in vivo* tumor models. Tumor immune infiltrate was assessed by flow cytometry. Cytokine and chemokine expression was evaluated using NanoString technology and qRT-PCR. Although EphA2 overexpression in NSCLC cells did not display proliferative advantage *in vitro*, it conferred a growth advantage *in vivo*. Analysis of lung tumor infiltrate revealed decreased natural killer and T cells in the EphA2-overexpressing tumors, as well as increased myeloid populations, including tumor-associated macrophages (TAMs). T cell activation, particularly in CD8 T cells, was decreased, while PD-1 expression was increased. These changes were accompanied by increased monocyte-attracting chemokines, specifically CCL2, CCL7, CCL8, and CCL12, and immunosuppressive proteins TGF-β and arginase 1. Our studies suggest EphA2 on tumor cells recruits monocytes and promotes their differentiation into TAMs that likely inhibit activation and infiltration of cytotoxic lymphocytes, promoting tumor immune escape. Further studies are needed to determine the molecular mechanisms by which EphA2 affects the recruitment of these cell types and to test the function of these myeloid cells.

Introduction

Targeted and immunotherapies have both emerged as cornerstones of anti-cancer treatment over the past several decades. Despite these advancements, not all patients derive durable clinical benefit from these therapeutic agents, and many efforts are underway to design the best combinations of targeted therapies and immune checkpoint inhibitors (ICIs) that will enhance responses while limiting toxicities[124,125]. However, in order to effectively combine these different treatment modalities, more research is needed to evaluate how one may impact the other – in particular, how targeted agents may already be altering the host anti-tumor immune response.

Despite the introduction of many novel therapies, lung cancer is still the most prevalent cancer that occurs among men and women combined and the leading cause of cancer-related death. A fraction of patients with NSCLC, the most common type of lung cancer, have experienced clinical benefit from single-agent ICIs and/or targeted agents, depending on the mutational profile, but one of the major challenges has been strategizing which combination therapies may be the most synergistic while least toxic and therefore should be tested in trials first[126,127].

EphA2 receptor tyrosine kinase (RTK) is a cell-surface protein that is overexpressed and implicated in the progression of many solid cancers including NSCLC, and it has become a prominent target for anti-cancer therapy. Currently, agents targeting EphA2, including kinase inhibitors, antibodies, peptide-drug conjugates, liposomal siRNA, chimeric antigen receptor (CAR)-T cells, and dendritic cell (DC) vaccines, are being tested in various cancer clinical trials around the world (NCT02252211, NCT04180371, NCT01591356, NCT01440998, NCT03423992, NCT00563290, NCT00371254, NCT02575261, NCT01876212, NCT00423735). Although the role of EphA2 within the cancer cell and tumor endothelium is well-studied[47,56], its impact on the tumor immune microenvironment is largely unknown[24]. Thus, we aim to evaluate how EphA2 expression in the tumor affects the immune landscape in NSCLC.

To test the impact of tumor-specific EphA2, we overexpressed EphA2 in murine NSCLC cells and found that EphA2 overexpression increases lung tumor burden *in vivo*. We examined immune infiltrate of tumor-bearing lungs by flow cytometry and found that lungs with EphA2-overexpressing tumors had decreased lymphocytic populations and activation of CD8 T cells but had conversely increased myeloid populations, including TAMs and monocytes, and PD-1 expression in T cells. In addition, gene expression analysis of lung tumors revealed that EphA2 overexpression increased levels of monocyte-attracting chemokines and myeloid-associated

immunosuppressive proteins. Together, these studies suggest that EphA2 in NSCLC cells recruits monocytes and promotes their transformation into TAMs, which inhibit the activation of anti-tumor T cells. This provides relevant insight into EphA2's impact on the immune landscape of NSCLC and the additional potential benefits of targeting EphA2 in cancer.

Materials and Methods

Cell culture

Lewis lung carcinoma (LLC) cells were a generous gift from Dr. Barbara Fingleton (Vanderbilt University). *Kras G12D* mutant, *Tp53* and *Stk11*/LKB1 knockout, GFP NSCLC cell line (KPL) from the C57BL/6 background was previously generated in the lab[128]. Both cell lines were maintained in DMEM (Corning #MT10013CV) supplemented with penicillin/streptomycin (Gibco #15140163) and 10% FBS (Gibco #A3160502). Luciferase-expressing KPL cells were generated by serial dilutions of KPL cells with lentiviral overexpression of the luciferase gene. Stable EphA2 overexpression was generated by lentiviral transduction of pCDH vector containing the human EphA2 cDNA sequence with subsequent puromycin selection (2 μg/ml) for four days and was compared with empty vector pCDH control.

Western blotting

Cells were washed with PBS and lysed on ice with RIPA buffer supplemented with a protease inhibitor cocktail (Sigma-Aldrich #4693124001) and phosphatase inhibitors (Sigma-Aldrich #4906845001). Lysates were electrophoresed on a 12% SDS-polyacrylamide gel and transferred to nitrocellulose membranes, which were blocked for a half hour with 5% nonfat dry milk in TBS-T buffer. Membranes were incubated with primary monoclonal antibodies against EphA2 (Cell Signaling Technologies #6997, 1/1000) and tubulin (Sigma-Aldrich #T4026, 1/2000) overnight at 4°C, followed by three washes with TBS-T and incubation with secondary antibodies goat anti-rabbit IRDye 800CW (LI-COR #926-32211) and anti-mouse IRDye 680LT (LI-COR #926-68020, 1/20,000) for 1 hour at room temperature. After washing with TBS-T, blots were imaged using LI-COR Odyssey.

Cell viability assays

For MTT assays, cells were seeded at a density of 1000 cells per well in 100 μl media in 96-well plates. At each indicated time point, 20 μl of 5 mg/ml thiazolyl blue tetrazolium bromide

(MTT) reagent (Thermo Fisher #M6494) in PBS was added per well and incubated at 37°C for 3 hours. Media was then aspirated, and 150 µl of isopropanol solution with 4mM HCl and 0.1% NP-40 was added to each well and rocked at room temperature for 10 minutes. The absorbance at 590 nm was read on a BioTek spectrophotometer and recorded using a Gen5 Microplate Reader. Cell viability was presented as a relative fold change from day 1 values. Each assay included six technical replicates and was repeated at least three independent times. For colony formation assays, cells were seeded at a density of 400 cells per well in 2 ml media in 12-well plates. After incubating for seven days, media was aspirated, and plates were washed x2 with PBS on ice, fixed with methanol for 10 minutes, and stained with 0.5% crystal violet in methanol for 10 minutes at room temperature. Plates were then rinsed under diH_2O and let out to dry overnight before image acquisition. Images were analyzed using NIH ImageJ, and colony formation was presented as percentage of total area. Each assay included three technical replicates and was repeated four times.

Animal models

Animals were housed in a non-barrier animal facility under pathogen-free conditions, 12-hour light/dark cycle, and access to standard rodent diet and water *ad libitum*. Experiments were performed in accordance with AAALAC guidelines and with Vanderbilt University Medical Center Institutional Animal Care and Use Committee approval. Wild-type C57BL/6 mice were purchased from Jackson Laboratory and bred to generate litters for experiments. Male athymic nude (*Foxn1*^{nu}) mice were purchased from Envigo for experiments testing tumor growth and immune infiltrate in the context of T cell deficiency. All other experiments utilized male and female immunocompetent wild-type C57BL/6 mice. Mice were co-housed with one to four littermates for at least two weeks prior to and during all experiments and compared with littermate controls whenever possible. All mice used for tumor experiments were six to ten weeks old at the onset on the experiment. Experimental cohorts were limited to litters that were born within two consecutive weeks. Sample sizes are as shown in the figures. At experimental endpoints, mice were euthanized by cervical dislocation.

Tumor models

For lung tumor colonization experiments, luciferase-expressing KPL cells suspended in PBS were injected via tail vein into seven to ten-week-old wild-type C57BL/6 mice, and mice underwent *in vivo* bioluminescence imaging with a PerkinElmer IVIS Spectrum several hours post-injection to verify successful delivery to the lungs. For experiments comparing lung tumor

growth between control and EphA2-overexpressing cells, $1x10^6$ KPL cells were injected in each mouse. For experiments equalizing tumor burden, either $4x10^6$ vector control or $1x10^6$ EphA2-overexpressing KPL cells were injected in each mouse. Mice were reimaged at one and two weeks post-injection and sacrificed at day 14-16. Lungs were weighed, imaged for GFP+ tumors, and processed for flow cytometry analysis. For subcutaneous tumor implantations, $1x10^6$ KPL cells suspended in a 1:1 mixture of PBS and Growth Factor-Reduced Matrigel (Corning #354230) were injected subcutaneously into the dorsal flanks of six to eight-week-old male and female mice. In experiments with athymic nude mice, tumors dimensions were measured by digital caliper at given time points every other day, and volume was calculated using the following formula: volume = length x width^2 x 0.52. Tumors were subsequently harvested, weighed, and processed for flow cytometry at day 14 post-implantation.

Flow cytometry

Lungs and subcutaneous tumors were minced and dissociated in RPMI-1640 media (Corning #MT10040CV) containing 2.5% FBS, 1 mg/ml collagenase IA (Sigma-Aldrich #C9891), and 0.25 mg/ml DNase I (Sigma-Aldrich #DN25) for 45 minutes at 37°C. Digested tissue was then filtered through a 70-µm strainer, and red blood cells were lysed using ACK Lysis Buffer (KD Medical #RGF-3015). Samples were washed with PBS and stained with Ghost Dye Violet V450 (Tonbo Biosciences #13-0863) or V510 (Tonbo Biosciences #13-0870) to exclude dead cells. After washing with buffer (0.5% BSA, 2mM EDTA in PBS), samples were blocked in αCD16/32 mouse Fc block (Tonbo Biosciences #70-0161) and stained for extracellular proteins using an antibody master mix made in buffer. After washing with buffer, cells were fixed with 2% PFA. Flow cytometry data was obtained on a BD 4-laser Fortessa using BD FACS Diva software v8.0.1 and analyzed using FlowJo software v10.6.1. Fluorescence minus one (FMO) samples were used as gating controls when needed. Antibodies used in flow panels are detailed in Table 2.1, and gating strategies used in analysis are detailed in Table 2.2. Each data point is generated after analyzing at least $5x10^5$ viable cells from a specimen from an individual mouse.

NanoString nCounter assay

Lung tumors were dissected and minced with surgical tools cleaned with RNaseZAP (Sigma-Aldrich #R2020), and RNA was extracted using RNeasy Micro Kit (Qiagen #74004). RNA concentration was assessed with a Nanodrop spectrophotometer, and RNA quality was determined by the Agilent 2100 Bioanalyzer System. 20 ng of RNA from each of twelve mice, six gender-matched littermate pairs, were used for input into nanoString nCounter hybridization

Table 2.1. Antibodies used in flow cytometry analysis.

Antibody target	Manufacturer	Catalog #	Fluorophore	Dilution	RRID
MHCII I-E/A	Tonbo Biosciences	75-5321	V450	1/250	AB_2621965
CD8a	BD Biosciences	560469	V450	1/250	AB_1645281
CD45.2	Tonbo Biosciences	35-0454	V450	1/500	AB_2621965
CD19	Tonbo Biosciences	35-0193	FITC	1/250	AB_2621682
CD3e	BD Biosciences	553061	FITC	1/250	AB_394594
CD44	Tonbo Biosciences	35-0441	FITC	1/250	AB_2621688
NK1.1	BD Biosciences	557391	PE	1/250	AB_396674
CD11b	eBiosciences	12-0112-82	PE	1/500	AB_2734869
CD25	eBiosciences	12-0251-81	PE	1/500	AB_465606
CTLA-4	BD Biosciences	561718	PE	1/250	AB_10895585
CD3e	BD Biosciences	561826	APC	1/500	AB_10896663
CD4	Biolegend	100516	APC	1/1000	AB_312719
F4/80	eBiosciences	17-4801-82	APC	1/250	AB_2784648
CD3e	Tonbo Biosciences	65-0031	PerCP-Cy5.5	1/250	AB_2621872
CD11b	Tonbo Biosciences	65-0112	PerCP-Cy5.5	1/500	AB_2621885
CD11c	BD Biosciences	560584	PerCP-Cy5.5	1/250	AB_1727422
F4/80	eBiosciences	45-4801-82	PerCP-Cy5.5	1/250	AB_914345
Ly6C	eBiosciences	45-5932-82	PerCP-Cy5.5	1/250	AB_2723343
Ly6G(Gr1)	eBiosciences	45-5931-80	PerCP-Cy5.5	1/500	AB_906247
Ly6G(Gr1)	Tonbo Biosciences	80-5931	rF710	1/1000	AB_2621999
CD8a	Tonbo Biosciences	80-0081	rF710	1/500	AB_2621977
MHCII I-E/A	Biolegend	107622	Ax700	1/1000	AB_493727
PD-1	BD Biosciences	565815	APC-R700	1/500	AB_2739366
CD4	Tonbo Biosciences	55-0041	PE-Cy5	1/2500	AB_2621816
CD11b	Tonbo Biosciences	55-0112	PE-Cy5	1/5000	AB_2621818
CD3e	BD Biosciences	552774	PE-Cy7	1/750	AB_394460
NKp46	eBiosciences	25-3351-82	PE-Cy7	1/750	AB_2573442
CD11c	BD Biosciences	561022	PE-Cy7	1/500	AB_2033997
CD69	BD Biosciences	552879	PE-Cy7	1/500	AB_394508
CD25	Tonbo Biosciences	60-0251	PE-Cy7	1/500	AB_2621843
CD45	BD Biosciences	557659	APC-Cy7	1/500	AB_396774

Table 2.2. Gating strategy used in flow cytometry analysis.

Cell population	Gating strategy
KPL cells	CD45-,GFP+,SSA^{hi}
Immune cells	CD45+, GFP-
NK cells (nude mice)	CD45+, GFP-, CD19-, NKp46+
B cells (nude mice)	CD45+, GFP-, CD19+, MHCII+
Gr1+ myeloid cells (nude mice)	CD45+, GFP-, CD11b^{hi}, Ly6G(Gr1)+, MHCII-
Gr1- myeloid cells (nude mice)	CD45+, GFP-, CD11b^{hi}, Ly6G(Gr1)-
Macrophages (nude mice)	CD45+, GFP-, CD11b^{hi}, F4/80+, Ly6G(Gr1)-
DCs (nude mice)	CD45+, GFP-, CD11c+, MHCII+, NKp46-, Ly6G(Gr1)-
CD4 T cells	CD45+, GFP-, CD3e+, NK1.1-, CD4+, CD8a-
CD8 T cells	CD45+, GFP-, CD3e+, NK1.1-, CD4-, CD8a+
NK cells	CD45+, GFP-, CD3e-, NK1.1+
Macrophages	CD45+, GFP-, CD11b^{hi}, F4/80+, Ly6C-
Monocytes	CD45+, GFP-, CD11b^{hi}, F4/80-, Ly6C+
DCs	CD45+, GFP-, CD11c+, MHCII+,F4/80-

and hybridized to the nanoString nCounter Mouse PanCancer Immune Profiling Panel probeset (nanoString Technologies #XT-CSO-MIP1-12) to measure gene expression. Raw count data was normalized by background correction, positive control correction, and housekeeping gene correction and $\log_2$ transformed using nanoString's nSolver software v3.0. This software was also used to generate pathway scores, differential gene expression analysis, and the volcano plot. Heatmap was generated with normalized data standardized by gene using Microsoft Excel 2016.

RT-PCR

RNA was isolated and measured as detailed above and then converted to cDNA using iScript cDNA Synthesis Kit (Bio-Rad #1708891). Quantitative RT-PCR was carried out with TaqMan Gene Expression Assay reagents, specifically TaqMan Fast Advanced Master Mix (Thermo Fisher #4444557) and probes (Table 2.3), using a StepOnePlus RT-PCR system (Applied Biosystems). Reactions were run in triplicate and mouse *Actb* was used as a housekeeping gene. Six gender-matched littermate pairs were used to validate nanoString hits, and data was presented as fold change of EphA2-overexpressing tumor samples with respect to their littermate control sample.

Table 2.3. TaqMan RT-PCR probes.

Target gene	Assay ID
Actb	Mm02619580_g1
Arg1	Mm00475988_m1
C5ar1	Mm00500292_s1
Ccl2	Mm00441242_m1
Ccl7	Mm00443113_m1
Ccl8	Mm01297183_m1
Ccl12	Mm01617100_m1
Ccr2	Mm99999051_gH
Csf1r	Mm01266652_m1
Tgfb1	Mm01178820_m1
Tgfb2	Mm00436955_m1
Tgfb3	Mm00436960_m1

Statistical analysis

All graphs and statistical analysis were completed using GraphPad Prism software v6.07. For comparisons of continuous variables between two groups, an unpaired, two-tailed student's t test with Welch correction or unpaired Mann-Whitney *U*-test was performed. For comparisons of continuous variables over time between two groups, a two-way analysis of

variance (ANOVA) was performed. For comparison of survival curves, a log-rank test was performed. For RT-PCR analysis, a one-sample Wilcoxon signed rank test was performed. A *P*-value less than 0.05 was considered statistically significant.

Results

EphA2 confers growth advantage to NSCLC *in vivo* but not *in vitro*

Because EphA2 has been shown to play both tumor-promoting and suppressing roles, we investigated whether EphA2 overexpression in our murine NSCLC cell lines could impact cell viability and tumor growth. We chose two NSCLC cell lines originating from the C57BL/6 background, LLC and a KRAS G12D mutant cell line containing loss of TP53 and STK11/LKB1 (KPL)[128], both of which are common alterations found concomitantly with KRAS mutations in human NSCLC samples[129,130]. We stably overexpressed EphA2 in these cells (Figure 2.1A) but found no changes in cell viability by MTT or colony formation assays *in vitro*, compared to vector control cells (Figure 2.1B, 2.1C). We next determined if EphA2 overexpression could impact tumor growth *in vivo* using two different models, subcutaneous implantation and tail vein injection for generation of lung tumors in immunocompetent, wild-type C57BL/6 mice. In both subcutaneous and lung tumor models, EphA2-overexpressing KPL cells grew dramatically larger tumors *in vivo*, as shown by bioluminescence imaging and gross lung specimens (Figure 2.1D-F). In addition, survival of tail vein-injected mice was significantly worse in mice injected with EphA2-overexpressing cells, compared to control cells (Figure 2.1G). Overall, these data suggest host factors contribute to EphA2's impact on *in vivo* growth, which is not apparent *in vitro*.

EphA2 overexpression in NSCLC does not significantly impact tumor burden or immune infiltration in nude mice

There are various host factors that may explain the discrepancy between our *in vitro* and *in vivo* results regarding the impact of EphA2 in the NSCLC cell, one of which includes the host immune system. Besides one study demonstrating that tumor-intrinsic EphA2 can inhibit anti-tumor immunity in pancreatic cancer[123], the effect of EphA2 on the tumor immune microenvironment has been largely unstudied. Thus, we set out to determine if the host immune system plays a role in EphA2-mediated KPL tumor growth *in vivo*. To test whether the adaptive or innate immune response may play a role, we first evaluated KPL tumor growth in athymic

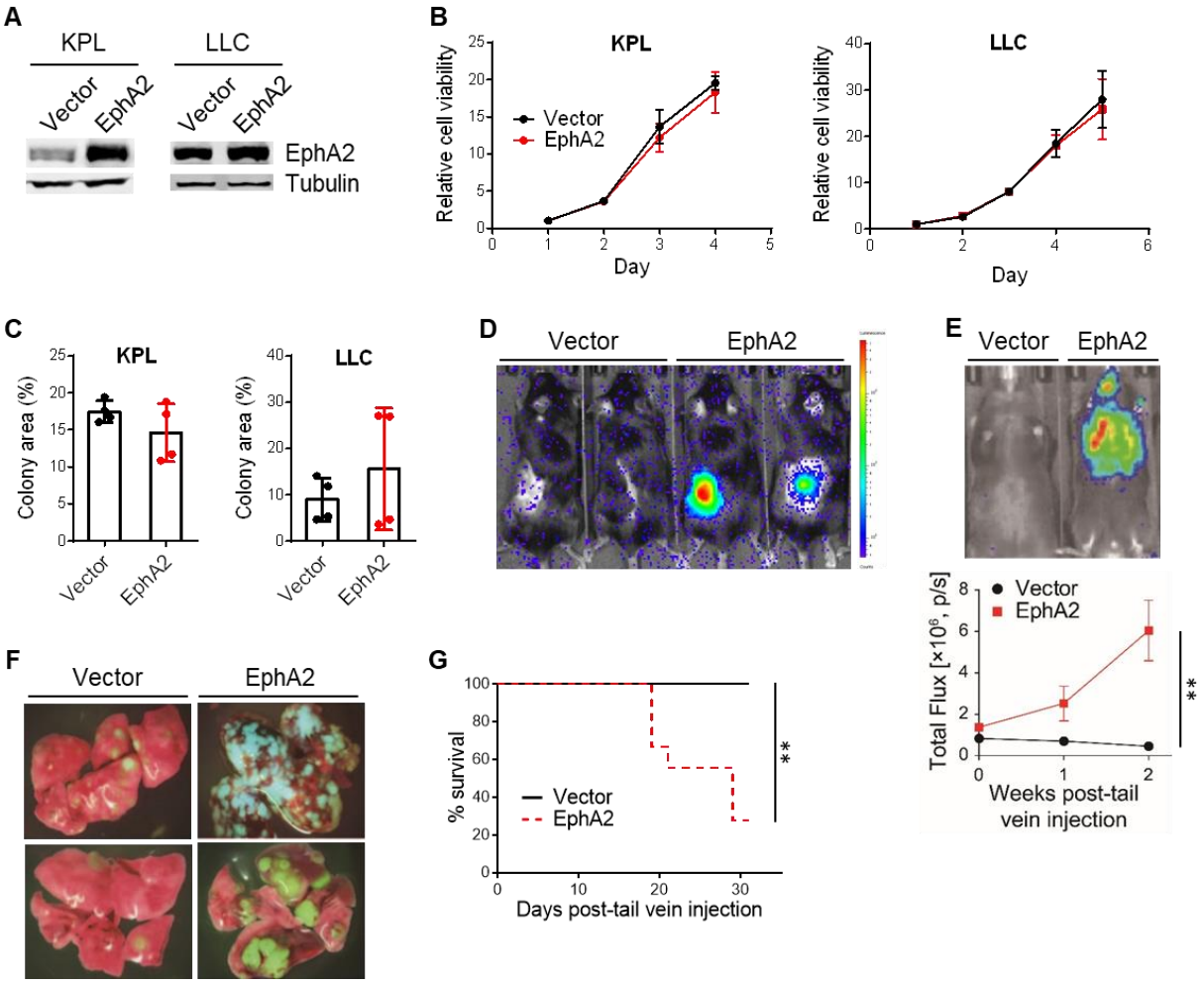

Figure 2.1. EphA2 confers growth advantage to NSCLC *in vivo* but not *in vitro*. (A) Confirmation of EphA2 overexpression in KPL and LLC cells by western blot. (B, C) *In vitro* cell viability of KPL and LLC cells with control and EphA2 overexpression by MTT and colony formation assays (n=4). (D) Representative image of bioluminescence signal in control and EphA2-overexpressing KPL tumors 14 days after subcutaneous implantation. (E) Representative image of bioluminescence signal 14 days after tail vein injection of control and EphA2-overexpressing KPL cells and quantification of bioluminescence signal at indicated time points (**p<0.01, two-way ANOVA) (F) Representative gross specimens of GFP+ vector and EphA2-overexpressing KPL tumor-bearing lungs. (G) Survival of mice injected with vector or EphA2-overexpressiong KPL cells via tail vein (**p<0.01, log-rank test). Data shown are averages ± SD.

nude mice, which have defective T cell adaptive immunity. We did not observe significant differences in tumor growth and weight between control and EphA2-overexpressing tumors in nude mice (Figure 2.2A). In addition, we performed flow cytometry analysis on the tumors and draining lymph nodes and found no differences in percentages of GFP+ KPL tumor cells and tumor-infiltrating immune cells (Figure 2.2B). We also observed no significant differences in subsets of immune cells, including natural killer (NK) cells, B cells, DCs, and myeloid cells, from both the tumors and draining lymph nodes in the nude mice (Figure 2.2C, 2.2D). These results

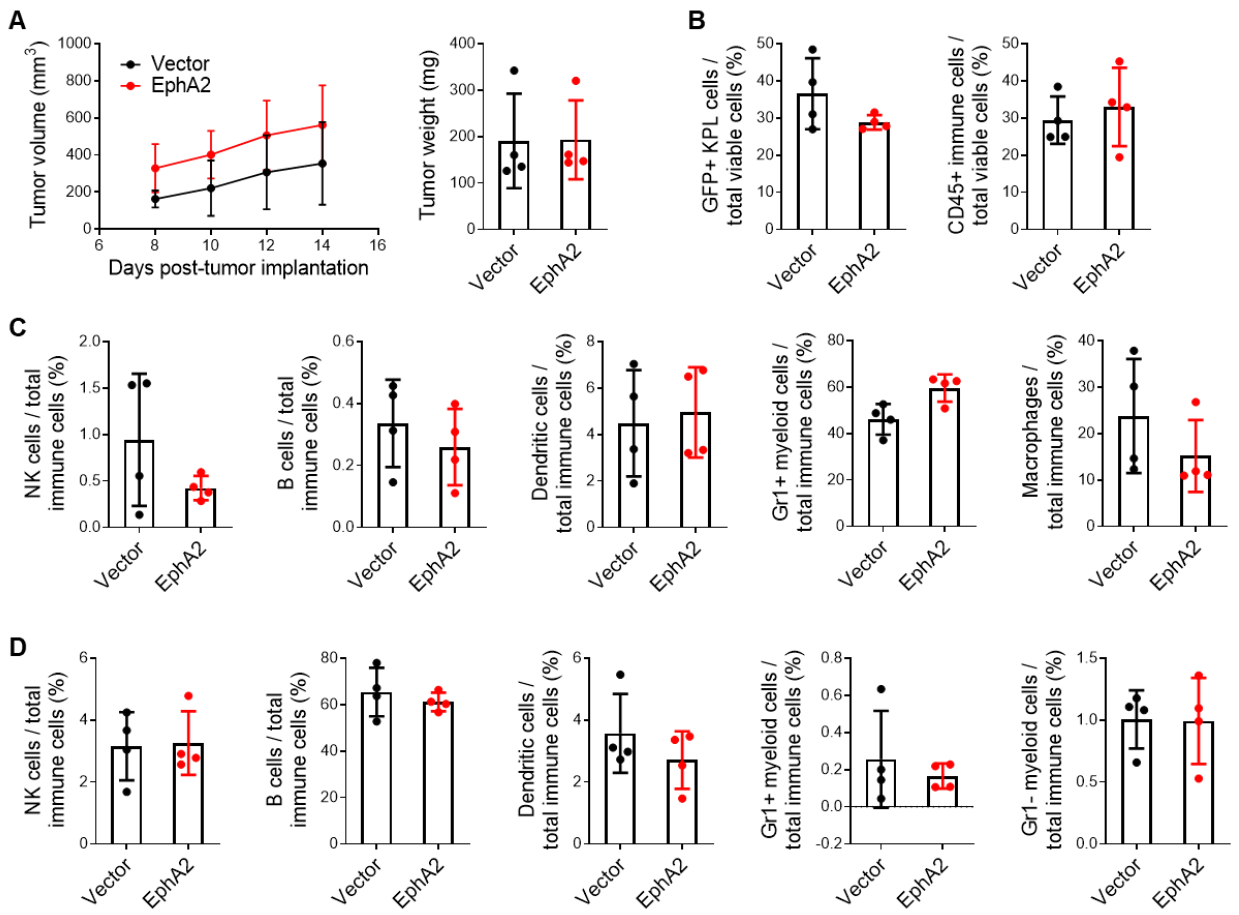

Figure 2.2. EphA2 overexpression in NSCLC does not significantly impact tumor burden or immune infiltration in nude mice. (A) Tumor volumes over time and weights on day 14 post-implantation of control and EphA2-overexpressing KPL subcutaneous tumors from nude mice. (B) Flow cytometric analysis of GFP+ KPL tumor cells and total tumor-infiltrating immune cells, as well as (C) tumor-infiltrating NK cells, B cells, DCs, macrophages, and Gr1+ myeloid cells. (D) Similar flow cytometry analysis of immune populations from draining inguinal lymph nodes. Data shown are averages ± SD (n=4 mice per group).

suggest that EphA2-mediated KPL tumor growth *in vivo* may require suppression of T cell adaptive immunity.

EphA2 overexpression in NSCLC decreases lymphocytic and increases myeloid infiltrate in tumor-bearing lungs

We returned to our tumor model with immunocompetent C57BL/6 mice to examine the tumor immune infiltrate, including the T cell populations. As before, wild-type mice were injected via tail vein with control or EphA2-overexpressing KPL cells, and lungs were harvested for flow cytometry analysis 14 days later. EphA2-overexpressing KPL tumor-bearing lungs had significantly higher percentages of GFP+ KPL tumor cells compared to control (Figure 2.3A).

Although the overall percentage of immune cells did not differ (Figure 2.3A), the lymphocytic populations, particularly CD4 and CD8 T cells and NK cells, were significantly decreased in the EphA2-overexpressing tumor-bearing lungs (Figure 2.3B). Conversely, myeloid populations, including macrophages and monocytes, were increased, while there was no change in DCs (Figure 2.3C). This data suggests that EphA2 in the tumor cell reshapes the tumor immune microenvironment of the lung and shifts it from a lymphocytic to a more myeloid response. This myeloid response presumably plays a greater tumor-promoting role and may suppress the anti-tumor response primarily led by the T cells.

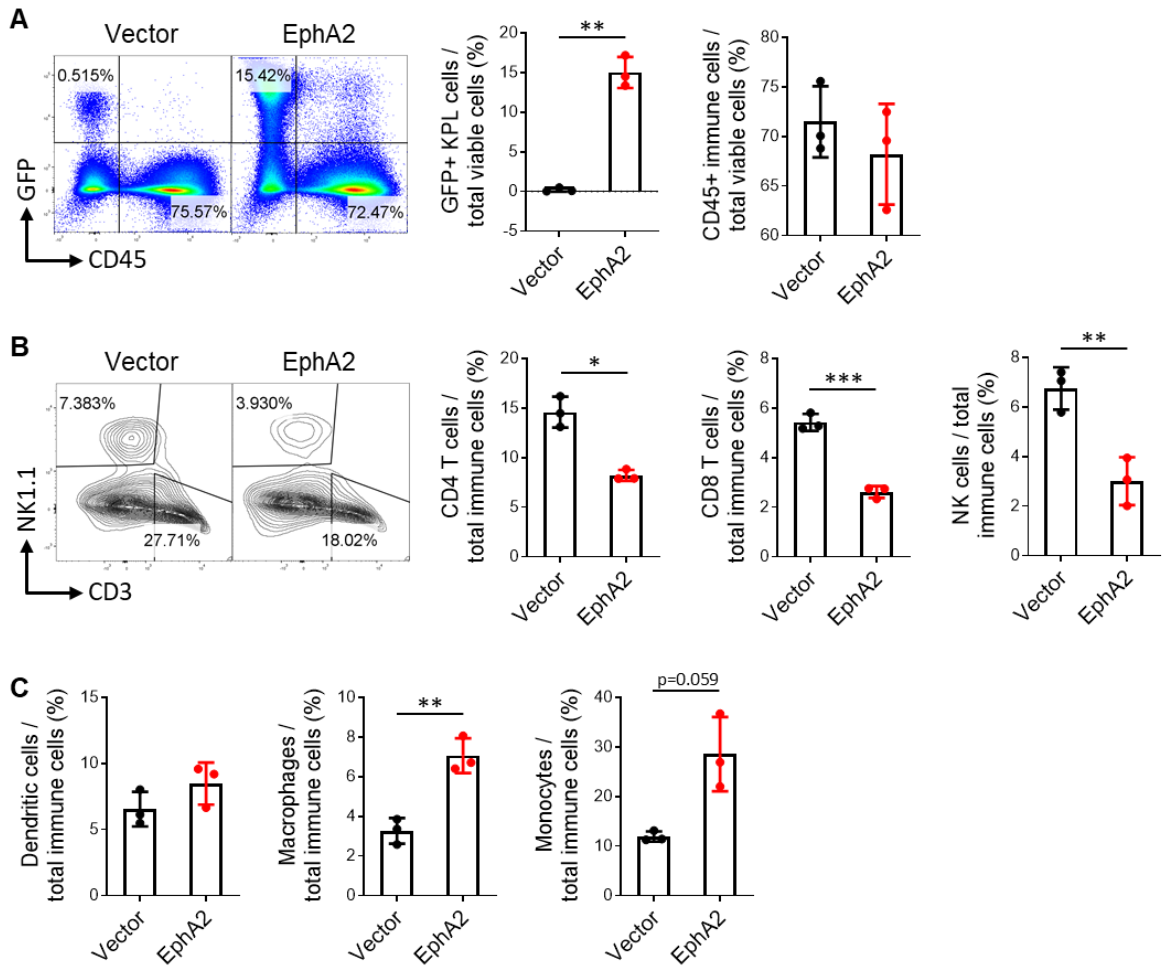

Figure 2.3. EphA2 overexpression in NSCLC decreases lymphocytic and increases myeloid infiltrate in tumor-bearing lungs. (A) Representative flow cytometry plots and quantification of GFP+ KPL and immune cells from vector control and EphA2-overexpressing tumor-bearing lungs on day 14 post-tail vein injection. (B) Similar flow plots and analysis of CD4 and CD8 T cells and NK cells, as well as (C) quantification of DCs, macrophages, and monocytes. Data shown are averages ± SD (n=3 mice per group, *p<0.05; **p<0.01; ***p<0.001, two-tailed unpaired student's t test with Welch correction).

EphA2 overexpression in NSCLC suppresses tumor-infiltrating T cells

Although we found a decrease in lymphocyte populations in EphA2-overexpressing tumor-bearing lungs, this result could also be explained by the dramatically greater tumor burden in these lungs, compared to the control lungs, which contained less than a percentage of KPL tumor cells (Figure 2.3A). Many previous studies have shown a correlation between tumor bulk and the quality of immune infiltrate, though it is difficult to discern which is the cause and which is the effect. In order to determine if tumor bulk contributes to the immune landscape we observe in Figure 2.3, we repeated the tail vein experiment controlling for tumor bulk by injecting four times the number of control KPL cells, compared to EphA2-overexpressing KPL cells. By day 16, there was comparable amount of KPL tumor burden in control and EphA2-overexpressing tumor-bearing lungs (Figure 2.4A). Flow cytometric analysis on these lungs did

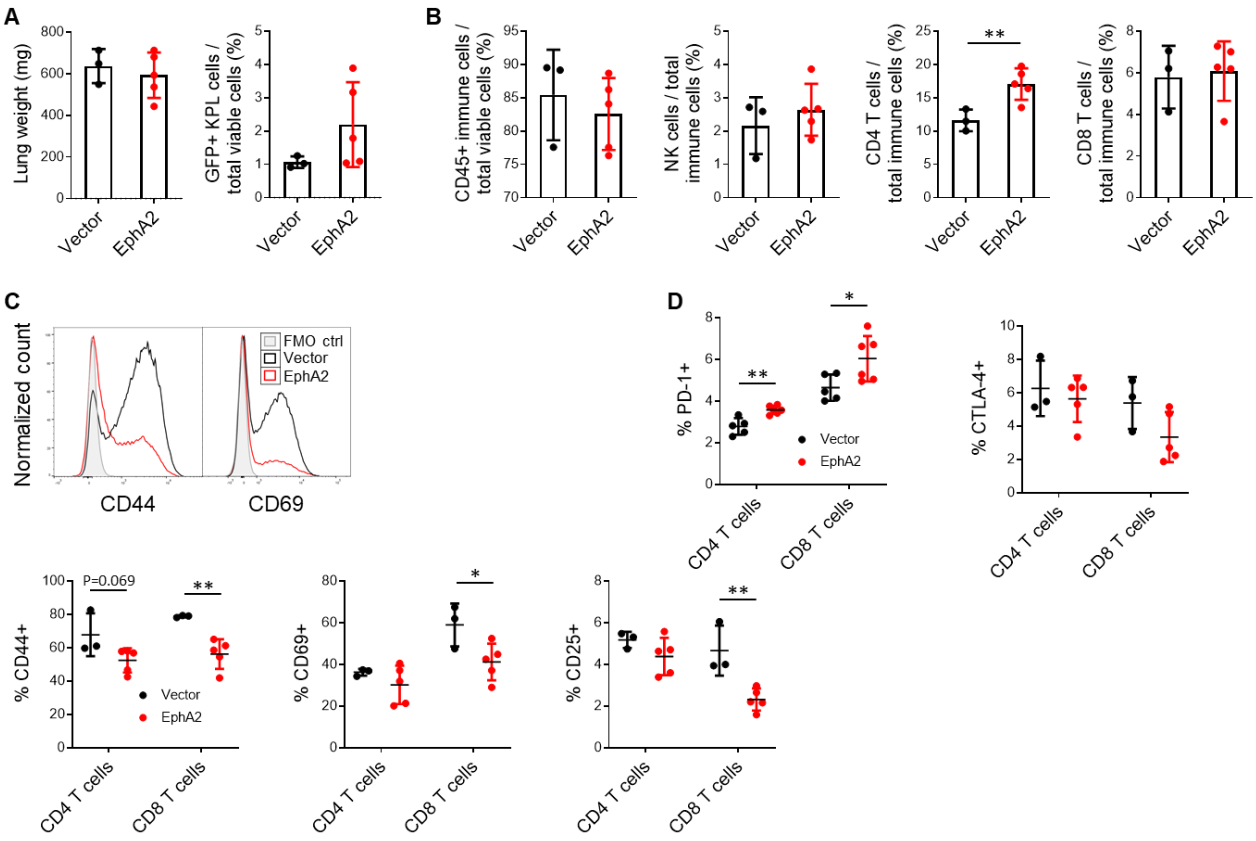

Figure 2.4. EphA2 overexpression in NSCLC suppresses tumor-infiltrating T cells. (A) Lung weights and quantification of GFP+ KPL cells via flow cytometry from vector control and EphA2-overexpressing tumor-bearing lungs with equalized tumor burden. (B) Flow cytometric analysis of total immune cells, CD4 and CD8 T cells, and NK cells in KPL-tumor bearing lungs. (C) Representative flow histograms of CD44 and CD69 expression on CD8 T cells and quantification of CD44, CD69, and CD25 activation markers on CD4 and CD8 T cells. (D) Quantification of PD-1 and CTLA-4 exhaustion markers on CD4 and CD8 T cells. Data shown are averages ± SD (n=3-6 mice per group, *p<0.05; **p<0.01, two-tailed unpaired student's t test with Welch correction).

not recapitulate results from the previous experiment, specifically no decrease in lymphocyte populations in EphA2-overexpressing tumor-bearing lungs (Figure 2.4B). Interestingly, there was an increase in CD4 T cells in the EphA2-overexpressing tumor-bearing lungs. These findings indicate that the differences in immune lung infiltrate we previously observed were at least partially due to increased KPL tumor burden from EphA2-overexpressing tumors compared to control tumors.

Although the proportion of CD8 T cells did not differ when tumor burden between control and EphA2-overexpressing KPL tumors were equalized, T cell activation status and effector function may still be different. Tumor-infiltrating T cells with upregulated expression of activation markers, such as CD44, CD69, and CD25, and downregulated expression of exhaustion markers like PD-1 and CTLA-4 indicate a higher T cell functional status that mediates a stronger and more enduring anti-tumor response[103,131]. We examined the expression of activation markers of T cells from KPL tumor-bearing lungs and found that EphA2 overexpression in the tumor significantly downregulates surface activation markers CD44, CD69, and CD25 on CD8 T cells (Figure 2.4C). Similar trends were also seen in CD4 T cells, though not significant (Figure 2.4C). In addition, tumor-specific EphA2 overexpression led to increased PD-1 expression in both CD4 and CD8 T cells, though not CTLA-4 (Figure 2.4D). These results indicate that EphA2 overexpression in KPL tumors inhibits CD8 T cell activation and may promote T cell exhaustion in the lung tumor microenvironment.

Gene expression profiling reveals higher expression of myeloid markers and chemoattractants in EphA2-overexpressing tumors

In order to understand the mechanism by which tumor-specific EphA2 suppresses CD8 T cell activation, we performed gene expression profiling of dissected control and EphA2-overexpressing lung tumors using nanoString's Mouse PanCancer Immune Profiling Panel. Gene pathway analysis yielded two significantly upregulated pathways in the EphA2-overexpressing tumors, cancer progression and macrophage functions, consistent with our observations on *in vivo* tumor burden and findings from flow cytometry (Figure 2.5A, 2.5B). Differential expression analysis of individual genes revealed 95 genes that were significantly different in expression between vector control and EphA2-overexpressing tumors with a $\log_2$ratio less than -0.5 or greater than 0.5 (Figure 2.5C).

Among these genes included a group of monocyte and macrophage surface markers (*Csf1r*, *Ccr2*, *Itgam*/CD11b, *Mrc1*/CD206), myeloid chemoattractants (*Ccl2*, *Ccl7*, *Ccl8*, *Ccl12*), and immunosuppressive proteins (*Arg1*, *Tgfb1*, *Tgfb2*, *Tgfb3*) (Figure 2.5D). CD11b is a

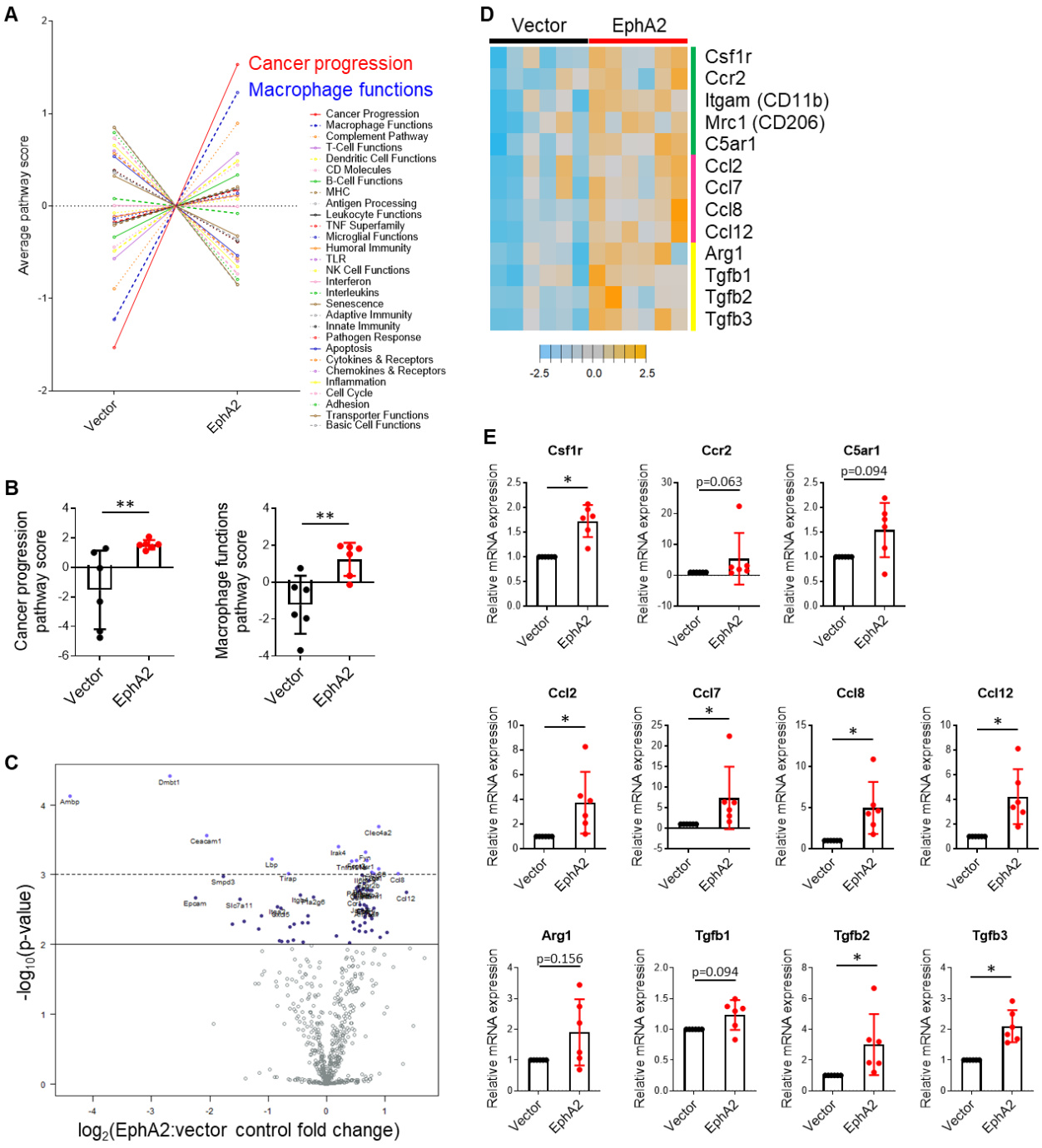

Figure 2.5. Gene expression profiling reveals higher expression of myeloid markers and chemoattractants in EphA2-overexpressing tumors. (A) Average pathway scores of vector control and EphA2-overexpressing KPL tumors calculated from normalized gene expression data using nanoString nSolver software. (B) Comparison of cancer progression and macrophage functions pathway scores between control and EphA2-overexpressing samples. (n=6 mice per group, $^{**}p<0.01$, unpaired Mann-Whitney test) (C) Volcano plot of statistically significant differentially expressed genes. (D) Heatmap depicting standardized expression of differentially expressed myeloid markers (green bar), myeloid-attracting chemokines (pink bar), and immunosuppressive proteins (yellow bar). (E) RT-PCR validation of nanoString hits. (n=6 mice per group, $^{*}p<0.05$, one-sample Wilcoxon signed rank test). Data shown are averages ± SD.

nonspecific myeloid marker, while CCR2, CSF1R, and CD206 are typically expressed in inflammatory monocytes and macrophages, with CD206 specifically detected in tumor-promoting M2 macrophages[132,133]. CCL2, CCL7, CCL8, and CCL12 all belong to the CCL chemokine family and have been shown to bind to CCR2 expressed on circulating monocytes and facilitate their recruitment[132–134]. Additionally, arginase 1 (ARG1) and TGF-β are well-known immunosuppressive proteins that are secreted in the tumor microenvironment by tumor-promoting cells such as M2 TAMs and subsequently inhibit CD8 T cell effector function[132,133]. We validated a majority of these genes using RT-PCR (Figure 2.5E).

In summary, gene expression analysis provided evidence that tumor-specific EphA2 increases the levels of myeloid chemoattractants, monocyte/macrophage lineage cells, and immunosuppressive proteins. We propose that EphA2 in the tumor cell upregulates expression of chemokines in the tumor milieu that recruit circulating monocytes into the tumor, where they differentiate into macrophages and are co-opted to serve tumor-promoting functions as polarized M2 TAMs (Figure 2.6). These tumor-promoting functions include secretion of proteins, such as arginase and TGF-β, that inhibit the expansion and activity of T cells, particularly anti-tumor CD8 cytotoxic lymphocytes. This leads to a shift towards a more myeloid and less lymphocytic infiltrate, as we observed in our flow cytometry studies, as well as decreased activation and increased exhaustion in T cells. Ultimately, the effect of EphA2 in the tumor dampens the anti-tumor immune response and perpetuates the vicious cycle of tumor immune escape and growth.

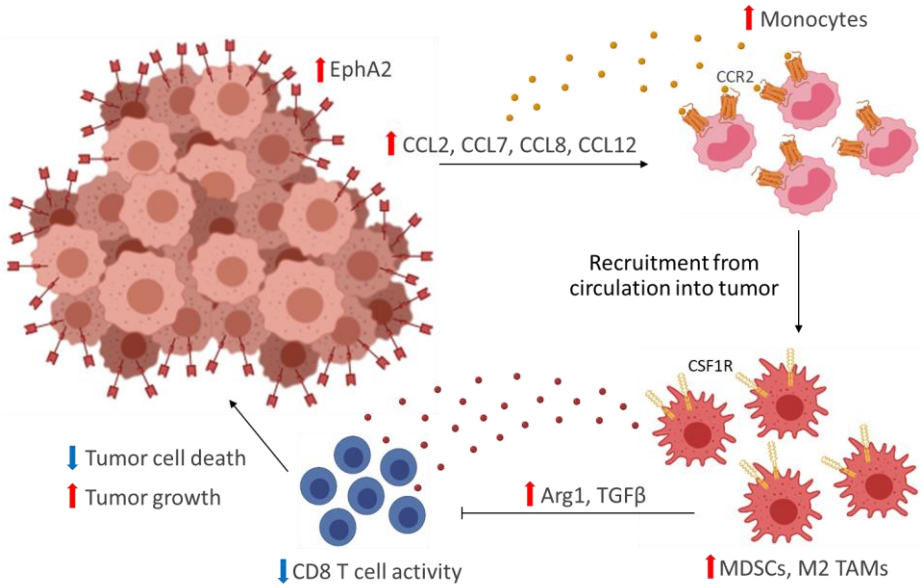

Figure 2.6. Proposed role of tumor-specific EphA2 on promoting NSCLC immune evasion.

Discussion

Our studies identify a novel mechanism that contributes to EphA2's pro-tumor effect in NSCLC. Although EphA2 has previously been shown to facilitate lung tumor growth and metastasis through tumor cell-intrinsic mechanisms[64,71], this is the first study that we are aware of that shows an immune-mediated phenotype. Despite these new insights, this work poses several unanswered questions. First, which cell types are critical for the EphA2-mediated effect on CD8 T cells? EphA2 overexpression in the cancer cell may directly upregulate myeloid-attracting chemokine expression in the tumor cells, but it may also indirectly affect expression in other stromal cells that can secrete these chemoattractants. Similarly, although we propose that the monocytes and macrophages in EphA2-overexpressing tumors are responsible for the higher levels of arginase and TGF-β, these immunosuppressive proteins can also be secreted from cancer or stromal cells. Further studies utilizing single-cell techniques will be required to elucidate the roles of each cell type in the tumor microenvironment. Additionally, the molecular mechanisms by which tumor-specific EphA2 alters the chemokine milieu and immune landscape of lung cancer may be very complex. EphA2 in the tumor cell can signal in an ephrin ligand-dependent or independent manner[57], and it can even be packaged into extracellular vesicles to initiate signaling from a distance[39]. Further molecular investigations are needed to better understand the signaling modalities and downstream pathways in the cancer cell that mediate this immune modulation.

Our findings are consistent with a recently published paper that demonstrated tumor cell-intrinsic EphA2 inhibits anti-tumor immunity in pancreatic cancer through regulation of *PTGS2*, the gene encoding cyclooxygenase-2 (COX2)[123]. Markosyan, et al. identified EphA2 from a screen of The Cancer Genome Atlas (TCGA) dataset evaluating genes that were inversely correlated with *CD8A* expression in human pancreatic adenocarcinomas, as well as other markers of cytotoxic T lymphocytes (CTLs). They went on to evaluate the effect of knocking out tumor cell-specific EphA2 in a mouse model of pancreatic cancer bearing a *Kras G12D* mutation, loss of *Tp53*, and a YFP marker (KPCY) and found that EphA2 knockout significantly increased T cell infiltration and activation, as we had observed in our murine KPL model of NSCLC. Interestingly, they found that EphA2 knockout decreased numbers of granulocytic MDSCs but did not affect macrophages. In addition, these authors identified *Ptgs2* from a RNAseq experiment examining the differentially expressed genes between EphA2 WT and KO tumors.

We can draw many parallels between our investigations and the studies performed by

Markosyan et al.; however, there are also some intriguing differences. Although both studies demonstrate that tumor cell-specific EphA2 has a detrimental impact on T cell-mediated immunity, one suggests that granulocytic myeloid cells play an intermediary role, while the other suggest monocytic myeloid cells. In addition, *Ptgs2* was not among the genes we found to be differentially expressed between control and EphA2-overexpressing KPL tumors. Furthermore, Markosyan et al. observed a decrease in tumor cell proliferation and *in vivo* tumor burden with EphA2 KO, but we observed no differences in growth *in vitro* or *in vivo* when we knocked out EphA2 in our KPL model via CRISPR/Cas9 (data not shown). Lastly, although the authors observed inverse correlations between *EPHA2* and CTL gene signatures in human pancreatic cancer, we did not discover any consistent trends between *EPHA2* and *CD3E*, *CD8B*, *GZMB*, *PRF1*, or *IFNG* expression from the TCGA lung adenocarcinoma dataset (data not shown). These discrepancies could be due to differences in cancer cell type and model and the EphA2 receptor/ephrin ligand balance in the tumor microenvironment, which can be very dissimilar between the pancreas and lung. Although EphA2 is implicated in tumor growth and metastasis of many types of solid cancers through ligand-independent signaling[20,48], it can also suppress cell growth via ligand-dependent signaling through ephrin-A1, its primary binding partner[58,73,77]. Because we observed no effect on cell viability *in vitro* or tumor growth *in vivo* with EphA2 knockout in our KPL lung model, perhaps EphA2 is playing a dual tumor promoter and suppressor role in this cell line. Whereas, in KPCY pancreatic tumors, EphA2 is more of a tumor promoter than suppressor. This would suggest that EphA2 is signaling differently in these two tumor types, or at least in these two particular models, and may explain why the immune phenotypes differ.

A note of caution that we feel compelled to point out is that our investigations rely heavily on an overexpression system, which has been shown in published studies to yield artifactual results[135–140] and likely also observed in many unpublished works. We used the same lentiviral vector to overexpress other genes in KPL cells, including a catalytically dead Cas9 (dCas9), and found that regardless of the gene, overexpression appeared to increase tumor burden *in vivo*, compared to vector control (data not shown). We then tried to overexpress EphA2 using a retroviral vector and discovered that this unfortunately did not recapitulate results we observed in tumor burden with the lentiviral vector (data not shown), though we did not evaluate the immune landscape. We also engineered KPL cells with loss of function of EphA2 via CRISPR/Cas9 and tested both single cell clones and multiclonal populations *in vivo*. Unfortunately, we did not observe significant differences in tumor burden between sgEphA2 cell populations and the sgLacz control cells (data not shown). After these observations, we were

hesitant to continue this avenue of inquiry, as some of our original data may be confounded by overexpression artifact. Despite this, we do believe a portion of our work reflects true biology, and not all the data are a result of artifact. This sentiment arises from recently published works that highlight EphA2's role in inhibiting anti-tumor immunity[123], as well as in monocyte and macrophage function[141–144], which provide some evidence of veracity of our studies. Discerning which results can be attributed to EphA2 and which to artifact is unfortunately an exceedingly challenging task. Our work not only highlights EphA2's potential impact on anti-tumor immunity, but also offers a cautionary tale of scientific rigor and reproducibility.

CHAPTER III

Host deficiency in ephrin-A1 inhibits breast cancer metastasis

The work presented in this chapter is published with the same title in *Faculty 1000 Research*, March 2020[144]

Abstract

The conventional dogma of treating cancer by focusing on the elimination of tumor cells has been recently refined to include consideration of the tumor microenvironment, which includes host stromal cells. Ephrin-A1, a cell surface protein involved in adhesion and migration, has been shown to be tumor suppressive in the context of the cancer cell. However, its role in the host has not been fully investigated. Here, we examine how ephrin-A1 host deficiency affects cancer growth and metastasis in a murine model of breast cancer. 4T1 cells were orthotopically implanted into the mammary fat pads or injected into the tail veins of ephrin-A1 wild-type (*Efna1*$^{+/+}$), heterozygous (*Efna1*$^{+/-}$), or knockout (*Efna1*$^{-/-}$) mice. Tumor growth, lung metastasis, and tumor recurrence after surgical resection were measured. Flow cytometry and immunohistochemistry (IHC) were used to analyze various cell populations in primary tumors and tumor-bearing lungs. While primary tumor growth did not differ between *Efna1*$^{+/+}$, *Efna1*$^{+/-}$, and *Efna1*$^{-/-}$ mice, lung metastasis and primary tumor recurrence were significantly decreased in knockout mice. *Efna1*$^{-/-}$ mice had reduced lung colonization of 4T1 cells compared to *Efna1*$^{+/+}$ littermate controls as early as 24 hours after tail vein injection. Furthermore, established lung lesions in *Efna1*$^{-/-}$ mice had reduced proliferation compared to those in *Efna1*$^{+/+}$ controls. Our studies demonstrate that host deficiency of ephrin-A1 does not impact primary tumor growth but does affect metastasis by providing a less favorable metastatic niche for cancer cell colonization and growth. Elucidating the mechanisms by which host ephrin-A1 impacts cancer relapse and metastasis may shed new light on novel therapeutic strategies.

Introduction

Over the past several decades, the conventional dogma of treating cancer by focusing on the elimination of rapidly dividing tumor cells has been gradually refined to include consideration of the environment in which the tumor thrives – the tumor microenvironment. The tumor microenvironment consists of both cancer cells and host stromal cells, such as endothelial cells, immune populations, and fibroblasts. Prominent discoveries regarding tumor-associated endothelium and immune cells have notably led to breakthrough therapeutic strategies with anti-angiogenic agents and immunotherapies, respectively[145–148]. Thus, understanding the host-tumor interactions involved in tumor growth and metastasis is critical for the development and application of new anti-cancer therapies.

As a result of new advancements in targeted and immunotherapies, the majority of patients with early stage disease have a very favorable prognosis. However, patients who later develop distant metastasis or who are diagnosed with disseminated disease at the onset are typically very difficult to treat effectively[14,16]. This is largely because our knowledge of how cancer cells spread is still limited. Cancer metastasis is a dynamic and complex process that requires tumor cells to undergo many steps, including adopting invasive properties, intravasating into proximal vasculature, surviving in circulation, evading immunosurveillance, extravasating from distant vasculature, and finally adapting to selective pressures of a new environment[17,18]. Each of these steps involves multiple interactions between cancer cells and different types of host stromal cells. As an example, breast cancer most commonly metastasizes to the lung, bone, liver, and brain, but how and why these cells travel and colonize these particular organs is still unknown[14,16]. A better understanding of how breast cancer metastasizes to these distant sites is greatly needed in order to develop more effective therapies and prevent spread of malignant disease.

Ephrin-A1 is a cell surface protein that regulates cell adhesion and migration[75,88,154–163,119,141,142,149–153], and its role in cancer has recently been investigated in several different solid tumors[164–170]. It belongs to the group of ephrin ligands that interact with the largest family of receptor tyrosine kinases (RTKs), the Eph receptors, and regulates various developmental processes, such as embryonic cardiovascular development and angiogenic remodeling[20,33,57]. It is expressed in various cell types, including epithelial, endothelial, and immune cells and is the primary ligand for EphA2 RTK, which has been implicated in cancer growth and metastasis in various solid tumors[20,23,24,33,57,171]. While ephrin-A1 expression in cancer cells has been shown to be tumor suppressive[75,78,154,172], its role in the host, has not been fully investigated. Here, we use ephrin-A1 knockout mice to examine how ephrin-A1 host deficiency affects cancer growth and

metastasis in a murine model of breast cancer.

To test the impact of ephrin-A1 host deficiency on cancer progression, we utilized an orthotopic 4T1 mammary tumor model, as well as two different models of metastasis. While primary tumor growth did not significantly differ between ephrin-A1 wild-type (*Efna1*$^{+/+}$), heterozygous (*Efna1*$^{+/-}$), and knockout (*Efna1*$^{-/-}$) mice, metastasis and primary tumor recurrence were significantly decreased in *Efna1*$^{-/-}$ mice. Results of analysis on tumor-infiltrating immune cell populations and vascularity in the primary tumor did not evidently explain the differences in metastasis between *Efna1*$^{+/+}$ and *Efna1*$^{-/-}$ mice. However, tumor cell lung colonization was reduced in *Efna1*$^{-/-}$ mice, and lung metastases in *Efna1*$^{-/-}$ mice were less proliferative than in their wild-type counterparts, suggesting that the metastatic niche in *Efna1*$^{-/-}$ mice is less hospitable for invading tumor cells. Together, our studies suggest that host deficiency of ephrin-A1 does not impact initial tumor growth but does affect metastasis through inhibiting cancer cell extravasation and proliferation at the metastatic niche.

Materials and Methods

Animal models

Animals were housed in a non-barrier animal facility under pathogen-free conditions, 12-hour light/dark cycle, and access to standard rodent diet and water *ad libitum*. Experiments were performed in accordance with AAALAC guidelines and with Vanderbilt University Medical Center Institutional Animal Care and Use Committee approval. All mice used in this study were immunocompetent BALB/c mice. Ephrin-A1 knockout (*Efna1*$^{-/-}$) mice were previously characterized by our lab[173]. To generate littermate controls, wild-type BALB/c mice were purchased from Jackson Laboratory and mated with *Efna1*$^{-/-}$ mice to generate heterozygote mating pairs. *Efna1*$^{+/+}$, *Efna1*$^{+/-}$ and *Efna1*$^{-/-}$ animals were identified by PCR analysis of genomic DNA using the following primers: Forward primer (5'-TGGTTATATCCCCCCACCTCACAC-3') and two allele-specific reverse primers (WT 5'-AAGGACTCCCATATCTCAGCGACG-3') and (KO 5'-AGACTGCCTTGGGAAAAGCG-3'). Mice were co-housed with one to four littermates for at least two weeks prior to and during all experiments and compared with littermate controls whenever possible. All mice used for tumor experiments were six to ten weeks old at the onset on the experiment. Experimental cohorts were limited to litters that were born within two consecutive weeks and that also had at least one *Efna1*$^{-/-}$ and *Efna1*$^{+/+}$ female littermate pair and, when applicable, at least one *Efna1*$^{+/-}$ female littermate. Sample sizes are as shown in the figures and range from three to twelve mice per group. At experimental endpoints, mice were

euthanized by cervical dislocation.

Cell culture

4T1 murine mammary adenocarcinoma cells were purchased from ATCC and maintained in DMEM (Corning #MT10013CV) supplemented with penicillin/streptomycin (Gibco #15140163) and 10% FBS (Gibco #A3160502). 4T1-GFP-luciferase clones were generated by serial dilutions of 4T1 cells with lentiviral overexpression of GFP and luciferase genes.

Tumor models

To reflect human breast cancer, only female mice were used for tumor experiments. For orthotopic mammary tumor implantations, $1x10^5$ 4T1 cells suspended in a 1:1 mixture of PBS and Growth Factor-Reduced Matrigel (Corning #354230) in a total volume of 100 µl were injected through the nipple into the fourth mammary fat pads of six to eight-week-old female mice. Tumor dimensions were measured by digital caliper at given time points every other day, and volume was calculated using the following formula: volume = length x $width^2$ x 0.52. To observe spontaneous lung metastases and primary tumor recurrence, mammary tumors were resected at day 14 post-implantation, along with draining inguinal lymph nodes and surrounding fat pads, and mice were ultimately sacrificed at day 32. At the time of surgical resection of primary tumors on day 14, tumors were weighed and cut in half to provide tissue for both flow cytometry analysis and cryosection staining. At the experimental endpoint on day 32, tumors were weighed, and lung metastases were counted in a blinded manner. For lung colonization experiments, 4T1-GFP-luciferase cells suspended in PBS were injected via tail vein, and mice underwent *in vivo* bioluminescence imaging with a PerkinElmer IVIS Spectrum several hours post-injection to verify successful and equal delivery of 4T1 cells. To observe gradual formation of GFP+ metastases, $1x10^5$ 4T1-GFP-luciferase cells were injected via tail vein, and mice were sacrificed at day 17. GFP+ lung metastases were counted in a blinded manner. The left lung lobe of each mouse was fixed in 10% formalin for subsequent formalin-fixed paraffin-embedded (FFPE) processing, sectioning, and H&E staining, while the other lung lobes were processed for flow cytometry analysis. To observe early colonization and proliferation of 4T1 cells, $5x10^5$ 4T1-GFP-luciferase cells labeled with CellTrace Violet dye (Invitrogen #C34571) were injected via tail vein. At 24 hours, mice were sacrificed, and lungs were perfused with PBS and processed for flow cytometry analysis.

Immunohistochemistry (IHC) and Immunofluorescence (IF)

FFPE lung sections were prepared and stained for PCNA (1:100, BD Biosciences #555567 raised in mouse, RRID: AB_395947) as described previously[174]. Slides were blinded, and the number of metastatic foci per section of lobe was quantified. Nuclear PCNA staining was analyzed using ImageJ v1.52o with the IHC Profiler plugin[175] and percentage of PCNA+ tumor cell nuclei were quantified. Each data point is an average of two sections of the left lung from an individual mouse. To prepare cryosections, mammary tumors were frozen in OCT Compound (Thermo Fisher Scientific #23-730-571) on dry ice and stored at -80°C. Sections (8 µm) were cut on a Leica Cryostat CM1950, fixed in 4% PFA, washed with PBS, permeabilized with 0.3% Triton X-100 (Sigma-Aldrich #X100), and blocked using M.O.M. Mouse Ig Blocking Reagent and Protein Concentrate (Vector Laboratories #PK-2200) per manufacturer recommendations and with 2.5% goat serum (Sigma-Aldrich #G9023) in PBS. Slides were then incubated over two nights at 4°C with primary antibodies against CD31 (1:150, Biolegend #102501 raised in rat, RRID: AB_312908) and αSMA (1:150, Dako #M085129-2 raised in mouse, RRID: AB_2811108) in blocking buffer. After washing with PBS, slides were incubated for one hour at room temperature in secondary antibodies goat anti-rat Ax594 (1:500, Invitrogen #A11007, RRID: AB_10561522) and anti-mouse Ax488 (1:500, Invitrogen #A11001, RRID: AB_2534069), washed with PBS, and mounted with ProLong Gold Antifade Mountant with DAPI (Invitrogen #P36931). Slides were blinded, and images were taken by an Olympus DP72 camera through a BX60 inverted fluorescence microscope and processed using CellSens Dimension software. A total of 12-40 20x fields of view were analyzed from each section using ImageJ. For αSMA analysis, images were evaluated for colocalization with CD31 staining, and data was displayed as a percentage of αSMA+ out of CD31+ area or integrated intensity. Each data point is an average of all fields of view of two to three tumor sections from an individual mouse.

Flow cytometry

Tumors and lungs were minced and dissociated in RPMI-1640 media (Corning #MT10040CV) containing 2.5% FBS, 1 mg/ml collagenase IA (Sigma-Aldrich #C9891), and 0.25 mg/ml DNase I (Sigma-Aldrich #DN25) for 45 minutes at 37°C. Digested tissue was then filtered through a 70-µm strainer, and red blood cells were lysed using ACK Lysis Buffer (KD Medical #RGF-3015). Samples were washed with PBS and stained with Ghost Dye Violet V510 (Tonbo Biosciences #13-0870) to exclude dead cells. After washing with buffer (0.5% BSA, 2mM EDTA in PBS), samples were blocked in αCD16/32 mouse Fc block (Tonbo Biosciences #70-0161)

Table 3.1. Antibodies used in flow cytometry analysis

Antibody target	Manufacturer	Catalog #	Fluorophore	Dilution	RRID
MHCII I-E/A	Tonbo Biosciences	75-5321	V450	1/250	AB_2621965
CD8a	BD Biosciences	560469	V450	1/250	AB_1645281
CD11b	Tonbo Biosciences	35-0112	FITC	1/250	AB_2621676
CD62L	Tonbo Biosciences	35-0621	FITC	1/100	AB_2621697
CD44	Tonbo Biosciences	50-0441	PE	1/5000	AB_2621762
CTLA-4	BD Biosciences	561718	PE	1/250	AB_10895585
CD31	BD Biosciences	561073	PE	1/750	AB_10563931
CD4	Biolegend	100516	APC	1/1000	AB_312719
Ly6C	BD Biosciences	560595	APC	1/500	AB_1727554
FoxP3	eBiosciences	50-5773-82	e660	1/100	AB_11218868
F4/80	eBiosciences	45-4801-82	PerCP-Cy5.5	1/250	AB_914345
CD3e	Tonbo Biosciences	65-0031	PerCP-Cy5.5	1/250	AB_2621872
Ly6G (Gr1)	Tonbo Biosciences	80-5931	rF710	1/1000	AB_2621999
CD8a	Tonbo Biosciences	80-0081	rF710	1/500	AB_2621977
PD-1	BD Biosciences	565815	APC-R700	1/500	AB_2739366
CD45	Biolegend	103109	PE-Cy5	1/5000	AB_312974
CD4	Tonbo Biosciences	55-0041	PE-Cy5	1/2500	AB_2621816
CD69	BD Biosciences	552879	PE-Cy5	1/1000	AB_394508
CD11b	Tonbo Biosciences	55-0112	PE-Cy5	1/5000	AB_2621818
EpCAM	Biolegend	118215	PE-Cy7	1/750	AB_1236477
CD11c	BD Biosciences	561022	PE-Cy7	1/500	AB_2033997
Ly6C	eBiosciences	25-5932-80	PE-Cy7	1/1000	AB_2573502
CD25	Tonbo Biosciences	60-0251	PE-Cy7	1/500	AB_2621843
CD11c	Biolegend	117323	APC-Cy7	1/500	AB_830646
CD45	BD Biosciences	557659	APC-Cy7	1/500	AB_396774

Table 3.2. Gating strategy used in flow cytometry analysis

Cell population	Gating strategy
CD8 T cells	CD45+,CD3e+,CD4-,CD8a+
CD4 T cells	CD45+,CD3e+,CD4+,CD8a-
Tregs	CD45+,CD3e+,CD4+,CD8a-,CD25+,FoxP3+
Monocytes	CD45+,CD11b+,Ly6G-,Ly6C+,F4/80-
Macrophages	CD45+,CD11b+,Ly6G-,Ly6C-,F4/80+
Granulocytes	CD45+,CD11b+,Ly6G+,Ly6C-/+,F4/80-
Dendritic cells	CD45+,CD11c+,MHCII+,F4/80-
Endothelial cells	CD45-,GFP-,EpCAM-,CD31+

and stained for extracellular proteins using an antibody master mix made in buffer. After washing with buffer, cells were fixed with 2% PFA. For FoxP3 intracellular staining, cells were permeabilized using the FoxP3 Transcription Factor Staining Kit (Tonbo Biosciences #TNB-0607-KIT) per manufacturer protocol. Flow cytometry data was obtained on a BD 4-laser Fortessa using BD FACS Diva software v8.0.1 and analyzed using FlowJo software v10.6.1. Fluorescence minus one (FMO) samples were used as gating controls when needed. Antibodies used in flow panels are detailed in Table 3.1, and gating strategies used in analysis are detailed in Table 3.2. Each data point is generated after analyzing at least $5x10^5$ viable cells from a specimen from an individual mouse.

Statistical analysis

All graphs and statistical analysis were completed using GraphPad Prism software v6.07. For comparisons between two groups, an unpaired Mann-Whitney *U*-test was performed. For comparisons between three groups, a Kruskal-Wallis *H*-test was performed, followed by post-hoc Mann-Whitney *U*-tests evaluating differences between the knockout and either the wild-type or heterozygote animals. A *P*-value less than 0.05 was considered statistically significant.

Results

Ephrin-A1-deficient hosts have reduced metastasis *in vivo*

We initially investigated the impact of ephrin-A1 host deficiency on primary tumor growth by implanting 4T1 cells in a mixture of PBS and Matrigel orthotopically into the mammary fat pads of syngeneic BALB/c female *Efna1*$^{+/+}$ and *Efna1*$^{-/-}$ mice. No difference in primary tumor growth or weight at 21 days post-implantation was observed (Figure 3.1A). To test the impact of ephrin-A1 host deficiency on spontaneous metastasis, 4T1 cells were implanted orthotopically as described above and surgically resected on day 14 post-implantation to allow for gradual development of endogenous metastases by day 32 (Figure 3.1B). As expected, primary tumors resected from *Efna1*$^{+/+}$ and *Efna1*$^{-/-}$ mice were not different in size (Figure 3.1C), and this was additionally verified with *Efna1*$^{+/+}$, *Efna1*$^{+/-}$, and *Efna1*$^{-/-}$ littermates (Figure 3.1D). However, at the experimental endpoint, the number of visible lung metastases and lung weights were significantly decreased in knockout mice (Figure 3.1E). Many of these mice not only harbored lung metastases but also tumors that had regrown at the original site of the resected primary tumor. Similar to our findings in lung metastases, the size of recurrent primary tumors was

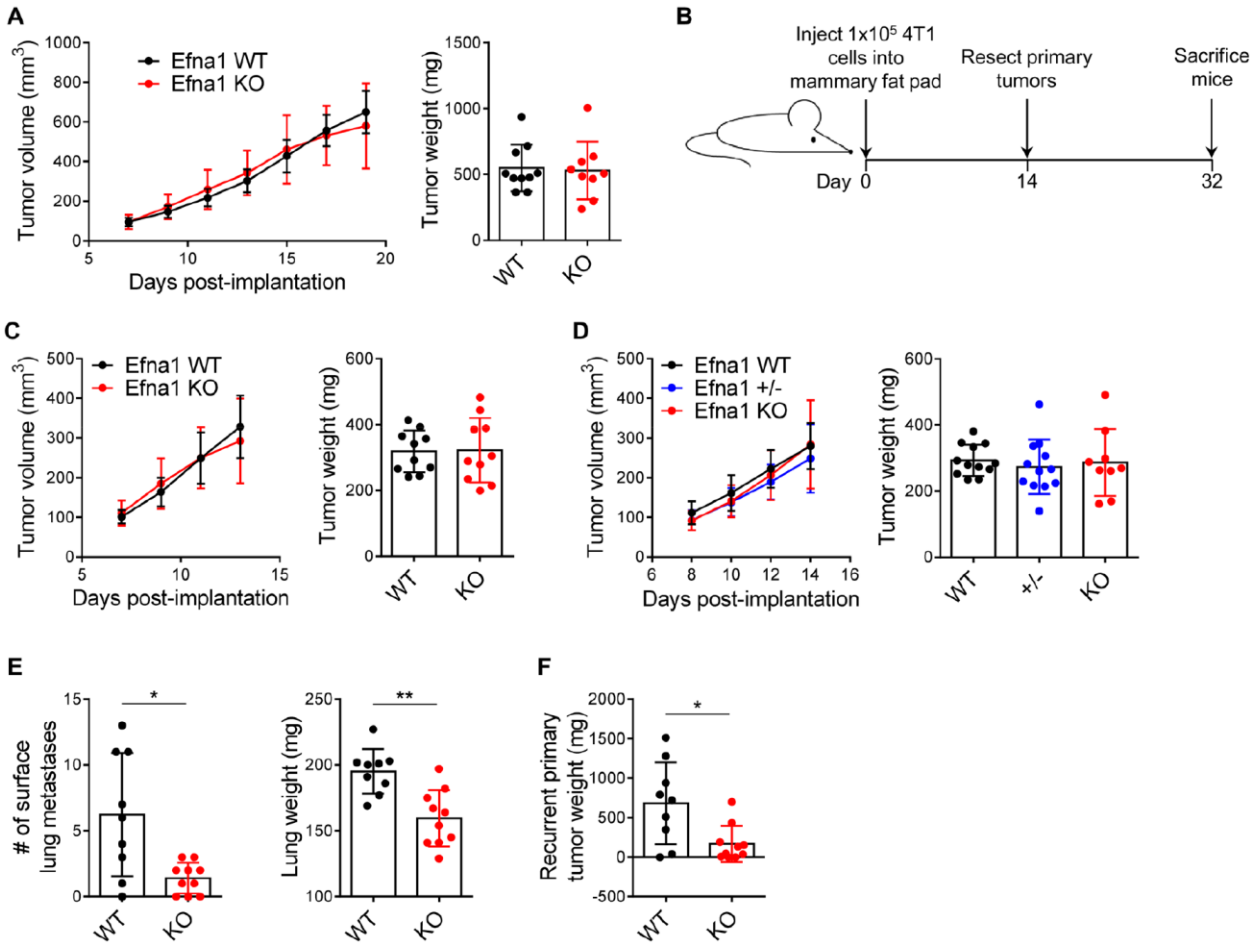

Figure 3.1. Ephrin-A1-deficient hosts have reduced metastasis and tumor recurrence but no difference in primary tumor growth. (A) 4T1 primary tumor growth curves in age-matched female *Efna1*$^{+/+}$ (WT) and *Efna1*$^{-/-}$ (KO) mice and resulting tumor weights at day 21 post-implantation. (B) Schematic diagram showing experimental procedure for evaluating spontaneous metastases. (C) 4T1 primary tumor growth curves in WT and KO mice and resultant tumor weights at time of surgical resection on day 14. (D) 4T1 primary tumor growth curves in WT, heterozygous (+/-) and KO littermates and resultant tumor weights at time of surgical resection on day 14. (E) Blinded quantification of visible lung metastases and lung weights from WT and KO mice at experimental endpoint on day 32. (F) Weights of recurrent 4T1 tumor at primary site 18 days after surgical resection. Data shown are averages ± SD with each data point representing an individual mouse (n=9-12 mice per group). *p<0.05, **p<0.01 (unpaired Mann-Whitney U-test).

significantly reduced in knockout mice (Figure 3.1F). Together, these results demonstrate that while host deficiency in ephrin-A1 may not affect initial tumor growth, it can impact metastatic spread and recurrence.

To complement our findings in our model of spontaneous metastasis, we evaluated the impact of ephrin-A1 host deficiency on experimental metastasis. 4T1 cells engineered to express GFP and luciferase (4T1-GFP-luciferase) were injected into the tail veins of *Efna1*$^{+/+}$, *Efna1*$^{+/-}$, and *Efna1*$^{-/-}$ littermates. *In vivo* bioluminescence imaging several hours after injection

illustrated comparable signal across all mice (Figure 3.2AB), indicating ephrin-A1 host deficiency did not impact tumor cell trafficking and lodging within the lung, at least in this short time frame. After harvesting the lungs 17 days later, we observed decreased GFP+ metastases in *Efna1*$^{-/-}$ mice, compared to both *Efna1*$^{+/+}$ and *Efna1*$^{+/-}$ littermates, which was additionally confirmed by flow cytometry (Figure 3.2C, D). Similarly, histological analysis revealed fewer metastatic foci in lungs from *Efna1*$^{-/-}$ mice (Figure 3.2E). These data align with our previous

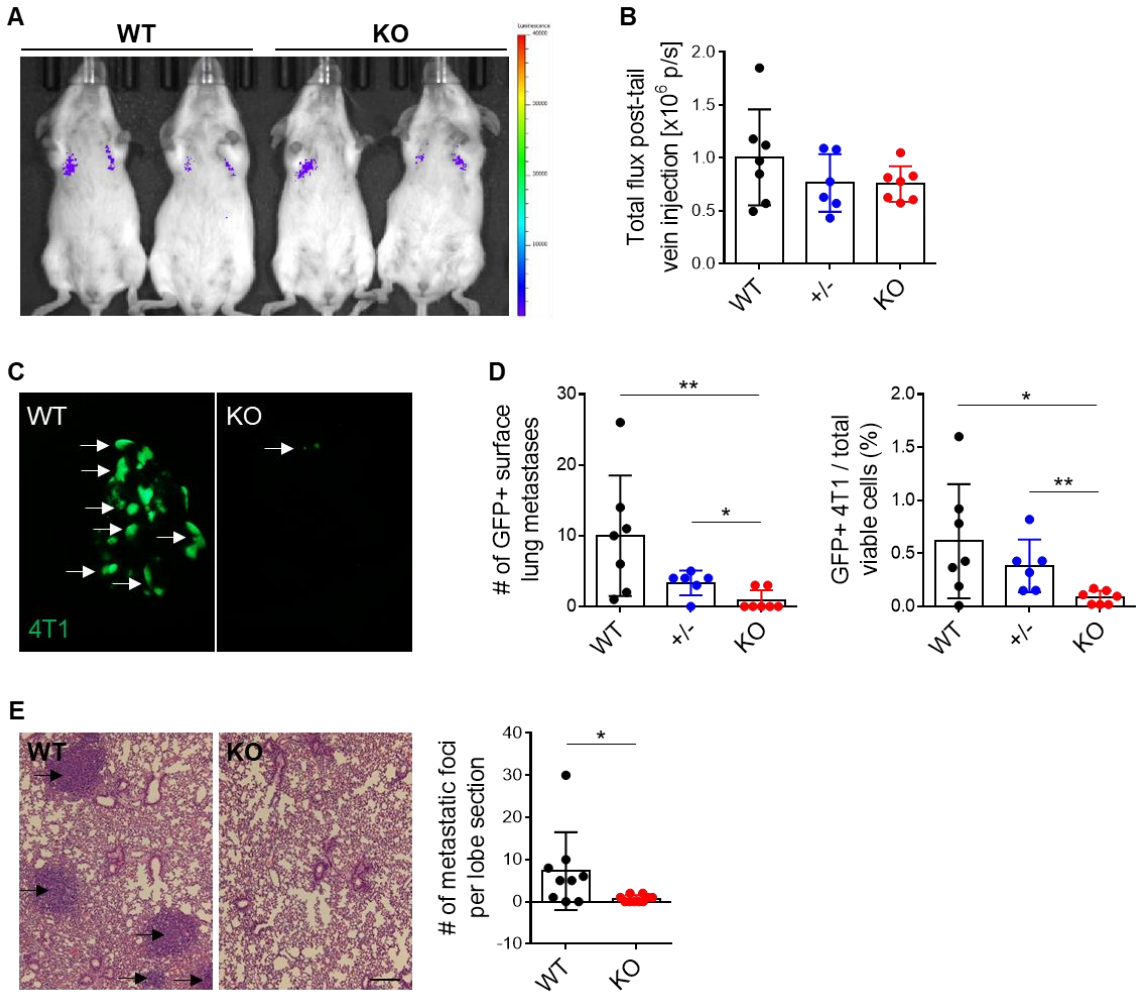

Figure 3.2. Ephrin-A1-deficient hosts have reduced cancer cell lung colonization. (A) Representative image of bioluminescence signal in WT and KO littermates several hours after tail vein injection of 1x10^5 4T1-GFP-luciferase cells. (B) Quantification of bioluminescence signal in WT, +/-, and KO littermates. (C) Representative images of GFP+ surface lung metastases in WT and KO littermates 17 days after tail vein injection. (D) Blinded quantification of GFP+ lung metastases in WT, +/-, and KO littermates and percentages of GFP+ 4T1 cells in the lung from flow cytometry analysis. (E) Representative H&E staining of left lung lobes from WT and KO littermates and blinded quantification of metastatic foci per lung section. Scale bar: 200 µm. Data shown are averages ± SD with each data point representing an individual mouse (n=4-9 mice per group). *p<0.05, **p<0.01 (unpaired Mann-Whitney U-test for comparisons between two groups, Kruskal-Wallis H-test with post-hoc unpaired Mann-Whitney U-test for comparisons between three groups).

observations on endogenous metastasis and suggest that host deficiency in ephrin-A1 inhibits circulating cancer cells from colonizing the lung.

Tumor-infiltrating immune populations are not significantly different in ephrin-A1-deficient hosts

Ephrin-A1 is expressed in several types of host cells, including immune cells and endothelial cells[23,24,171]. Thus, we sought to determine how the ephrin-A1-deficient host immune system and endothelium may mitigate metastasis. Among immune cells, ephrin-A1 can be expressed in B and T cells, monocytes, and macrophages[23]. The role of ephrin-A1 in B cells is largely unknown[176]. However, in T cells, monocytes, and macrophages, ephrin-A1 has been shown to regulate cell adhesion and migration[117,118,141,142,155,156,177,178]. These immune cell populations play a critical role in overall anti-tumor immunity and immunosurveillance. Dendritic cells (DCs) and T cells, particularly CD8 cytotoxic T cells, are the primary drivers of the adaptive anti-tumor response in solid tumors and increased infiltration of these cell types is correlated with better prognosis and enhanced response to immunotherapies[101,179]. Conversely, regulatory T cells (Tregs) suppress effector functions of T cells and typically inhibit the anti-tumor response[103,131]. Between the two ends of this spectrum, myeloid populations, such as monocytes, macrophages, and granulocytes, can either promote or suppress an anti-tumor response, depending on their polarization and functionality[102,180].

Because of ephrin-A1's known role in adhesion and chemotaxis of immune cells, we performed flow cytometry analysis on 4T1 primary tumors harvested from *Efna1*$^{+/+}$, *Efna1*$^{+/-}$, and *Efna*$^{-/-}$ littermates. To our surprise, we found no significant differences in total infiltrating immune cells, CD4 or CD8 T cells, DCs, Tregs, or myeloid populations in *Efna1*$^{+/+}$, *Efna1*$^{+/-}$, and *Efna*$^{-/-}$ littermates (Figure 3.3A, B). DCs were decreased in *Efna*$^{-/-}$ mice, though not significantly with these sample sizes. While there were no apparent differences in the immune microenvironment of the mammary tumors, the immune microenvironment of the lung is distinct from that of the mammary gland and may impact the metastatic niche. To investigate this, we performed flow cytometry analysis on 4T1 tumor-bearing lungs generated from our model of experimental metastasis. Similar to the results we obtained from the 4T1 primary tumors, we did not see significant differences in immune populations in tumor-bearing lungs harvested from *Efna1*$^{+/+}$, *Efna1*$^{+/-}$, and *Efna1*$^{-/-}$ littermates, except for a modest increase in macrophages in knockout mice (Figure 3.3C, D).

Although the percentage of tumor infiltrating T cells in *Efna1*$^{+/+}$ and *Efna1*$^{-/-}$ mice is comparable, their activation status and effector function may still be different. Tumor-infiltrating

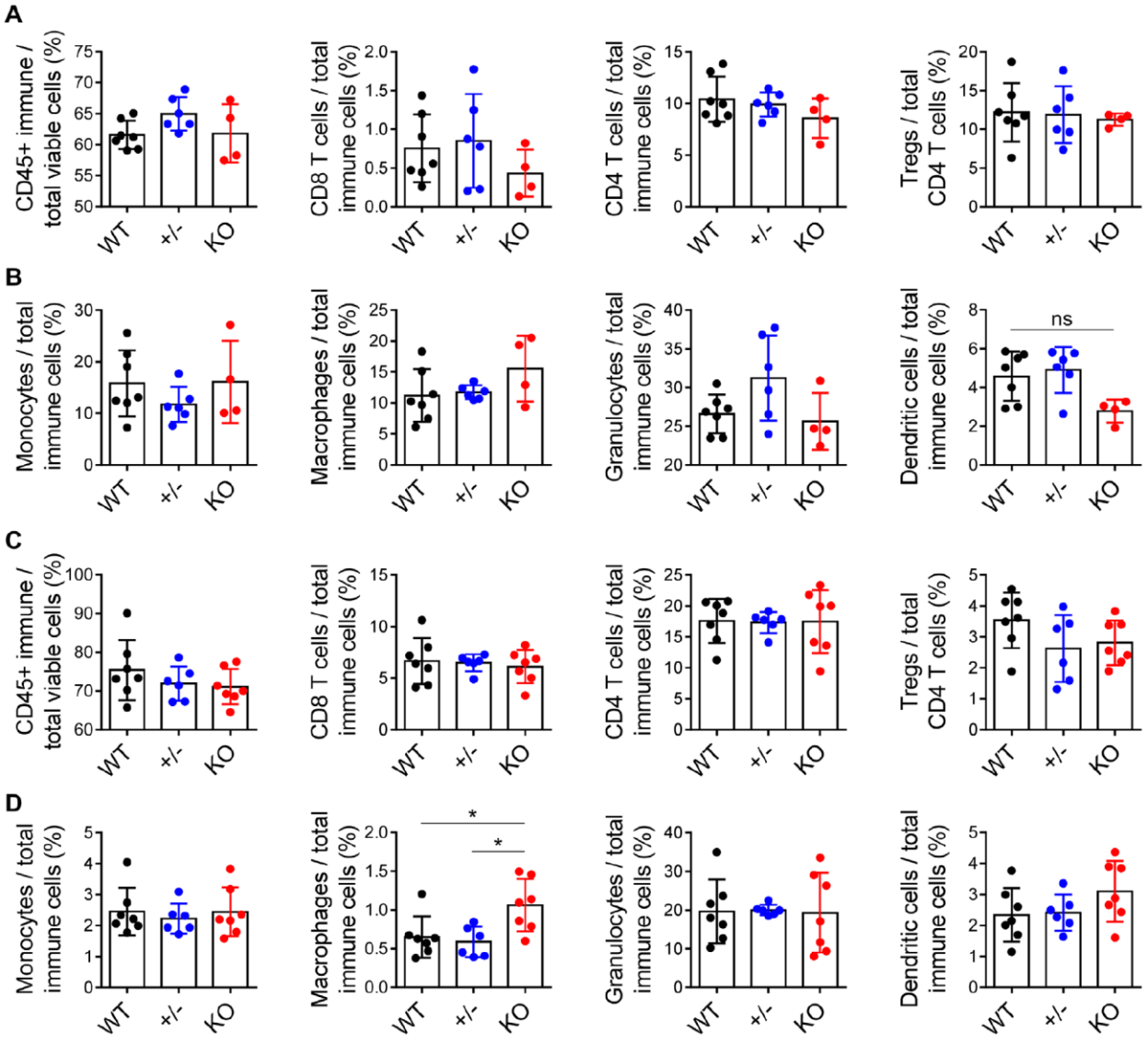

Figure 3.3. Tumor-infiltrating immune populations are not significantly different in ephrin-A1-deficient hosts. (A) Flow cytometric analysis of total immune cells, T cells, and T regulatory (Treg) cells, as well as (B) monocytes, macrophages, granulocytes, and dendritic cells, in 4T1 primary tumors resected from WT, +/-, and KO littermates at day 14 post-implantation. (C, D) Similar analyses of immune populations in tumor-bearing lungs harvested from WT, +/-, and KO littermates 17 days after tail vein injection of 4T1-GFP-luciferase cells. Data shown are averages ± SD with each data point representing an individual mouse (n=3-7 mice per group). *p<0.05 (Kruskal-Wallis H-test with post-hoc unpaired Mann-Whitney U-test).

T cells with upregulated expression of activation markers, such as CD44, CD69, and CD25, and downregulated expression of antigen-naïve markers like CD62L and exhaustion markers like PD-1 and CTLA-4 indicate a higher T cell functional status that mediates a stronger and more enduring anti-tumor response[103,131]. We assessed these markers on T cells in 4T1 primary tumors and tumor-bearing lungs from *Efna1*$^{+/+}$ and *Efna1*$^{-/-}$ littermates using flow cytometry.

However, we did not observe consistent increases in activation or decreases in naïve or exhaustion markers in knockout-derived T cells (data not shown, included in *Underlying data*). In summary, host deficiency in ephrin-A1 does not significantly affect tumor-infiltrating immune cells in both primary tumors and tumor-bearing lungs. Thus, the reduction of lung metastases in *Efna1*$^{-/-}$ hosts *in vivo* is unlikely due to host immunity.

Tumor vascularity and pericyte coverage are not significantly different in ephrin-A1-deficient hosts

In addition to the anti-tumor immune response, another host factor that can impact metastasis is the tumor vasculature. Angiogenesis is the formation of new blood vessels from a pre-existing network and is required for solid tumor growth and progression. Blood vessels can supply nutrients that support tumor growth and provide an entry for hematological dissemination and invasion[145,181]. These new blood vessels are typically hastily constructed in response to the high release of growth factors, such as vascular endothelial growth factor (VEGF), from tumor cells[82,83]. Thus, tumor vessels tend to be disorganized, leaky, and poorly covered by pericytes, which normally support the integrity of the endothelium. Ephrin-A1 is expressed in the vascular endothelium and has been shown to promote angiogenesis *in vitro* and in several *in vivo* models[87,90,95–97,182]. Therefore, we hypothesized that tumors in *Efna1*$^{-/-}$ mice may have reduced tumor vasculature and increased endothelial pericyte coverage compared to *Efna1*$^{+/+}$ controls.

To evaluate tumor vascularity and vessel function, we co-stained cryosections of 4T1 primary tumors from *Efna1*$^{+/+}$ and *Efna1*$^{-/-}$ littermates with CD31 and αSMA, markers for endothelial cells and pericytes, respectively. Colocalization of αSMA with CD31 acts as an indicator for functional endothelium within tumors. Surprisingly, we did not observe a change in CD31+ area or intensity in 4T1 tumors from *Efna1*$^{+/+}$ and *Efna1*$^{-/-}$ littermates (Figure 3.4A, B). Furthermore, pericyte coverage on tumor vessels remained the same in tumors from *Efna1*$^{+/+}$ and *Efna1*$^{-/-}$ littermates (Figure 3.4A, C). Together, these data suggest that loss of ephrin-A1 in the host does not affect tumor vessel formation and function in the primary tumor.

Ephrin-A1-deficient lung microenvironment provides a less favorable metastatic niche

Our results from analysis of the immune infiltrate and vasculature of primary tumors, coupled with the significant difference in experimental lung metastasis between *Efna1*$^{+/+}$ and *Efna1*$^{-/-}$ mice, suggest that host factors critical to this metastatic phenotype are more likely to lie downstream of the primary tumor site. These steps include tumor cell trafficking to the lung vasculature, extravasation, and adaptation to new selective pressures of the lung

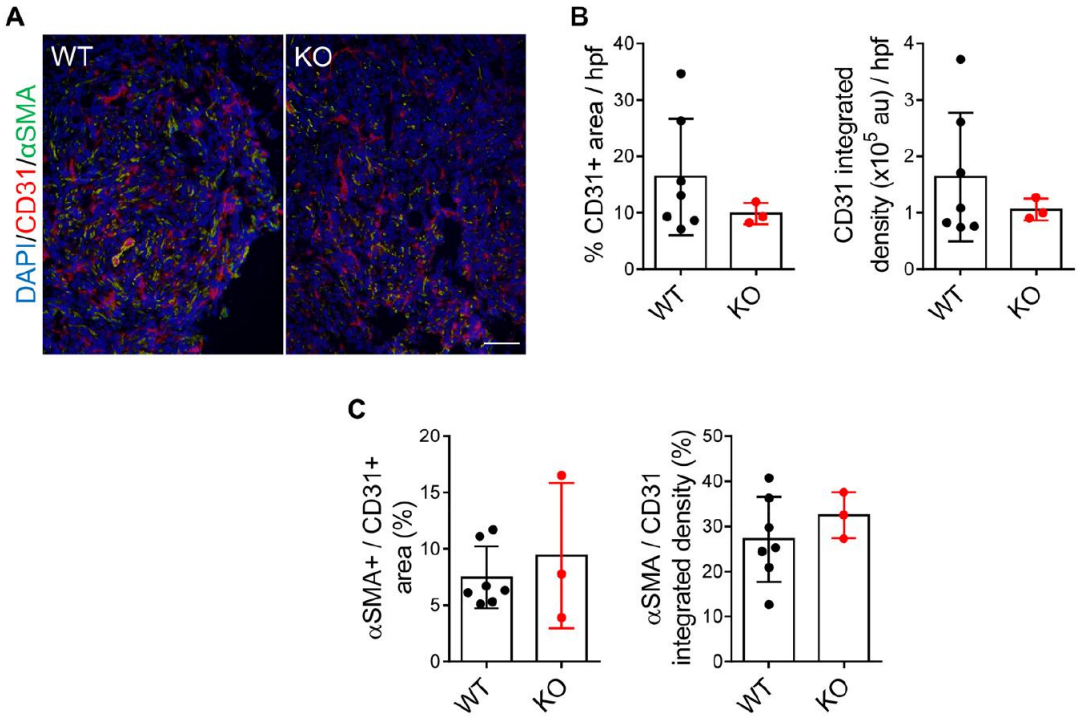

Figure 3.4. Tumor vascularity and pericyte coverage are not significantly different in ephrin-A1-deficient hosts. (A) Representative images of CD31 (red), αSMA (green), and DAPI (blue) staining on cryosections of 4T1 primary tumors harvested from WT and KO littermates at day 14 post-implantation. Scale bar: 100 μm. (B) Quantification of CD31+ area and integrated intensity in arbitrary units (au) per high power field (hpf) of view. (C) Quantification of αSMA colocalization with CD31 as a percentage of αSMA+ over CD31+ stained area and integrated density. Data shown are averages ± SD with each data point representing an individual mouse (*n*=3-7 mice per group).

microenvironment. 4T1 cell trafficking to the lung was not significantly different between *Efna1*$^{+/+}$ and *Efna1*$^{-/-}$ littermates after tail vein injections (Figure 3.2A, B). Thus, we aimed to evaluate extravasation and adaptation to the lung metastatic niche in *Efna1*$^{+/+}$ and *Efna1*$^{-/-}$ hosts.

To test extravasation of 4T1 cells *in vivo*, we injected 4T1-GFP-luciferase cells labeled with CellTrace Violet dye into the tail veins of *Efna1*$^{+/+}$ and *Efna1*$^{-/-}$ littermates. This dye is retained only in the labeled tumor cells and diminished after subsequent cell divisions, enabling quantification of short-term cell proliferation. At 24 hours after injection, we perfused the lungs with PBS to flush out remaining cells in the pulmonary vasculature and processed the lungs for flow cytometry. Decreased GFP+ 4T1 cells were found in ephrin-A1-deficient lungs compared to wild-type controls (Figure 3.5A), suggesting that fewer cancer cells had extravasated into the lung parenchyma at this timepoint. This result may be partly due to decreased vascularity of ephrin-A1-deficient lungs at baseline. The percentage of CD31+ endothelial cells was slightly lower in knockout lungs but not significantly so with this sample size (Figure 3.5B). Moreover, this was not due to decreased proliferation of the 4T1 cells within the 24-hour timeframe, as the

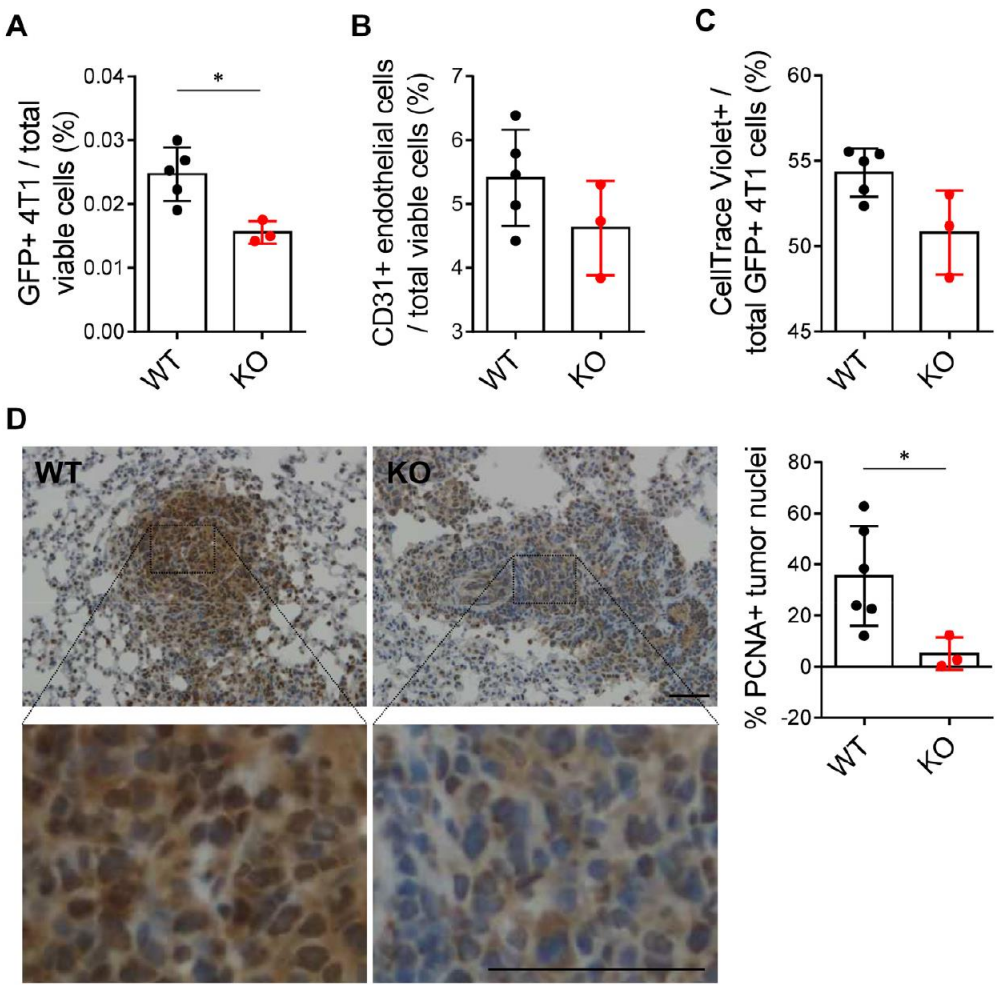

Figure 3.5. Ephrin-A1-deficient lung microenvironment provides a less favorable metastatic niche. (A) Quantification of GFP+ 4T1 cells and (B) CD31+ endothelial cells by flow cytometry in perfused lungs harvested from WT and KO littermates 24 hours post-tail vein injection. (C) Percentage of GFP+ 4T1 cells in perfused WT and KO lungs that still contained CellTrace Violet dye, indicating reduced proliferation. (D) Representative images of PCNA staining on FFPE sections of tumor-bearing lungs from WT and KO littermates 17 days after tail vein injection of 4T1-GFP-luciferase cells. Higher magnification images and blinded quantification of PCNA+ tumor cell nuclei shown. Scale bar: 50 µm. Data shown are averages ± SD with each data point representing an individual mouse (n=3-6 mice per group). *p<0.05 (unpaired Mann-Whitney U-test).

amount of retained CellTrace Violet dye was not higher in 4T1 cells that had extravasated in knockout lungs compared to wild-type lungs (Figure 3.5C). Together, these data suggest that extravasation of 4T1 cells is inhibited in knockout mice, compared to wild-type controls, and ephrin-A1 deficiency in the host lung may play a role in this process.

While decreased extravasation of tumor cells may explain in part the decreased lung metastases in *Efna1*$^{-/-}$ mice, another possibility is that once tumor cells have extravasated and established in the lung, they have reduced fitness of survival in ephrin-A1-deficient lungs, compared to wild-type lungs. There are many stressors in the lung metastatic niche that could

impact the adaptability of the tumor cell. We used tumor proliferation index as a marker to evaluate how well tumor cells have adapted to a metastatic niche. Since no differences were observed in proliferation of 4T1 cells that had newly extravasated into the lung parenchyma of *Efna1*$^{+/+}$ and *Efna1*$^{-/-}$ littermates within the short 24-hour timeframe (Figure 3.5C), we next assessed proliferation of tumor cells in lung micrometastases that had established over 17 days after tail vein injection (Figure 3.2). There was a significant decrease in cell proliferation in metastatic foci established in *Efna1*$^{-/-}$ mice, compared to *Efna1*$^{+/+}$ controls, as indicated by PCNA staining (Figure 3.5D). These findings suggest that reduced tumor cell lung colonization in *Efna1*$^{-/-}$ hosts is due to both decreased extravasation of cancer cells and decreased proliferation in the metastatic niche.

Discussion

In conclusion, host deficiency in ephrin-A1 inhibits metastasis by providing a less hospitable metastatic niche for cancer cell extravasation and colonization of the lung. Our data from 4T1 primary tumor specimens demonstrated no differences in primary tumor growth, infiltrating immune cell populations, and vascularity. This led us to investigate the metastatic process downstream from the primary tumors. We then found that lung colonization in knockout mice was decreased compared to wild-type mice as early as 24 hours post-tail vein injection of 4T1 cells, in part due to decreased extravasation. Moreover, the metastases that established in *Efna1*$^{-/-}$ lungs were not only reduced in number but also less proliferative compared to those in wild-type lungs. These studies offer insight on how host expression of ephrin-A1 may impact tumor growth and dissemination, but they also lead to additional questions.

Our ephrin-A1 knockout model is not tissue-specific nor inducible, which creates challenges in identifying specific mechanisms that contribute to our observed phenotype. For example, ephrin-A1 is highly expressed in embryonic stages of development and plays a known role in neuronal and mammary development[87,183–187]. The transcriptional and epigenetic changes that occur *in utero* and during early physiological development as a result of ephrin-A1 deficiency in various tissues may all contribute to the observed phenotype; however, dissecting which changes are directly downstream of ephrin-A1 and critical to metastasis may be quite difficult. This challenge is further augmented when we consider the many cell types that can express ephrin-A1, especially immune, endothelial, and epithelial cells. Additionally, ephrin-A1 on these cell types presumably interacts with EphA receptors on various stromal and tumor cells. In the absence of host ephrin-A1, forward signaling in these EphA receptors may be

reduced, or it may be conserved through compensatory interaction with other ephrin-A ligands. If other ephrin-A1 ligands do not compensate for the lack of ephrin-A1, perhaps EphA receptors in these cells are available fore more ligand-independent signaling. These are all reasonable hypotheses that may be supported with more molecular and biochemistry studies.

Many studies have demonstrated ephrin-A1's role in immune cell adhesion and migration. Although we did not observe significant differences in tumor immune infiltrate, this does not preclude a role for ephrin-A1 in these cell populations. Immune cells engage in a complex network of crosstalk, and it is possible that loss of ephrin-A1 in one cell type may mask the effects it has in another. One intriguing difference we observed was an increase in macrophages in *Efna1*$^{-/-}$ tumor-bearing lungs. However, we have not determined if this difference occurs in the specific context of a stressor, such as tumor metastasis, or if knockout mice have increased macrophages at baseline. Because ephrin-A1 has been shown to impact monocyte chemotaxis and adhesion to the endothelium, it is reasonable to hypothesize that ephrin-A1 may affect recruitment of monocytes from circulation into lung tissue where they differentiate into macrophages. Macrophages in the lung are known to play a role in forming the pre-metastatic niche and maintaining a metastatic niche[188]. Though we demonstrate increased macrophages in ephrin-A1-deficient lungs, it remains to be seen if these macrophages are polarized towards an anti-tumor or a pro-tumor response. Nevertheless, this offers evidence of a novel role of ephrin-A1 in macrophage recruitment, differentiation or survival, which requires further investigation.

In addition, ephrin-A1 has been shown to regulate expression of adhesion molecules on endothelial cells and promote angiogenesis. Modulation of surface expression of adhesion proteins, such as ICAM-1 and VCAM-1, on endothelial cells impact binding to immune cells and cancer cells[18,24]. Thus, it is possible that ephrin-A1 on endothelial cells may mediate cancer cell transendothelial migration through modulation of these adhesion proteins. While this result may be consistent with published literature, in contrast to ephrin-A1's known role in angiogenesis, we did not observe differences in angiogenesis between tumors from *Efna1*$^{+/+}$ and *Efna1*$^{-/-}$ hosts. This discrepancy may be due to a couple reasons. First, most studies reporting on ephrin-A1's impact on angiogenesis have shown its effect through EphA receptor signaling on the endothelial cell, not necessarily through ephrin-A1 directly in the endothelium[87,95–97]. Loss of ephrin-A1 in the endothelium and other host tissues is unlikely to completely abrogate EphA receptor signaling in the endothelium, as other ephrin ligands are able to promiscuously bind to the same EphA receptors and may even compensate for the loss of ephrin-A1[20]. Second, some of these studies use soluble ephrin-A1, instead of membrane-bound or cell-surface ephrin-A1.

In our *Efna1*$^{-/-}$ model, both cell-surface, membrane-bound ephrin-A1 and soluble, secreted ephrin-A1 are lost *in vivo*, and these two forms of ephrin-A1 have been shown to have competing effects[157].

The different forms of ephrin-A1, as well as the range of interactions with various Eph receptors, show how potentially complex the molecular mechanisms can be when considering host deficiency of ephrin-A1. A clue into this complicated investigation can be found in our data obtained with ephrin-A1 heterozygote controls. When comparing tumor metastasis and immune infiltrate, results from *Efna1*$^{+/-}$ mice were much more comparable to wild-type than knockout littermate controls. This suggests that ephrin-A1 has a genetically dominant effect – one wild-type allele may be sufficient to induce the wild-type phenotype.

Although we focused our inquiries on primary mammary tumors and lung metastases, there is much more to be explored. 4T1 cells, like human breast cancer, metastasize to other organ sites, such as the bone, liver, and brain. The lungs in *Efna1*$^{-/-}$ hosts may or may not be the only organ that provides a less favorable environment for colonizing tumor cells than those in *Efna1*$^{+/+}$ hosts. We observed differences in recurrent primary tumor, in addition to lung metastases, which may indicate that tumor cell apoptosis or senescence is altered in knockout hosts. If this is the case, one may infer that primary tumors should also be smaller in knockout mice. Although we did not observe differences in primary tumors, it is possible that the number of 4T1 cells that were injected and the amount of Matrigel used to implant these cells, though small, may have obscured these results.

While much of the published literature on ephrin-A1 focuses on its tumor suppressive role in the tumor cell, this novel study demonstrates that its role in the host tissues may be tumor-promoting. This suggests that the function of ephrin-A1 is cell-type dependent and that if there is a way to target ephrin-A1 in host tissues, rather than in the tumor, targeting host ephrin-A1 to inhibit metastasis may be a strategy worth considering. Further elucidating the mechanisms by which ephrin-A1 in host cells impact cancer relapse and metastasis may enhance our understanding of the metastatic process and ultimately shed new light on novel therapeutic strategies.

Data availability

Harvard Dataverse: Host deficiency in ephrin-A1 inhibits breast cancer metastasis; https://dataverse.harvard.edu/dataverse/hostEfna1metastasis.

This project contains the following underlying data:

Harvard Dataverse: 4T1 primary tumor dimensions and weights. https://doi.org/10.7910/DVN/AGKDWV. (4T1 primary tumor dimensions from digital caliper measurements, volume calculations, and weights (related to Figure 3.1A, C, D.)

Harvard Dataverse: 4T1 recurrent primary and spontaneous lung metastases. https://doi.org/10.7910/DVN/FU8JEY. (Spontaneous 4T1 lung metastases quantification and recurrent primary tumor weights (related to Figure 3.1E, F.)

Harvard Dataverse: Images and quantification of 4T1-GFP-luciferase spontaneous lung metastases. https://doi.org/10.7910/DVN/2ANDYX. (Experimental 4T1-GFP-luciferase lung metastases quantification and images (related to Figure 3.2C-E.))

Harvard Dataverse: 4T1-GFP-luciferase bioluminescence images and quantification post-tail vein injection. https://doi.org/10.7910/DVN/39D0YR. (4T1-GFP-luciferase bioluminescence quantification and images (related to Figure 3.2A, B).)

Harvard Dataverse: 4T1 primary tumor flow cytometry. https://doi.org/10.7910/DVN/ZRX2RG. (Flow cytometry files (fcs), gating and analysis (wsp), and panels (xlsx) containing immune profiling of 4T1 primary mammary tumors from *Efna1* $^{+/+}$, *Efna1* $^{+/-}$, and *Efna1* $^{-/-}$ littermate mice (related to Figure 3.3A, B))

Harvard Dataverse: 4T1-GFP-luciferase tumor-bearing lung flow cytometry. https://doi.org/10.7910/DVN/S06NQ1. (Flow cytometry files (fcs), gating and analysis (wsp), and panels (xlsx) containing immune profiling of 4T1-GFP-luciferase tumor-bearing lungs from *Efna1* $^{+/+}$, *Efna1* $^{+/-}$, and *Efna1* $^{-/-}$ littermate mice (related to Figure 3.2D, 3C, D).)

Harvard Dataverse: 4T1-GFP-luciferase 24-hr lung colonization flow cytometry. https://doi.org/10.7910/DVN/G7TAAE. (Flow cytometry files (fcs), gating and analysis (wsp), and panels (xlsx) containing profiling of 24-hr 4T1-GFP-luciferase tail vein injected lungs from *Efna1* $^{+/+}$ and *Efna1* $^{-/-}$ littermate mice (related to Figure 3.5A-C).)

Harvard Dataverse: CD31 and aSMA images and quantification of 4T1 primary tumors. https://doi.org/10.7910/DVN/MOYPE7. (4T1 primary tumor CD31 and αSMA staining quantification and images (related to Figure 3.4A-C).)

Harvard Dataverse: PCNA images and quantification of 4T1-GFP-luciferase lung metastases. https://doi.org/10.7910/DVN/8AJKFM. (Lung metastasis PCNA staining quantification and images (related to Figure 3.5D).)

CHAPTER IV

CONCLUSIONS AND FUTURE DIRECTIONS

Conclusions

In the last several decades, remarkable advancements have been made to target genomic alterations of cancer cells, as well as aspects of the tumor microenvironment, such as the host vasculature and immune system. Despite these novel treatment strategies, progress in improving both progression-free survival and quality of life of cancer patients has been relatively incremental compared to the billions of dollars in both public and private funding, as well as the resources and sacrifices that have been poured into research. Complete responses to therapy are still quite rare. Nevertheless, both basic and translational research are indispensable for the continued progress towards the cure for cancer. Only with our utmost dedication and professional discipline to continue collaborative and rigorous research will we be able to win more battles in the war against cancer.

This thesis sought to examine the EphA2/ephrin-A1 axis in host-tumor interactions. These studies not only reveal novel insight into how tumor-specific EphA2 impacts the host immune system and how host-specific ephrin-A1 impacts tumor metastasis, but also further elucidates the complexity of regulatory networks involved in host-tumor interactions. However, this thesis falls short of identifying the molecular mechanisms involving EphA2 and ephrin-A1 in the tumor microenvironment, and more investigations are required on this front. In addition, these experiments were conducted with the utmost rigor, which has led to tangential discoveries of how seemingly minor factors can lead to significant issues in reproducibility of data. This work not only provides a basis for continued investigation of the EphA2/ephrin-A1 axis in host-tumor interactions, but also a cautionary lesson in the rigor and reproducibility of science.

Future directions

This work builds upon decades' worth of research on the Eph receptor and ephrin ligand family. Despite these new contributions, this thesis perhaps raises more questions than answers, opening up many exciting avenues of inquiry. A selection of these questions is discussed below.

What underlying molecular mechanisms mediate EphA2 and ephrin-A1's impact on the tumor microenvironment?

As reviewed in Chapter I, the various cell types that express EphA2 and ephrin-A1 and the different signaling modalities that occur in these cells make it incredibly challenging to pinpoint mechanisms that contribute to an *in vivo* phenotype. In the first project that models tumor-specific overexpression of EphA2 in NSCLC, we found that EphA2 overexpression did not significantly increase cell viability of KPL and LCC cells *in vitro*, suggesting that the balance between tumor-promoting, ligand-independent signaling and tumor-suppressing, ligand-dependent signaling is maintained even in the presence of exogenous EphA2 overexpression (Figure 2.1B, 2.1C). However, whether this balance is maintained in three-dimensional (3D) tumoroid growth *in vitro* has not been explored. In fact, how EphA2/ephrin-A1 engagement changes from 2D to 3D culture remains largely unknown. One may speculate that 3D culture would increase the opportunity of canonical EphA2/ephrin-A1 ligand-dependent signaling due to increased areas of cell-to-cell contact; however, tumoroid cultures also depend on exogenous growth factors, such as EGF, which activate RTK signaling and potentially more ligand-independent EphA2 signaling.

In addition to factors that may modulate EphA2/ephrin-A1 signaling in a 3D growth system, there is an abundance of other factors to consider when utilizing an *in vivo* model. Both EphA2 and ephrin-A1 are expressed in normal lung epithelium, albeit at lower levels than in tumors[64,71]. How do EphA2/ephrin-A1 interactions between tumor and normal epithelium differ from interactions among tumor cells? What about interactions between tumor cells and other stromal cells that express EphA2 or ephrin-A1, including endothelial cells, immune cells, and fibroblasts? These are all questions that are difficult to examine but may be addressed, at least in part, by using single-cell and spatial techniques. For example, multiplexed immunofluorescence (mIF) in theory could be leveraged to identify tumor and different stromal populations, as well as cell surface EphA2 and ephrin-A1 expression. Analysis of phosphoresidues on EphA2, particularly S897 and Y588/Y594, may help determine if EphA2 is signaling in a more ligand-independent or dependent fashion, respectively. Furthermore, EphA2 can be packaged into extracellular vesicles and facilitate signaling in a manner that does not require cell-cell contact[39,189]. Preliminary data demonstrate that EphA2 overexpression in a human *KRAS* mutant NSCLC cell line increases the amount of EphA2 packaged into extracellular vesicles (Figure 4.1). Thus, overexpression of EphA2 in the cancer cell may induce a plethora of signaling changes in the tumor microenvironment.

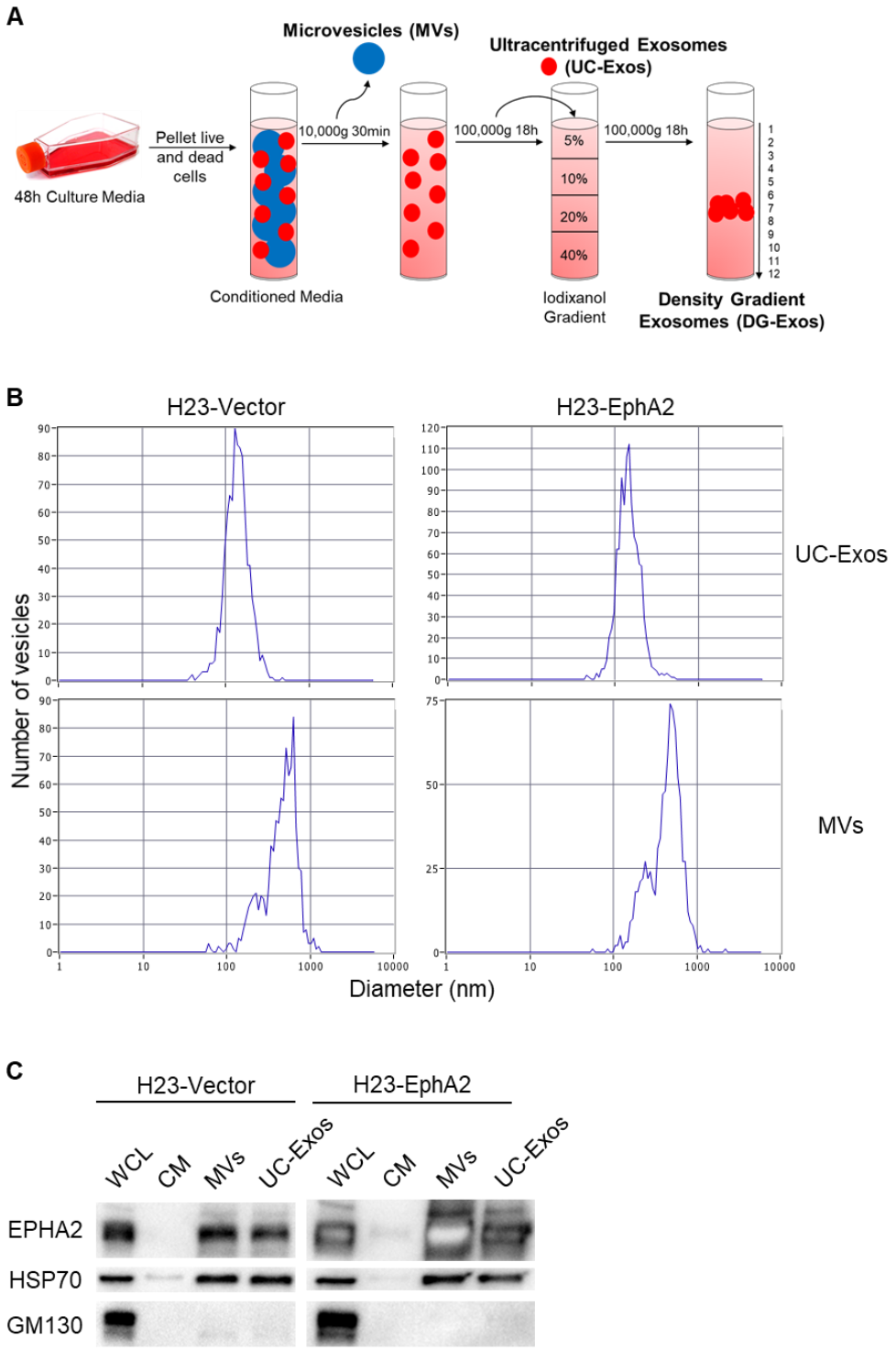

Figure 4.1. EphA2 expression is higher in extracellular vesicles derived from EphA2-overexpressing H23 NSCLC cells. (A) Schematic depicting isolation of microvesicles (MVs) and exosomes from H23 control (H23-Vector) and EphA2-overexpressing cells (H23-EphA2). (B) Histogram depicting sizes of isolated MVs and ultracentrifuged exosomes (UC-Exos). (C) Western blot showing protein expression of EphA2, positive vesicle marker HSP70, and negative vesicle marker GM130 from whole cell lysate (WCL), conditioned media (CM), MVs, and UC-Exos derived from H23-Vector and H23-EphA2 cells. (Courtesy of Aaron Lim, Kim Rathmell lab)

Deficiency of ephrin-A1 in host tissues can also lead to a diverse array of signaling changes. In ephrin-A1 KO animals, canonical signaling between ephrin-A1 and EphA2 is completely abrogated. This not only results in the absence of ephrin-A1 reverse signaling and soluble ephrin-A1 stimulation but may also increase opportunity for EphA2 to engage with other ephrin ligands or signal in a ligand-independent manner. Interestingly, in ephrin-A1 KO mice, we found dramatically higher cell-surface EphA2 expression in host lung epithelial and endothelial cells, compared to WT littermates (Figure 4.2A). Furthermore, 4T1 cells injected via tail vein and harvested from lungs of ephrin-A1 KO mice also trend towards increased EphA2 expression, compared to those from WT littermates (Figure 4.2B). When ephrin-A1 binds to EphA2, this typically leads to endocytosis of the EphA2/ephrin-A1 complex; hence, the observed increase in EphA2 surface expression in ephrin-A1 KO host cells may be due to the lack of ephrin-A1-mediated internalization of the receptor or loss of feedback inhibition. In addition, increased EphA2 expression in 4T1 cancer cells from KO hosts appears counterintuitive given the metastasis phenotypes observed in KO versus WT littermates (Chapter III). Based on the current literature, one would hypothesize that increased EphA2 expression on tumor cells in ephrin-A1 KO mice would lead to greater tumor growth. However, we instead see decreases in the number of lung metastases and in cell proliferative index in metastatic lesions in KO mice (Chapter III). Thus, the conventional reasoning that suggests EphA2 overexpression in tumor cells leads to greater ligand-independent signaling, which leads to increased cancer growth and progression, may not always be true. Instead, factors in the host tissues likely modulate the relationship between EphA2 tumor expression and tumor burden *in vivo*. Ironically, this observed discrepancy in EphA2's role in the tumor cell is perfectly consistent with the

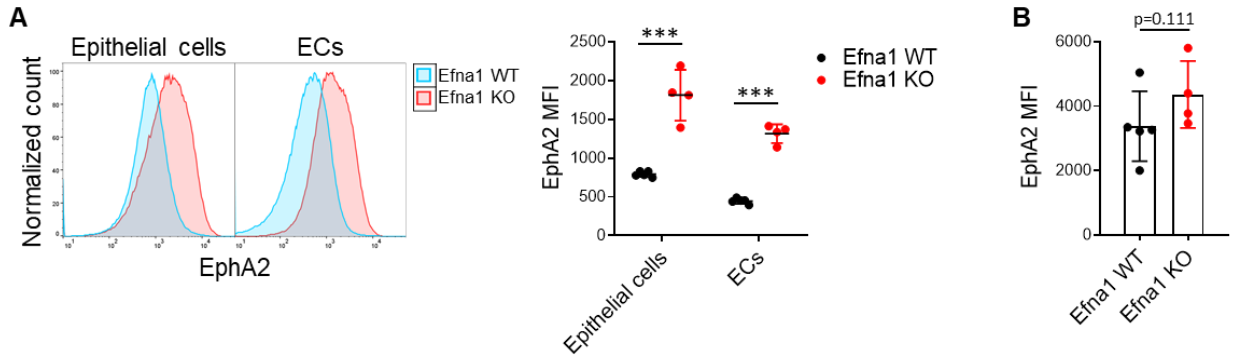

Figure 4.2. EphA2 surface expression is higher in cells derived from ephrin-A1 KO mice. (A) Representative flow histograms and quantification of EphA2 median fluorescence intensity (MFI) on lung epithelial cells (EpCAM+, GFP-, CD45-, CD31-) and ECs (CD31+, EpCAM-, GFP-, CD45-) from ephrin-A1 WT and KO littermates. (B) Quantification of EphA2 MFI on 4T1 cells (GFP+, CD45-, CD31-) 24 hours after tail vein injection into WT and KO littermates. Data shown are averages ± SD (n=4-5 mice per group, ***p<0.001, unpaired Mann-Whitney test).

controversial discoveries surrounding EphA2's dual role as a tumor promoter and tumor suppressor. Our findings indicate that ephrin-A1 ligand expression in host tissues influences which role EphA2 plays in the tumor cell, though further molecular studies must be performed to explore this host-tumor interaction. One preliminary experiment that could be done is to overexpress or knockout EphA2 in the cancer cells and evaluate their ability to grow tumors and metastases *in vivo* in ephrin-A1 KO versus WT hosts. This may provide further insight into whether the reduced metastases we observe in the KO mice is partially due to tumor-specific EphA2.

How well do these findings on EphA2 and ephrin-A1 in these mouse models generalize to other cancer types and translate to human pathophysiology?

The two projects that encompass Chapters II and III both focus on only one cancer type, lung and breast cancer, respectively. Naturally, a future direction would be to investigate if these findings were specific to the cancer cell lines and mouse models we utilized, or if they can be generalized to other cancers. Besides NSCLC cell lines, we have a number of other murine cancer cell lines, such as MMTV-PyMT, E0771, 4T1, B16, RENCA, and CT26, in which EphA2 expression can be modulated and tested *in vivo* in immunocompetent syngeneic mice. Ideally, these studies would also be complemented with a spontaneous tumor model; however, the generation of an inducible tissue-specific EphA2 knockout mouse would be needed. In addition, RENCA and CT26 cells are both derived from the Balb/c background, on which we have our ephrin-A1 knockout mouse model. Investigations on ephrin-A1 in host tissues would not only benefit from exploration of other tumor types, but also the generation of an inducible ephrin-A1 KO since ephrin-A1 has been shown to impact developmental processes.

An even more important question perhaps is whether our findings in mouse models are relevant to human cancers. Our experiences have shown that host-tumor interactions involving EphA2 and ephrin-A1 may be regulated differently in human cancer cells and tumors, compared to their murine counterparts. For example, previous work demonstrated that PD-L2 is upregulated by cytokines, such as IFN-γ and TNF-α, in human KRAS mutant NSCLC cell lines, and knockdown of EphA2 by siRNA or shRNA downregulated cytokine-induced PD-L2 expression[190]. However, we discovered that murine NSCLC cell lines, both KPL and LLC, do not express PD-L2 at baseline, and PD-L2 expression was not induced by IFN-γ, TNF-α, or IL-4 in these cells (data not shown). In addition, tumor cells derived from murine lung tumors and analyzed by flow cytometry do not express PD-L2 either; although, PD-L2 expression was seen on immune cells derived from the tumors, including macrophages and DCs (data not shown).

This data suggests that PD-L2 is not expressed in murine lung cancer cells, which makes evaluation of tumor-intrinsic EphA2's regulation of PD-L2 challenging to perform *in vivo*.

One published study found that *EPHA2* mRNA expression inversely correlated with cytotoxic T cell markers in pancreatic tumors archived by the TCGA[123]. Despite these promising results and our data using the murine KPL NSCLC model, we did not observe consistent trends between EPHA2 and *CD3E*, *CD8B*, *GZMB*, *PRF1*, or *IFNG* expression from the TCGA lung adenocarcinoma dataset (data not shown). Similarly, because we found reduced breast cancer metastases in ephrin-A1 KO mice compared to WT littermates, we analyzed *EFNA1* gene expression in publicly available datasets containing breast tumor and adjacent normal samples. However, we did not observe a consistent trend between *EFNA1* expression in adjacent normal tissue and stage of disease (Figure 4.3), though we did not control for other clinical characteristics. The human data discussed in this section, although not consistent with our murine studies, are only correlative by nature. Future evaluation of the EphA2/ephrin-A1 axis in human tumor samples would require more granular data.

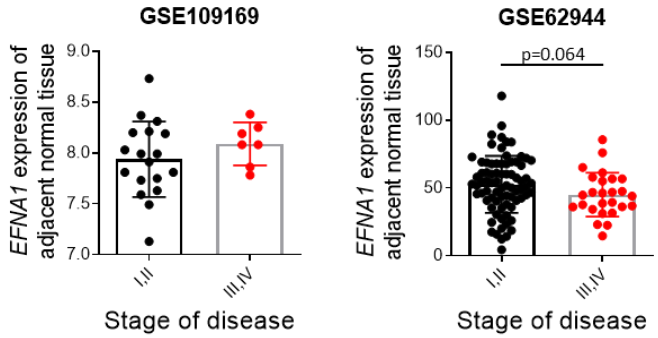

Figure 4.3. *EFNA1* mRNA expression in adjacent normal tissue from breast cancer patients with early versus advanced stage disease. Comparison of adjacent normal *EFNA1* expression between early (I, II) and late stage of disease (III, IV) using publicly available processed microarray (GSE109169[191]) and RNAseq data (GSE62944[192]). Data shown are averages ± SD (unpaired, two-tailed student's t test with Welch correction).

Knowing how complex EphA2 and ephrin-A1 interactions are in the tumor microenvironment, what is the best way to target this axis?

As we and others have demonstrated, EphA2 and ephrin-A1 interactions in the tumor microenvironment are exceedingly complex. Therefore, efforts to target EphA2 in cancer have faced notable barriers. For example, MEDI-547, a first-in-class EphA2-targeting antibody-drug conjugate (ADC), was halted in phase 1 trials due to unacceptable hemorrhage and coagulation related toxicities[193]. This ADC was engineered to deliver auristatin, a microtubule inhibitor,

specifically into EphA2-expressing cancer cells. These toxicities were thought to be partially due to the ADC's unintended targeting of EphA2 on the endothelium or an off-target effect on another protein, rather than nonspecific toxicity from auristatin[57,194,195]. The fact that this agent previously promised high efficacy with no observed toxicities in preclinical models[196–198] but failed miserably in trials is yet another testament to the differences in EphA2's effect between the mouse and human.

Another drug that has been tested for targeting of EphA2 is dasatinib, a small molecule tyrosine kinase inhibitor (TKI) originally developed to inhibit BCR-ABL and SRC family kinases and was discovered to have off-target inhibition on EphA2[199,200]. This quality, along with the fact that it is already approved for treatment of leukemia, has led to several trials testing dasatinib in patients with EphA2-expressing solid tumors (NCT01440998, NCT00895960, NCT00563290, NCT01876212, NCT00371254, NCT00423735). However, several phase II trials have shown that dasatinib provides no clinical benefit in pancreatic cancer, glioblastoma, and melanoma[201–203]. It is possible that dasatinib as a conventional TKI primarily inhibits the kinase activity of EphA2, which is typically activated as a result of ligand-dependent signaling, rather than ligand-independent, tumor-promoting signaling.

Despite the failures in the clinic thus far, EphA2 remains an attractive target, and several alternative strategies of targeting EphA2 are currently being developed and tested. These strategies primarily target cell-surface EphA2 to facilitate drug delivery into tumor cells, rather than aim to inhibit EphA2 signaling. Currently, EphA2-directed peptide-drug conjugates[204], nanoparticles[194,205], and CAR-T cells[113,114] are under development and testing in trials, and whether they are more efficacious or less toxic than their previous EphA2-targeting counterparts remains to be seen. What we have learned from previous trials is that the binding specificity of an agent to EphA2 on tumor cells is critical for limiting toxicities, and the mechanism by which it may inhibit EphA2 signaling is equally important. Based on the unanticipated outcomes of targeting EphA2 in patients, it is apparent that we require a better understanding of not only EphA2 in the tumor cell, but also EphA2 and perhaps ephrin-A1 in host tissues.

Concluding remarks

The discoveries presented in this thesis provide novel insight into EphA2 and ephrin-A1's roles in the tumor microenvironment. Yet, much more work is needed to fully understand all the implications of the EphA2/ephrin-A1 axis in human cancer. In this era of modern medicine,

the basic research and scientific reasoning behind anti-cancer treatment strategies and agents lag behind the clinical ambition to test these strategies and agents – the efforts to target EphA2 in cancer are no exception. Thus, it is imperative that we and the greater scientific community continue to dive deeper into the mechanisms that drive the onset and progression of cancer and seek an even better understanding of its underlying complexities in order to achieve the next breakthroughs in anti-cancer treatment.

APPENDIX A

Eph receptor tyrosine kinases in tumor immunity

The work presented in this appendix is published with the same title in *Cancer Research*, November 2016[24]

Abstract

The family of Eph receptor tyrosine kinases and their ephrin ligands regulate a diverse array of physiological processes, such as axonal guidance, bone remodeling, and immune cell development and trafficking. Eph/ephrin interactions have also been implicated in various pathological processes, including inflammation, cancer, and tumor angiogenesis. Because Eph receptors play prominent roles in both the immune system and cancer, they likely impact the tumor immune microenvironment, an area in which Eph receptors remain understudied. Here, we provide the first comprehensive review of Eph receptors in the context of tumor immunity. With the recent rise of cancer immunotherapies as promising therapeutic interventions, further elucidation of the roles of Eph receptors in the tumor immune microenvironment will be critical for understanding and developing novel targets against tumor immune evasion.

Introduction

Over the past several decades, the paradigm of cancer research and anticancer therapy has shifted from a focus on solely targeting tumor cells to a broader approach of understanding and remodeling the tumor microenvironment. The tumor microenvironment contains a diverse population of host cells, among which include immune cells that are often hijacked by cancer cells to fulfill the tumor's agenda for growth and metastasis. Recently, increasing attention has been directed towards investigating cancer cell evasion of immune destruction, and breakthroughs in this field have led to novel strategies for immunotherapy.

Overview of tumor immunity

In 2013, Chen and Mellman proposed a model of the "cancer-immunity cycle," a multi-step process that includes the release of cancer cell antigens, antigen presentation, priming and activation of T-cells, trafficking of T-cells to tumors, and recognition and killing of cancer cells by cytotoxic T-lymphocytes (CTLs)[101]. This model of tumor immunity, though simplified and lacking other important players like natural killer cells, provides an organized approach to identifying vulnerabilities capitalized by cancer cells. The best-studied examples thus far include inhibition of T-cell activation through cytotoxic T-lymphocyte antigen 4 (CTLA-4) and exhaustion of T-cell effector function through programmed death 1 (PD-1) receptor signaling. Therapeutic anti-CTLA-4 (ipilimumab) and anti-PD-1 monoclonal antibodies (nivolumab, pembrolizumab) have proven successful in the clinic. However, these checkpoint inhibitors are collectively only approved for melanoma, renal cell carcinoma (RCC), non-small cell lung cancer, and Hodgkin lymphoma. Typically, only 15-40% of patients respond favorably to checkpoint inhibitor monotherapy[206–208], though response rates up to 61% have been reported for combination ipilimumab and nivolumab therapy[208]. Thus, it is clear that other critical factors in tumor immunity have yet to be characterized and explored as targets.

The Eph receptor tyrosine kinase family

The Eph receptor tyrosine kinase (RTK) family comprises the largest group of surface receptors and are categorized into EphA or EphB subclasses based on sequence homology and preferential binding to their ephrin-A and ephrin-B ligands, respectively[20]. In humans, nine EphA (EphA1-8,10) and five EphB (EphB1-4,6) receptors are expressed, along with five ephrin-A and three ephrin-B ligands. Unlike most RTKs, Eph receptors interact with ligands that are often membrane-bound, allowing both "forward signaling" in the receptor-bound cell and "reverse signaling" in the ephrin-bound cell (Figure A.1A). In addition to "forward signaling," Eph receptors can signal in the absence of ligand binding and kinase activation through cross-talk with other RTKs, such as HER2[32,42]. Eph receptors are involved in a wide range of physiological and pathological processes, including inflammation and cancer. Although their roles in immune cell development, migration, and activation[209,210], as well as their involvement in tumorigenesis, tumor angiogenesis, and cancer stem cells, have been reviewed extensively, the junction between these two areas has yet to be rigorously examined[47,211,212]. Here, we attempt to

bridge this gap and provide the first comprehensive review of Eph RTKs in the context of tumor immunity.

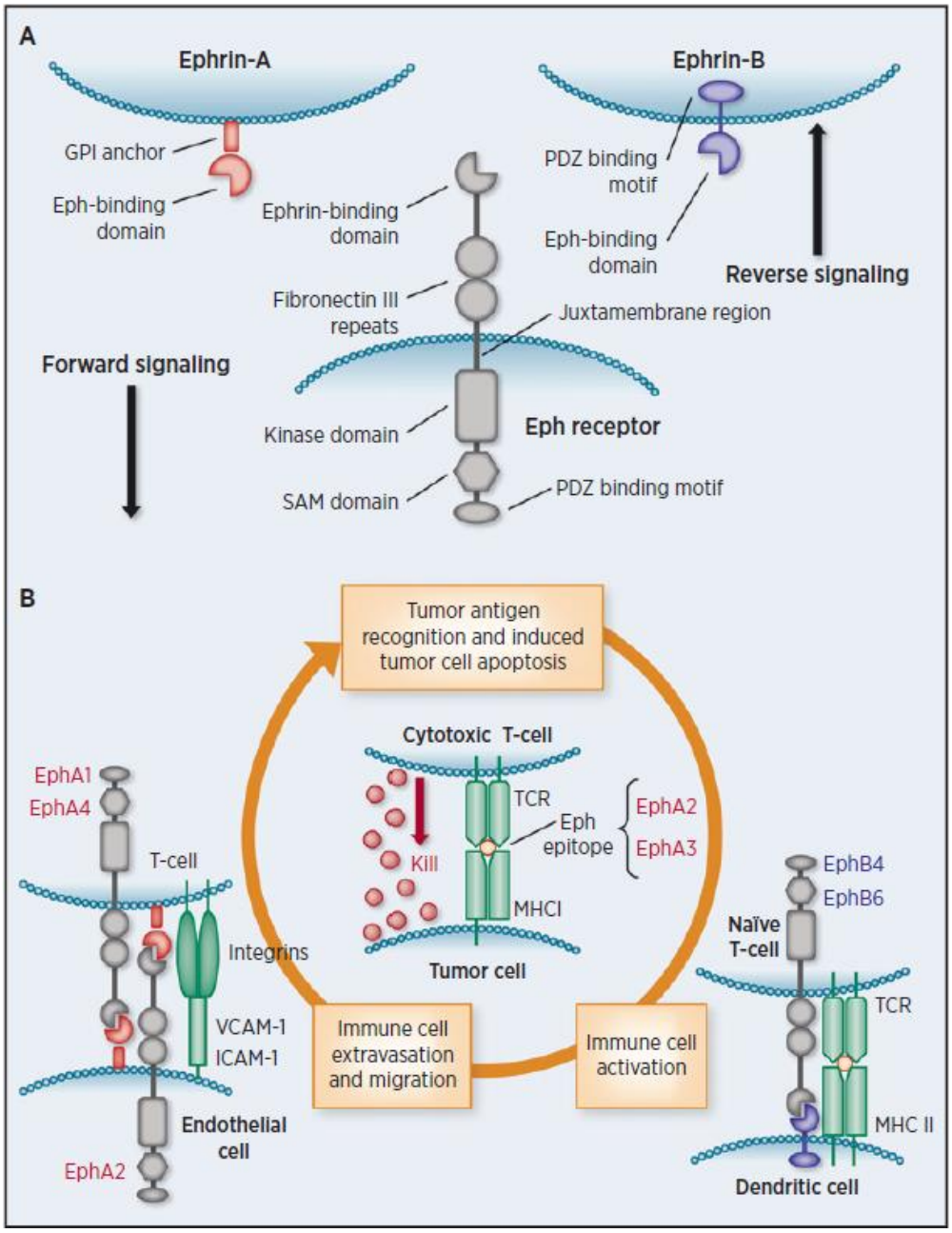

Figure A.1. Eph receptors and ephrin ligands – roles in the cancer-immunity cycle. (A) Structural elements of an Eph receptor and ephrin ligands. (B) Graphical summary of potential roles of Eph receptors in the cancer-immunity cycle. EphA receptors are sources of immunogenic TAAs and may interact with ephrins in the vasculature to regulate lymphocyte trafficking to tumor cells. Additionally, EphB receptors may serve as co-stimulation molecules that activate T cells against tumor cells.

Eph receptor-derived tumor-associated antigens

The first Eph receptor identified as a tumor-associated antigen (TAA) was EphA3[213], which is overexpressed in several malignancies, including melanoma. In this study, a CD4+ T-cell clone isolated from a melanoma patient with an exceptionally favorable clinical course was found to recognize an EphA3 epitope and elicit selective immunoreactivity against melanoma cell lines.

Subsequently, EphA2 has become the best-studied source of TAAs in the Eph family (Figure A.1B). At baseline expression levels, EphA2 typically binds its main ligand ephrin-A1 and facilitates epithelial cell-to-cell adhesion. However, when overexpressed in many solid tumors, such as melanoma, glioma, RCC, and breast and lung cancer, EphA2 signals in a ligand-independent fashion through cross-talk with EGFR and HER2, and promotes tumor growth and angiogenesis[32,163].

Multiple EphA2-derived epitopes are recognized by human CD4+ or CD8+ T-cells[105,214]. One particular epitope ($EphA2_{883-891}$) from the C-terminus of human EphA2 induces significant immunoreactivity in CD8+ T-cells via MHC I-restricted presentation against RCC and glioma cell lines *in vitro*[105,107,108]. Reactive T-cell clones were isolated from both healthy donors and patients with glioma or RCC; however, they were only identified after *ex vivo* expansion and antigen stimulation. Whether these $EphA2_{883-891}$-specific T-cells are generated spontaneously and confer antitumor activity in humans remains unknown. Further investigation will likely require a more direct and sensitive method of detecting specific T-cell clones while minimizing *ex vivo* manipulation.

These early studies led to several preclinical investigations adopting vaccinations with EphA2 peptide-pulsed dendritic cells (DCs) in mouse tumor models of syngeneic glioma, sarcoma, melanoma, and colorectal carcinoma[109,110,215]. Additionally, ephrin-A1 has been used to activate DCs in a rat glioma model[216]. The data from these preclinical models suggest that these DC vaccines induce immune responses and decrease tumor burden, though the findings invite further investigation. In these studies, antigen-specific cytotoxic T-cell clones were isolated from vaccinated animals, and *in vivo* depletion of CD8+ T-cells blocked the reduction in tumor size induced by vaccination. However, both primary tumor and metastasis models in these cases were non-orthotopic and not ideal representations of human disease. Furthermore, none of the studies analyzed tumor-infiltrating immune populations or reported on the effects on survival. Interestingly, the mouse EphA2 peptides used to stimulate DCs in these studies are not homologous to $EphA2_{883-891}$ in humans. This highlights the differences in MHC molecules

across species and their different binding affinities for peptides, which becomes a significant barrier to translating these models into treatments for patients. Thus, future research in this area will likely benefit from using humanized mouse models.

A few studies mentioned above[107–109] have led EphA2 to become a prominent target for immunotherapy in glioma and provided rationale for clinical trials to test the safety of combination peptide vaccines with $EphA2_{883\text{-}891}$ plus other TAAs in patients with gliomas[111,112,115]. Reports on toxicity and preliminary efficacy demonstrate that the peptide vaccinations are generally well-tolerated and elicit clinical and immunologic T-cell responses. However, the data contains wide interpatient variability and does not control for key confounding factors, such as prior chemotherapy and/or radiation regimens, that can have a notable impact on immune function. Later phase trials will hopefully provide greater insight on the efficacy of combination peptide vaccines in patients with glioma. Currently, a vaccine trial testing a group of TAAs, including $EphA2_{883\text{-}891}$, in combination with dasatinib, an inhibitor of Src and EphA2, is ongoing in patients with melanoma (NCT01876212). Despite these advances, $EphA2_{883\text{-}891}$ and other TAAs used in peptide vaccines can only be presented and potentially induce responses in patients with the MHC I haplotype HLA-A2. This greatly limits the patient population that may respond to such therapies.

Although the discussion thus far has focused on CTL function in relation to TAA immunogenicity, a few studies also examine the roles of other immune cell subsets, such as CD4+ T-cells. For example, Tatsumi et al. identifies MHC II-restricted EphA2 epitopes and examines the immunoreactivity of CD4+ T-cell subsets from RCC patients against these peptides[105]. They found that Th1 polarization of CD4+ T-cells is greater in patients with stage I disease, while Th2 polarization and regulatory T cell (Treg) differentiation, both generally considered to be immunosuppressive and tumor-promoting responses, are increased in patients with more advanced disease. In *in vivo* models, Yamaguchi et al. provide preliminary evidence that CD4+ T-cells can partially mediate antitumor responses induced by EphA2 peptide-pulsed DCs[110,215]. Further elucidation of the effects of EphA2 peptide and DC vaccines on T-cell subsets, as well as novel investigations on other immune cell populations, will broaden our understanding of the mechanisms and advance development of these anticancer therapies.

Eph receptor-mediated immune cell trafficking

Besides inducing immunologic responses, Eph receptors can regulate immune cell

trafficking. EphA2 is expressed on endothelial cells and may mediate lymphocyte adhesion to vessel walls, the first step in lymphocyte extravasation. Expression of both EphA2 and its main ligand ephrin-A1 is upregulated in activated endothelium *in vitro*, and stimulation of EphA2 signaling through ephrin-A1 binding leads to increased expression of adhesion proteins, such as E-selectin and VCAM-1, that bind to leukocyte integrins[116]. Conversely, EphA2 binding to ephrin-A1 on T-cells results in reverse signaling that promotes T-cell adhesion to VCAM-1 and another vascular adhesion protein ICAM-1[217] (Figure A.1B). However, these interactions have not been tested in a co-culture system or transendothelial migration model. Although cursory evidence suggests that EphA2 signaling may be modulating the NF-κB pathway to affect expression of adhesion proteins[218], further mechanistic studies are needed to elucidate the signaling pathways downstream of both EphA2 and ephrin-A1 that may lead to changes in lymphocyte adhesion to endothelial cells. Furthermore, since these *in vitro* studies were conducted in the context of atherosclerosis, whether the adhesion induced by EphA2 and ephrin-A1 binding facilitates lymphocyte extravasation through activated tumor vessels remains to be investigated.

In addition to *in vitro* investigations, the interaction between ephrin-A1 and EphA2 has been studied in various lung injury and inflammation mouse models[122,218]; however, their effects on lung vasculature remain equivocal and are likely model-dependent. For example, Carpenter et al. report that EphA2 knockout mice have reduced vascular permeability, immune cell infiltration, and chemokine production in a bleomycin-induced lung injury model[218], while Okazaki et al. conclude that the same knockout mice have increased immune cell infiltration and inflammatory cytokine production in *Mycoplasma* and ovalbumin-induced inflammatory lung models compared to their wild-type counterparts[122]. Further *in vivo* studies are needed to clarify the effect of EphA2 in the lung vasculature.

Two other binding partners of ephrin-A1 are EphA1 and EphA4, which are expressed in T-cells and mediate T-cell chemotaxis *in vitro*[120,219,220] (Figure A.1B). Ephrin-A1 stimulation of CD4+ and CD8+ T-cells promotes chemotaxis in response to stromal cell-derived factor 1α (SDF-1α)/CXCL12 and macrophage inflammatory protein 3β (MIP-3β)/CCL19 *in vitro*. EphA1 is expressed on CD4+ and CD8+ T-cells and facilitates migration of both T-cell subsets via recruitment of FAK-like kinase Pyk2, Src kinase Lck, Rho-GEF Vav1, and PI3K[219,220]. On the other hand, EphA4 is not expressed on CD8+ T-cells but facilitates CD4+ T-cell migration through activation of Vav1 and Src kinases Lck and Fyn, as well as potential dimerization with EphA1[120,220]. Surprisingly, administration of a pan-Src inhibitor appears to increase T-cell chemotaxis in response to CCL19 and CXCL12[219,220]. These chemokines both regulate

lymphocyte homing, though CXCL12 in particular is overexpressed in several types of cancer and can promote tumor growth, metastasis and angiogenesis through signaling of its receptor CXCR4 on cancer cells[221]. Thus, evaluation of EphA receptor roles in T-cell recruitment to tumors, especially those that are driven by CXCL12/CXCR4, may provide additional insight in the immune microenvironment of these tumors.

Although the association between EphA receptors and T-cell trafficking is well-established, some evidence suggests that EphB receptors regulate monocyte migration. Interactions between ephrin-B2 on endothelial cells and EphB4 expressed on monocytes inhibit their chemotaxis and transendothelial migration[222,223]. Though these studies are framed in the context of atherosclerosis, ephrin-B2 also plays a crucial role in angiogenesis through regulation of VEGFR signaling[224,225] and may affect monocyte trafficking through the tumor vasculature. In addition to T-cell and monocyte recruitment, there is sparse literature on Eph/ephrin involvement in trafficking of other immune cells, mainly B-cells[226] and dendritic cells[227].

Although these investigations examining Ephs/ephrins in immune cell chemotaxis and migration have not utilized cancer models, much of the understanding gained from this work can be easily applied and tested in the context of tumor immunity. EphA/ephrin-A1 interactions between lymphocytes and endothelial cells may play a role in lymphocyte infiltration of tumors, while EphB/ephrin-B2 may have similar functions in monocytes and tumor-associated macrophages. Additional research in Eph/ephrin interactions in the immune system will help redress inconsistencies in our current understanding and perhaps reveal novel targets in the tumor microenvironment or treatment strategies.

Eph receptors in immune cell activation

The balance between costimulatory and inhibitory signals from DCs to naïve T-cells can direct the fate of T-cells towards differentiation into a tumor fighting or immunosuppressive subclass, like Tregs, or apoptosis, leading to immune tolerance of tumor cells. Although little is known about EphB/ephrin-B interactions in facilitating T-cell trafficking, their role in T-cell costimulation has been well-characterized[228–231] (Figure A.1B).

In murine T-cells, *in vitro* stimulation of EphB receptors by ephrin-B1, B2, or B3 leads to EphB co-localization with the T-cell receptor (TCR) complex and T-cell activation, indicated by MAPK pathway signaling, T-cell proliferation, IFN-γ secretion, and cytotoxic activity[228–230]. Likewise, stimulation of EphB6 expressed on human T-cells with ephrin-B2 yields similar

results[231]. EphB6 activation leads to increased expression of T-cell activation markers CD25 and CD69 and secretion of several proinflammatory cytokines, including IFN-γ and TNF-α, though not IL-2, the main cytokine upregulated in T-cells by canonical antigen-presenting cell costimulation. The traditional costimulatory B7 molecules on DCs induce IL-2 transcription in T-cells and their survival, whereas other costimulatory receptors, such as those in the TNF receptor family, promote proliferation and differentiation without affecting IL-2 levels. Thus, EphB6 appears to function similarly to this last group of costimulatory receptors and, because it promotes IFN-γ secretion and cytotoxic activity, may promote CTL differentiation. Further evidence of this is demonstrated in EphB6 knockout mice that have impaired T-cell activation and function and reduced TCR downstream signaling proteins, such as activated ZAP-70, LAT, PLC-γ, and Erk1/2[232].

Despite the evidence presented in these studies, EphB/ephrin-B involvement in T-cell activation is likely more complex. For example, other EphB receptors expressed on T-cells, such as EphB4, may share redundant functions with EphB6 in stimulating T-cell proliferation45. Moreover, the concentration of available ephrin-B1 and B2 may modulate costimulatory function. Kawano et al. show that high concentrations of ephrin-B1 and B2, though not ephrin-B3, can inhibit instead of stimulate T-cell activation through EphB4 signaling[233]. Nguyen et al. report that ephrin-B2 and EphB2 expressed on mesenchymal stromal/stem cells (MSCs) can suppress T-cell activation via interaction with EphB4 and ephrin-B1 on T-cells, respectively[234]. The collective interactions of EphBs and ephrin-Bs between T-cells and MSCs increase expression of TGF-β1, indoleamine 2,3-dioxygenase (IDO), and inducible nitric oxide synthase (iNOS), all three of which are immunosuppressive factors that can promote tumor immune evasion[235].

Besides EphB/ephrin-B involvement in T-cell costimulation and suppression, very little is known about the roles of other Eph receptors in activating immune cells, except scant evidence suggesting that EphA2 expressed on dendritic cells may help activate B-cells[236]. Given the overwhelming evidence of EphB/ephrin-B engagement in T-cell costimulation, the activation of T-cells against TAAs and their differentiation into tumor-suppressing CTLs may be affected by EphB/ephrin-B interactions. Further investigation in this area using cancer models may provide insight into how we may capitalize on Eph/ephrin relationships to accentuate the antitumor immune response.

Concluding remarks

Eph receptors are sources of immunogenic TAAs and have critical functions in the immune system that likely impact the tumor immune microenvironment (Figure A.1B). Thus, modulating Eph receptor activities, in principle, could be leveraged to improve tumor immune therapies. However, much is still unknown about how Eph receptors regulate tumor immunity. First, many of the studies investigating Eph receptors in immune responses have yet to be translated in cancer models. Second, since the EphA2 receptor is often not mutated in human cancer, it is unclear if the immune system distinguishes EphA2 peptide-MHC complexes on tumor cells from those on normal tissue. Third, Eph receptor kinase inhibitors have been developed[71,237], but their impact on the immune system is unknown. Finally, while EphA2 is expressed on dendritic cells[227], its role in tumor immunity remains to be investigated. In summary, although there is abundant literature on Eph receptors and ephrins in cancer biology, as well as immunology, this family of RTKs is highly understudied in the context of tumor immunity. This gap in our current knowledge identifies a distinct opportunity for new discoveries that may advance our understanding of the tumor microenvironment and pave the way for novel immunotherapeutic targets.

APPENDIX B

Thrombocytopenia in patients with melanoma receiving immune checkpoint inhibit therapy

The work presented in this appendix is published with the same title in *Journal of Immunotherapy for Cancer*, February 2017[238]

Abstract

Immune checkpoint inhibitors, including antibodies against programmed death 1 (PD-1) and cytotoxic T-lymphocyte antigen 4 (CTLA-4), are being used with increasing frequency for the treatment of cancer. Immune-related adverse events (irAEs) including colitis, dermatitis, and pneumonitis are well described, but less frequent events are now emerging with larger numbers of patients treated. Herein we describe the incidence and spectrum of thrombocytopenia following immune checkpoint inhibitor therapy and two severe cases of idiopathic thrombocytopenic purpura (ITP). A 47-year-old female with recurrent BRAF mutant positive melanoma received combination anti-PD-1 and anti-CTLA-4. Two weeks later, she presented with mucosal bleeding, petechiae, and thrombocytopenia and was treated with standard therapy for ITP with steroids and intravenous immunoglobulin (IVIG). Her diagnosis was confirmed with bone marrow biopsy, and given the lack of treatment response, she was treated with rituximab. She began to have recovery and stabilization of her platelet count that ultimately allowed her to be retreated with PD-1 inhibition with no further thrombocytopenia. A second patient, a 45-year-old female with a BRAF wild-type melanoma, received anti-PD-1 monotherapy and became thrombocytopenic 43 days later. Three weeks of steroid treatment improved her platelet count, but thrombocytopenia recurred and required additional steroids. She later received anti-CTLA-4 monotherapy and developed severe ITP with intracranial hemorrhage . Her ITP resolved after treatment of prednisone, IVIG, and rituximab and discontinuation of checkpoint inhibition. In a retrospective chart review of 2,360 patients with melanoma treated with checkpoint inhibitor therapy, <1% experienced thrombocytopenia following immune checkpoint inhibition, and of these, most had spontaneous resolution and did not require treatment. Thrombocytopenia, especially ITP, induced by immune checkpoint inhibitors appears to be an uncommon irAE that

is manageable with observation in mild cases and/or standard ITP treatment algorithms. In our series, the majority of patients had mild thrombocytopenia that resolved spontaneously or responded to standard corticosteroid regimens. However, in two severe cases, IVIG and rituximab, in addition to steroids, were required. Checkpoint inhibition was resumed successfully in the first patient but rechallenge was not tolerated by the second patient.

Background

Immune checkpoint inhibitors, including antibodies against programmed death 1 (PD-1) receptor, are quickly becoming a staple in our arsenal of anti-cancer agents. PD-1 signaling normally inactivates effector T cells when bound to its ligands PD-L1 and PD-L2; thus, inhibition of this pathway reinvigorates T cell antitumor responses[239]. Nivolumab and pembrolizumab are monoclonal antibodies that block PD-1 and have demonstrated substantial benefit in melanoma, non-small cell lung cancer, renal cell carcinoma, Hodgkin lymphoma, and numerous other cancers[240].

Although inhibitors of PD-1 provide significant therapeutic benefit, many immune-related adverse events (irAEs) have emerged with these therapies. The most common irAEs include dermatologic toxicities and thyroid dysfunction[207,241,242]. Other clinically significant toxicities include colitis, hypophysitis, pneumonitis, and hepatitis[241–243]. These events arise from dysregulation of self-tolerance that is normally mediated by PD-1/PD-L1 interactions[244]. Additionally, anti-PD-1 (specifically nivolumab) may be combined with ipilimumab, an antibody against cytotoxic T-lymphocyte antigen 4 (CTLA-4), which when bound to costimulatory molecules on antigen-presenting cells inactivates T cells. Ipilimumab works synergistically with anti-PD-1 agents and improves antitumor efficacy but also increases the frequency and severity of irAEs[207,241,242].

Recently, cases of hematologic irAEs were reported with anti-PD-1 therapy, specifically autoimmune hemolytic anemia and immune thrombocytopenic purpura (ITP)[245–248]. Although cases of thrombocytopenia induced by either pembrolizumab or ipilimumab alone have been reported, its incidence, spectrum of severity, and development of ITP have not been established[249,250]. Given the rapid rise of immunomodulatory therapy use in numerous cancers, there is a clear need to identify and characterize these hematologic irAEs. Here, we report two cases of severe ITP resulting from checkpoint inhibitor therapy and the largest multi-institutional case series of thrombocytopenia induced by checkpoint inhibitor therapy.

A 47-year-old patient presented in 2011 with stage IIb melanoma on her left forearm, which was removed by wide local excision with a concurrent negative sentinel lymph node biopsy. Four years later, she presented with recurrent metastatic melanoma with a *BRAF*^{V600M} mutation. She initially responded to combination BRAF and MEK inhibition but developed progressive disease within five months. Two weeks later, she received her first infusion of combination ipilimumab and nivolumab. She developed bleeding from mucosal areas and petechiae fifteen days following her first dose of combination checkpoint inhibitor therapy with severe thrombocytopenia (PLT < 5000/uL) and an elevated immature platelet fraction of 15.4% (0.9 to 7.0% normal range). She had no history of autoimmune or coagulation disorders, and the remainder of her laboratory evaluation was unrevealing. She was presumed to have new-onset ITP and was started on methylprednisolone and intravenous immunoglobulin (IVIG) (Figure B.1). After five days of steroids and IVIG without significant improvement in her platelet count, a bone marrow biopsy revealed a hypercellular marrow with increased megakaryocytes (Figure B.2), further supporting the diagnosis of ITP. Her treatment was escalated to weekly rituximab with addition of a single dose of romiplostim, a thrombopoietin analog. Seven days after steroids

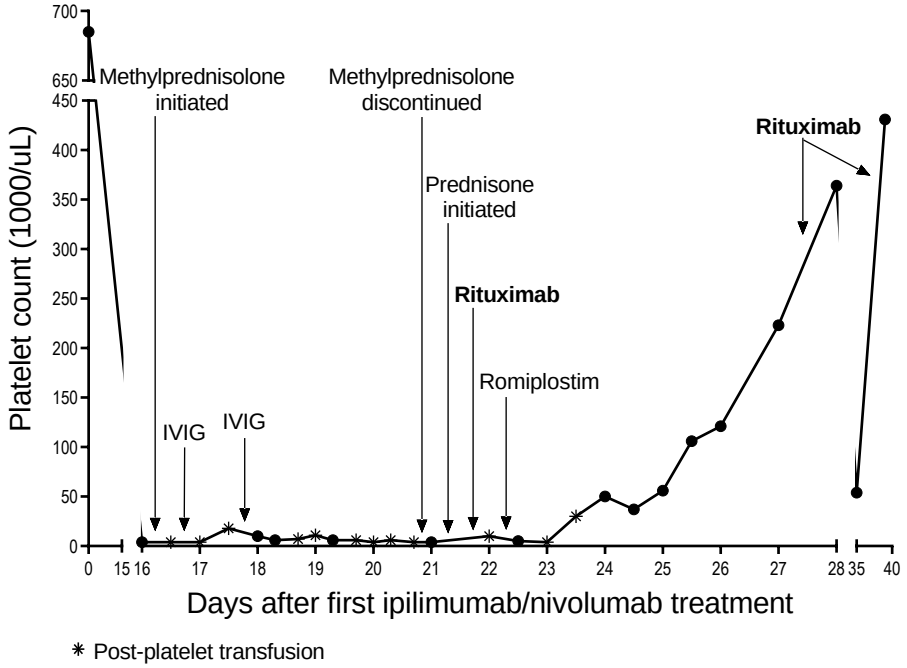

Figure B.1. Checkpoint inhibitor-induced ITP refractory to glucocorticoids subsequently responds to second-line treatment.

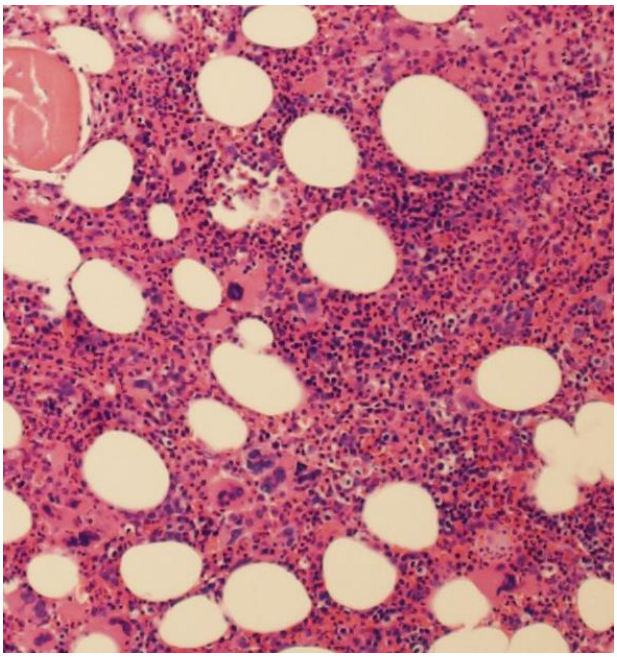

Figure B.2. Bone marrow from patient with checkpoint inhibitor-induced ITP before rituximab treatment. H&E stained section of the bone marrow biopsy, 100 x magnification. The bone marrow is moderately hypercellular for age with trilineage hematopoiesis and increased megakaryocytes (black arrows) with a range of morphologies and mild clustering. These findings, coupled with the patient's peripheral thrombocytopenia and elevated IPF, are compatible with a diagnosis of ITP.

and IVIG, and two days after rituximab, her platelet counts began to improve, reaching normal range (137,000 to 397,000/uL) by one week, and she subsequently did not require additional platelet transfusions (Figure B.1). Between her second and third infusion of rituximab, she transiently relapsed to a platelet count of 54,000/uL. She received a total of four doses of rituximab in accordance with standard therapy for ITP. Eight days after her last dose, she was rechallenged with nivolumab monotherapy and subsequently experienced a partial response with no relapse of her ITP.

A second patient, a 45-year-old female with a BRAF wild-type melanoma, received nivolumab as neoadjuvant therapy in a clinical trial and became thrombocytopenic (49,000/uL) 43 days later. She was asymptomatic and was treated with prednisone for three weeks, with elevation of platelet levels to baseline (307,000/uL). However, thrombocytopenia recurred with a platelet nadir of 28,000/uL, and she required an additional 12-week steroid taper before her platelets recovered. She later developed metastatic disease to the brain and underwent resection of a large frontal lesion, as well as gamma knife irradiation to several smaller lesions. Due to limited treatment options, she was administered ipilimumab monotherapy, eight months after receiving nivolumab. Within eight days, her platelet count decreased from 75,000 to 8,000/uL, and two days later, she developed hemorrhage in her intracranial metastasis with no detectable platelets. Her ITP ultimately resolved after treatment with prednisone, IVIG, and rituximab and discontinuation of ipilimumab.

To assess the incidence and clinical patterns of thrombocytopenia, including potential

cases of ITP, following immune checkpoint inhibition, we performed retrospective reviews of electronic medical records at Georgetown Lombardi Cancer Center, Memorial Sloan Kettering Cancer Center, Moffitt Cancer Center, MD Anderson Cancer Center, and Vanderbilt-Ingram Cancer Center. Patients with melanoma were included if they experienced thrombocytopenia following treatment with a checkpoint inhibitor that was clinically diagnosed as ITP or was not attributable to another cause. The project was approved by IRBs of respective institutions with waiver of consent. Statistical analysis was performed using R version 3.3.0.

We assessed the frequency of thrombocytopenia induced by treatment with checkpoint inhibitors across these five institutions and identified 11 cases, several presumed to be ITP based on clinical diagnostic criteria. A total of 2,360 patients with melanoma receiving checkpoint inhibitor therapy were reviewed, suggesting an incidence of well under 1%. These patients were Caucasian men (58%) or women (42%) with melanoma; none had a previous diagnosis of ITP or a history of thrombocytopenia prior to initiation of treatment. Various checkpoint inhibitor regimens were represented (Table B.1). The average time to onset of checkpoint inhibitor-induced thrombocytopenia was 70 days (range, 12 to 173 days), and the average platelet count was 61,000/uL (range, <5,000 to 104,000/uL) with an average decrease of 70% from baseline (range, 38 to 99%). No significant differences were found among the differing checkpoint inhibitor regimens.

Of the 11 patients, four required immunosuppressive treatment with corticosteroids, and two of those cases were refractory to steroids. A higher percentage of patients treated with ipilimumab (single agent or combined with nivolumab) required immunosuppressive treatment (75%, 3 of 4) compared to those treated with anti-PD-1 monotherapy (14%, 1 of 7). The majority of patients displayed no clinical signs or symptoms of thrombocytopenia and required no therapies with spontaneous resolution (Table B.1). Our first case described in detail above had the most severe episode of thrombocytopenia with confirmed ITP by bone marrow biopsy.

Conclusions

Thrombocytopenia, especially ITP, induced by immune checkpoint inhibitors appears to be a relatively uncommon irAE that is manageable with standard treatment algorithms. In our series, the majority of patients had mild thrombocytopenia that resolved spontaneously or responded to standard corticosteroid regimens. However, in two severe cases, steroids, IVIG, and rituximab were administered with ultimate recovery. In the first case, nivolumab

Table B.1. Patients with thrombocytopenia and/or confirmed new-onset ITP following checkpoint inhibitor therapy for melanoma

	Case 1	Case 2	Case 3	Case 4	Case 5	Case 6	Case 7	Case 8	Case 9	Case 10	Case 11
Age, years / sex	52 / F	80 / M	55 / F	44 / M	67 / M	45 / F	53 / M	48 / F	36 / F	56 / M	69 / M
Checkpoint inhibitor(s) and dosage(s)	Ipi (3 mg/kg) + nivo (1 mg/kg)	Pembro (2 mg/kg)	Ipi (3 mg/kg) + nivo (1 mg/kg)	Ipi (3 mg/kg)	Ipi (3 mg/kg) + nivo (1 mg/kg)	Nivo (3 mg/kg)	Pembro (2 mg/kg)	Pembro (2 mg/kg)	Pembro (2 mg/kg)	Nivo (3 mg/kg)	Nivo (3 mg/kg)
Best response to therapy	PR	PR	PR	PD	N/A	PD	N/A	SD	PD	SD	N/A
Time to TP onset, days	15	21	50	62	68	43	12	173	40	130	151
Other irAEs	None	Neurological	Endocrine, skin	GI	Neurological, liver	None	Neurological, liver	Skin	None	None	None
Counts at TP onset											
WBC, 10^3/uL	15.4	5.8	7	12.8	3.8	6	3.7	11.9	8.1	4.9	4
HCT, %	34	43.5	37.8	N/A	35.8	40.7	35.3	31.3	28.2	41	28.5
PLT, 10^3/uL	Less than 5	104	61	18	86	49	53	89	58	73	74
% PLT decrease from baseline	99%	38%	80%	91%	40%	84%	69%	53%	74%	N/A	75%
Signs and symptoms of TP	Hematochezia, petechiae, gingival bleeding, epistaxis	None	None	Epistaxis	Bleeding from tumor	None	None	None	None	None	None
Confirmation of ITP	Bone marrow biopsy	—	Peripheral smear	—	—	—	—	—	—	—	—
Treatment 1 / highest PLT	MePRDL + IVIG / 18	None required	None required	Prednisolone + IVIG / 30	Prednisone / 118	Prednisone / 307	None required	None required	None required	None required	None required
Treatment 2 / highest PLT	Rituximab + prednisone / 364	—	—	None required	None required	*Prednisone / 269	—	—	—	—	—

Entries with "—" indicate not applicable to patient

Abbreviations: Ipi, ipilimumab; Nivo, nivolumab; Pembro, pembrolizumab; PR, partial response; PD, progression of disease; SD, stable disease; N/A, not available; TP, thrombocytopenia; GI, gastrointestinal; irAEs, immune-related adverse events; WBC, white blood count; HCT, hematocrit; PLT, platelet; MePRDL, methylprednisolone; IVIG: intravenous immunoglobulin

*Patient relapsed after initial steroid treatment

monotherapy was resumed with excellent tolerance. On the other hand, the second patient relapsed with subsequent immune checkpoint inhibition.

Primary ITP is a disorder caused by the formation of autoantibodies targeting platelet antigens, leading to thrombocytopenia[251]. ITP is a diagnosis of exclusion and may be challenging given the lack of specific testing and a wide differential diagnosis. ITP is thought to occur after an inciting event activates or alters the immune system, such as an infection, hematopoietic malignancy, or pharmacologic immune checkpoint inhibition[252]. However, most cases are idiopathic in etiology. A majority of acute cases (50-90%) are responsive to standard corticosteroid and IVIG therapy, though a fraction of cases require second-line treatment, usually involving a combination of rituximab and a thrombopoietin agonist[253]. In mouse models, there is loss of peripheral self-tolerance through alteration of immune homeostasis and evidence of regulatory T cell (Treg) deficiency associated with ITP[254]. Comparison of bone marrow between patients with ITP and normal donors revealed that those with ITP have lower levels of Tregs and abnormal levels of Th1 and Th17 cells[252]. Recent work demonstrated that patients with chronic ITP exhibit lower levels of PD-1 expression in total peripheral blood samples, compared with healthy controls[255,256]. A single case report showed that a patient who developed nivolumab-induced ITP had higher PD-1 expression on B cells[247].

Our experience suggests that thrombocytopenia, including ITP, may rarely complicate immune checkpoint inhibitor therapy but is usually mild and can resolve spontaneously or with standard treatment algorithms. The onset of ITP varies substantially, though a majority occurs within the first 12 weeks after initiation of checkpoint inhibition, consistent with other irAEs[257–259]. Although our observations on checkpoint inhibitor rechallenge after resolution of ITP are limited, our experience suggests that increased clinical vigilance should be used, especially with ipilimumab.

Declarations

This work was approved by IRBs of all contributing institutions with waiver of consent, including the Vanderbilt University Medical Center IRB, Memorial Sloan Kettering Cancer Center IRB, Georgetown University Medical Center IRB, Moffitt Cancer Center IRB, and MD Anderson IRB. A general research consent was signed by study participants to cover the identifying data in the manuscript, including Table B.1.

REFERENCES

1. Hanahan, D. & Weinberg, R. A. The hallmarks of cancer. *Cell* **100**, 57–70 (2000).
2. Hanahan, D. & Weinberg, R. A. Hallmarks of cancer: The next generation. *Cell* **144**, 646–674 (2011).
3. Siegel, R. L., Miller, K. D. & Jemal, A. Cancer statistics, 2020. *CA. Cancer J. Clin.* **70**, 7–30 (2020).
4. Falzone, L., Salomone, S. & Libra, M. Evolution of cancer pharmacological treatments at the turn of the third millennium. *Frontiers in Pharmacology* **9**, 1300 (2018).
5. Travis, W. D. *et al.* The 2015 World Health Organization Classification of Lung Tumors: Impact of Genetic, Clinical and Radiologic Advances since the 2004 Classification. *Journal of Thoracic Oncology* **10**, 1243–1260 (2015).
6. Weinstein, I. B. & Joe, A. K. Mechanisms of Disease: Oncogene addiction - A rationale for molecular targeting in cancer therapy. *Nature Clinical Practice Oncology* **3**, 448–457 (2006).
7. Skoulidis, F. & Heymach, J. V. Co-occurring genomic alterations in non-small-cell lung cancer biology and therapy. *Nature Reviews Cancer* **19**, 495–509 (2019).
8. Chan, B. A. & Hughes, B. G. M. Targeted therapy for non-small cell lung cancer: Current standards and the promise of the future. *Translational Lung Cancer Research* **4**, 36–54 (2015).
9. Canon, J. *et al.* The clinical KRAS(G12C) inhibitor AMG 510 drives anti-tumour immunity. *Nature* **575**, 217–223 (2019).
10. Weigelt, B., Geyer, F. C. & Reis-Filho, J. S. Histological types of breast cancer: How special are they? *Molecular Oncology* **4**, 192–208 (2010).
11. Prat, A. & Perou, C. M. Deconstructing the molecular portraits of breast cancer. *Mol. Oncol.* **5**, 5–23 (2011).
12. 5-Year Relative Survival by Stage at Diagnosis: Lung and Bronchus Cancer. *Surveillance, Epidemiology, and End Results (SEER) Program, SEER 18 Research Data (2009-2015)* (2020). Available at: https://seer.cancer.gov/statfacts/html/lungb.html. (Accessed: 27th March 2020)
13. 5-Year Relative Survival by Stage at Diagnosis: Female Breast Cancer. *Surveillance, Epidemiology, and End Results (SEER) Program, SEER 18 Research Data (2009-2015)* (2020). Available at: https://seer.cancer.gov/statfacts/html/breast.html. (Accessed: 27th March 2020)
14. Chiang, A. C. & Massagué, J. Molecular basis of metastasis. *New England Journal of Medicine* **359**, 2814 (2008).
15. Riihimäki, M. *et al.* Metastatic sites and survival in lung cancer. *Lung Cancer* **86**, 78–84 (2014).
16. Weigelt, B., Peterse, J. L. & Van't Veer, L. J. Breast cancer metastasis: Markers and models. *Nature Reviews Cancer* **5**, 591–602 (2005).
17. Chaffer, C. L. & Weinberg, R. A. A perspective on cancer cell metastasis. *Science* **331**, 1559–1564 (2011).
18. Strilic, B. & Offermanns, S. Intravascular Survival and Extravasation of Tumor Cells. *Cancer Cell* **32**, 282–293 (2017).
19. Reymond, N., D'Água, B. B. & Ridley, A. J. Crossing the endothelial barrier during metastasis. *Nature Reviews Cancer* **13**, 858–870 (2013).
20. Kania, A. & Klein, R. Mechanisms of ephrin-Eph signalling in development, physiology and disease. *Nature Reviews Molecular Cell Biology* **17**, 240–256 (2016).
21. Himanen, J. P. *et al.* Crystal structure of an Eph receptor-ephrin complex. *Nature* **414**, 933–938 (2001).
22. Himanen, J. P. *et al.* Ligand recognition by A-class Eph receptors: crystal structures of the EphA2 ligand-binding domain and the EphA2/ephrin-A1 complex. *EMBO Rep.* **10**, 722–728 (2009).
23. Darling, T. K. & Lamb, T. J. Emerging roles for Eph receptors and ephrin ligands in immunity. *Frontiers in Immunology* **10**, 1473 (2019).
24. Shiuan, E. & Chen, J. Eph receptor tyrosine kinases in tumor immunity. *Cancer Research* **76**, 6452–6457 (2016).
25. Wybenga-Groot, L. E. *et al.* Structural basis for autoinhibition of the EphB2 receptor tyrosine

kinase by the unphosphorylated juxtamembrane region. *Cell* **106**, 745–757 (2001).
26. Kullander, K. & Klein, R. Mechanisms and functions of Eph and ephrin signalling. *Nature Reviews Molecular Cell Biology* **3**, 475–486 (2002).
27. Zisch, A. H. *et al.* Replacing two conserved tyrosines of the EphB2 receptor with glutamic acid prevents binding of SH2 domains without abrogating kinase activity and biological responses. *Oncogene* **19**, 177–187 (2000).
28. Fang, W. Bin, Brantley-Sieders, D. M., Hwang, Y., Ham, A.-J. L. & Chen, J. Identification and functional analysis of phosphorylated tyrosine residues within EphA2 receptor tyrosine kinase. *J. Biol. Chem.* **283**, 16017–26 (2008).
29. Menges, C. W. & McCance, D. J. Constitutive activation of the Raf-MAPK pathway causes negative feedback inhibition of Ras-PI3K-AKT and cellular arrest through the EphA2 receptor. *Oncogene* **27**, 2934–2940 (2008).
30. Macrae, M. *et al.* A conditional feedback loop regulates Ras activity through EphA2. *Cancer Cell* **8**, 111–118 (2005).
31. Fang, W. Bin *et al.* Overexpression of EPHA2 receptor destabilizes adherens junctions via a RhoA-dependent mechanism. *J. Cell Sci.* **121**, 358–368 (2008).
32. Brantley-Sieders, D. M. *et al.* The receptor tyrosine kinase EphA2 promotes mammary adenocarcinoma tumorigenesis and metastatic progression in mice by amplifying ErbB2 signaling. *J. Clin. Invest.* **118**, 64–78 (2008).
33. Lisabeth, E. M., Falivelli, G. & Pasquale, E. B. Eph receptor signaling and ephrins. *Cold Spring Harb. Perspect. Biol.* **5**, a009159 (2013).
34. Kao, T. J. & Kania, A. Ephrin-Mediated cis-Attenuation of Eph Receptor Signaling Is Essential for Spinal Motor Axon Guidance. *Neuron* **71**, 76–91 (2011).
35. Yin, Y. *et al.* EphA receptor tyrosine kinases interact with co-expressed ephrin-A ligands in cis. *Neurosci. Res.* **48**, 285–295 (2004).
36. Carvalho, R. F. *et al.* Silencing of EphA3 through a cis interaction with ephrinA5. *Nat. Neurosci.* **9**, 322–330 (2006).
37. Wykosky, J. *et al.* Soluble monomeric EphrinA1 is released from tumor cells and is a functional ligand for the EphA2 receptor. *Oncogene* **27**, 7260–7273 (2008).
38. Ieguchi, K. *et al.* ADAM12-cleaved ephrin-A1 contributes to lung metastasis. *Oncogene* **33**, 2179–2190 (2014).
39. Takasugi, M. *et al.* Small extracellular vesicles secreted from senescent cells promote cancer cell proliferation through EphA2. *Nat. Commun.* **8**, 1–11 (2017).
40. Sato, S. *et al.* EPHB2 carried on small extracellular vesicles induces tumor angiogenesis via activation of ephrin reverse signaling. *JCI Insight* **4**, (2019).
41. Gong, J., Körner, R., Gaitanos, L. & Klein, R. Exosomes mediate cell contact-independent ephrin-Eph signaling during axon guidance. *J. Cell Biol.* **214**, 35–44 (2016).
42. Arvanitis, D. & Davy, A. Eph/ephrin signaling: Networks. *Genes and Development* **22**, 416–429 (2008).
43. Zantek, N. D. *et al.* E-Cadherin Regulates the Function of the EphA2 Receptor Tyrosine Kinase. *Cell Growth Differ.* **10**, 629 (1999).
44. Miao, H., Burnett, E., Kinch, M., Simon, E. & Wang, B. Activation of EphA2 kinase suppresses integrin function and causes focal-adhesion-kinase dephosphorylation. *Nat. Cell Biol.* **2**, 62–69 (2000).
45. Larsen, A. B. *et al.* Activation of the EGFR gene target EphA2 inhibits epidermal growth factor-induced cancer cell motility. *Mol. Cancer Res.* **5**, 283–293 (2007).
46. Hirai, H., Maru, Y., Hagiwara, K., Nishida, J. & Takaku, F. A novel putative tyrosine kinase receptor encoded by the eph gene. *Science (80-.).* **238**, 1717–1720 (1987).
47. Pasquale, E. B. Eph receptors and ephrins in cancer: Bidirectional signalling and beyond. *Nature Reviews Cancer* **10**, 165–180 (2010).
48. Brantley-Sieders, D. M. Clinical relevance of Ephs and ephrins in cancer: Lessons from breast, colorectal, and lung cancer profiling. *Seminars in Cell and Developmental Biology* **23**, 102–108 (2012).
49. Prickett, T. D. *et al.* Analysis of the tyrosine kinome in melanoma reveals recurrent mutations in ERBB4. *Nat. Genet.* **41**, 1127–1132 (2009).
50. Bardelli, A. *et al.* Mutational analysis of the tyrosine kinome in colorectal cancers. *Science (80-.).*

300, 949 (2003).
51. Ruhe, J. E. *et al.* Genetic alterations in the tyrosine kinase transcriptome of human cancer cell lines. *Cancer Res.* **67**, 11368–11376 (2007).
52. Davies, H. *et al.* Somatic mutations of the protein kinase gene family in human lung cancer. *Cancer Res.* **65**, 7591–7595 (2005).
53. Ding, L. *et al.* Somatic mutations affect key pathways in lung adenocarcinoma. *Nature* **455**, 1069–1075 (2008).
54. Sjöblom, T. *et al.* The consensus coding sequences of human breast and colorectal cancers. *Science (80-.).* **314**, 268–274 (2006).
55. Greenman, C. *et al.* Patterns of somatic mutation in human cancer genomes. *Nature* **446**, 153–158 (2007).
56. Taylor, H., Campbell, J. & Nobes, C. D. Ephs and ephrins. *Current Biology* **27**, R90–R95 (2017).
57. Barquilla, A. & Pasquale, E. B. Eph Receptors and Ephrins: Therapeutic Opportunities. *Annu. Rev. Pharmacol. Toxicol.* **55**, 465–487 (2015).
58. Beauchamp, A. & Debinski, W. Ephs and ephrins in cancer: Ephrin-A1 signalling. *Seminars in Cell and Developmental Biology* **23**, 109–115 (2012).
59. Lodola, A., Giorgio, C., Incerti, M., Zanotti, I. & Tognolini, M. Targeting Eph/ephrin system in cancer therapy. *European Journal of Medicinal Chemistry* **142**, 152–162 (2017).
60. Kou, C.-T. J. & Kandpal, R. P. Differential Expression Patterns of Eph Receptors and Ephrin Ligands in Human Cancers. *Biomed Res. Int.* **2018**, (2018).
61. Wen, Q. *et al.* EphA2 affects the sensitivity of oxaliplatin by inducing EMT in oxaliplatin-resistant gastric cancer cells. *Oncotarget* **8**, 47998–48011 (2017).
62. Miao, B. *et al.* EPHA2 is a mediator of vemurafenib resistance and a novel therapeutic target in melanoma. *Cancer Discov.* **5**, 274–287 (2015).
63. Zhuang, G. *et al.* Elevation of receptor tyrosine kinase EphA2 mediates resistance to trastuzumab therapy. *Cancer Res.* **70**, 299–308 (2010).
64. Amato, K. R. *et al.* EPHA2 blockade overcomes acquired resistance to EGFR kinase inhibitors in lung cancer. *Cancer Res.* **76**, 305–318 (2016).
65. Duxbury, M. S., Ito, H., Zinner, M. J., Ashley, S. W. & Whang, E. E. EphA2: A determinant of malignant cellular behavior and a potential therapeutic target in pancreatic adenocarcinoma. *Oncogene* **23**, 1448–1456 (2004).
66. Zelinski, D. P., Zantek, N. D., Stewart, J. C., Irizarry, A. R. & Kinch, M. S. EphA2 overexpression causes tumorigenesis of mammary epithelial cells. *Cancer Res.* **61**, 2301–6 (2001).
67. Miao, H. *et al.* EphA2 promotes infiltrative invasion of glioma stem cells in vivo through cross-talk with Akt and regulates stem cell properties. *Oncogene* **34**, 558–567 (2015).
68. Landen, C. N. *et al.* Therapeutic EphA2 gene targeting in vivo using neutral liposomal small interfering RNA delivery. *Cancer Res.* **65**, 6910–6918 (2005).
69. Udayakumar, D. *et al.* Epha2 is a critical oncogene in melanoma. *Oncogene* **30**, 4921–4929 (2011).
70. Song, W., Ma, Y., Wang, J., Brantley-Sieders, D. & Chen, J. JNK signaling mediates epha2-Dependent tumor cell proliferation, motility, and cancer stem cell-Like properties in non-Small cell lung cancer. *Cancer Res.* **74**, 2444–2454 (2014).
71. Amato, K. R. *et al.* Genetic and pharmacologic inhibition of EPHA2 promotes apoptosis in NSCLC. *J. Clin. Invest.* **124**, 2037–2049 (2014).
72. Koshikawa, N. *et al.* Proteolysis of EphA2 converts it from a tumor suppressor to an oncoprotein. *Cancer Res.* **75**, 3327–3339 (2015).
73. Yeddula, N., Xia, Y., Ke, E., Beumer, J. & Verma, I. M. Screening for tumor suppressors: Loss of Ephrin receptor A2 cooperates with oncogenic KRas in promoting lung adenocarcinoma. *Proc. Natl. Acad. Sci. U. S. A.* **112**, E6476–E6485 (2015).
74. Dunne, P. D. *et al.* EphA2 expression is a key driver of migration and invasion and a poor prognostic marker in colorectal cancer. *Clin. Cancer Res.* **22**, 230–242 (2016).
75. Yang, N. Y. *et al.* Crosstalk of the EphA2 receptor with a serine/threonine phosphatase suppresses the Akt-mTORC1 pathway in cancer cells. *Cell. Signal.* **23**, 201–212 (2011).
76. Miao, H. *et al.* EphA2 Mediates Ligand-Dependent Inhibition and Ligand-Independent Promotion of Cell Migration and Invasion via a Reciprocal Regulatory Loop with Akt. *Cancer Cell* **16**, 9–20 (2009).

77. Miao, H. *et al.* Activation of EphA receptor tyrosine kinase inhibits the Ras/MAPK pathway. *Nat. Cell Biol.* **3**, 527–530 (2001).
78. Liu, D. P., Wang, Y., Koeffler, H. P. & Xie, D. Ephrin-A1 is a negative regulator in glioma through down-reguation of EphA2 and FAK. *Int. J. Oncol.* **30**, 865–871 (2007).
79. Folkman, J. & Klagsbrun, M. Angiogenic factors. *Science (80-.).* **235**, 442–447 (1987).
80. Nishida, N., Yano, H., Nishida, T., Kamura, T. & Kojiro, M. Angiogenesis in cancer. *Vascular Health and Risk Management* **2**, 213–219 (2006).
81. Weis, S. M. & Cheresh, D. A. Tumor angiogenesis: Molecular pathways and therapeutic targets. *Nature Medicine* **17**, 1359–1370 (2011).
82. Baluk, P., Hashizume, H. & McDonald, D. M. Cellular abnormalities of blood vessels as targets in cancer. *Current Opinion in Genetics and Development* **15**, 102–111 (2005).
83. Nagy, J. A., Chang, S. H., Shih, S. C., Dvorak, A. M. & Dvorak, H. F. Heterogeneity of the tumor vasculature. *Seminars in Thrombosis and Hemostasis* **36**, 321–331 (2010).
84. Vasudev, N. S. & Reynolds, A. R. Anti-angiogenic therapy for cancer: Current progress, unresolved questions and future directions. *Angiogenesis* **17**, 471–494 (2014).
85. Jain, R. K. Normalization of tumor vasculature: An emerging concept in antiangiogenic therapy. *Science* **307**, 58–62 (2005).
86. McBride, J. L. & Ruiz, J. C. Ephrin-A1 is expressed at sites of vascular development in the mouse. *Mech. Dev.* **77**, 201–204 (1998).
87. Ogawa, K. *et al.* The ephrin-A1 ligand and its receptor, EphA2, are expressed during tumor neovascularization. *Oncogene* **19**, 6043–6052 (2000).
88. Ieguchi, K. *et al.* ADAM12-cleaved ephrin-A1 contributes to lung metastasis. *Oncogene* **33**, 2179–2190 (2014).
89. Song, Y., Zhao, X.-P., Song, K. & Shang, Z.-J. Ephrin-A1 Is Up-Regulated by Hypoxia in Cancer Cells and Promotes Angiogenesis of HUVECs through a Coordinated Cross-Talk with eNOS. *PLoS One* **8**, e74464 (2013).
90. Brantley-Sieders, D. M., Fang, W. Bin, Hwang, Y., Hicks, D. & Chen, J. Ephrin-A1 Facilitates Mammary Tumor Metastasis through an Angiogenesis-Dependent Mechanism Mediated by EphA Receptor and Vascular Endothelial Growth Factor in Mice. *Cancer Res.* **66**, 10315–10324 (2006).
91. Brantley-Sieders, D. M. & Chen, J. Eph receptor tyrosine kinases in angiogenesis: From development to disease. *Angiogenesis* **7**, 17–28 (2004).
92. Hunter, S. G. *et al.* Essential role of Vav family guanine nucleotide exchange factors in EphA receptor-mediated angiogenesis. *Mol. Cell. Biol.* **26**, 4830–42 (2006).
93. Brantley-Sieders, D. M. *et al.* EphA2 receptor tyrosine kinase regulates endothelial cell migration and vascular assembly through phosphoinositide 3-kinase-mediated Rac1 GTPase activation. *J. Cell Sci.* **117**, 2037–49 (2004).
94. Cheng, N. *et al.* Blockade of EphA receptor tyrosine kinase activation inhibits vascular endothelial cell growth factor-induced angiogenesis. *Mol. Cancer Res.* **1**, 2–11 (2002).
95. Brantley, D. M. *et al.* Soluble Eph A receptors inhibit tumor angiogenesis and progression in vivo. *Oncogene* **21**, 7011–7026 (2002).
96. Brantley-Sieders, D. M. *et al.* Impaired tumor microenvironment in EphA2-deficient mice inhibits tumor angiogenesis and metastatic progression. *FASEB J.* **19**, 1884–1886 (2005).
97. Chen, J. *et al.* Inhibition of retinal neovascularization by soluble EphA2 receptor. *Exp. Eye Res.* **82**, 664–673 (2006).
98. Cheng, N. *et al.* Inhibition of VEGF-Dependent Multistage Carcinogenesis by Soluble EphA Receptors. *Neoplasia* **5**, 445–456 (2003).
99. Brantley-Sieders, D. M. *et al.* EphA2 receptor tyrosine kinase regulates endothelial cell migration and vascular assembly through phosphoinositide 3-kinase-mediated Rac1 GTPase activation. *J. Cell Sci.* **117**, 2037–49 (2004).
100. Dobosz, P. & Dzieciątkowski, T. The Intriguing History of Cancer Immunotherapy. *Frontiers in Immunology* **10**, 2965 (2019).
101. Chen, D. S. & Mellman, I. Oncology meets immunology: The cancer-immunity cycle. *Immunity* **39**, 1–10 (2013).
102. Gabrilovich, D. I. & Nagaraj, S. Myeloid-derived suppressor cells as regulators of the immune system. *Nature Reviews Immunology* **9**, 162–174 (2009).
103. Jiang, Y., Li, Y. & Zhu, B. T-cell exhaustion in the tumor microenvironment. *Cell Death and*

Disease **6**, e1792–e1792 (2015).
104. Rahma, O. E. & Hodi, F. S. The Intersection between Tumor Angiogenesis and Immune Suppression. *Clin. Cancer Res.* (2019). doi:10.1158/1078-0432.CCR-18-1543
105. Tatsumi, T. *et al.* Disease Stage Variation in CD4+ and CD8+ T-Cell Reactivity to the Receptor Tyrosine Kinase EphA2 in Patients with Renal Cell Carcinoma. *Cancer Res.* **63**, 4481 LP – 4489 (2003).
106. Alves, P. M. S. *et al.* EphA2 as Target of Anticancer Immunotherapy. *Cancer Res.* **63**, 8476 LP – 8480 (2003).
107. Hatano, M. *et al.* EphA2 as a glioma-associated antigen: A novel target for glioma vaccines. *Neoplasia* **7**, 717–722 (2005).
108. Jian, G. Z. *et al.* Antigenic profiling of glioma cells to generate allogeneic vaccines or dendritic cell-based therapeutics. *Clin. Cancer Res.* **13**, 566–575 (2007).
109. Hatano, M. *et al.* Vaccination with EphA2-derived T cell-epitopes promotes immunity against both EphA2-expressing and EphA2-negative tumors. *J Transl. Med* **2**, 1–9
110. Yamaguchi, S. *et al.* Dendritic cell-based vaccines suppress metastatic liver tumor via activation of local innate and acquired immunity. *Cancer Immunol. Immunother.* **57**, 1861–1869 (2008).
111. Pollack, I. F. *et al.* Antigen-specific immune responses and clinical outcome after vaccination with glioma-associated antigen peptides and polyinosinic-polycytidylic acid stabilized by lysine and carboxymethylcellulose in children with newly diagnosed malignant brainstem and nonbrainstem gliomas. *J. Clin. Oncol.* **32**, 2050–2058 (2014).
112. Okada, H. *et al.* Induction of robust type-I CD8+ T-cell responses in WHO grade 2 Low-grade glioma patients receiving peptide-based vaccines in combination with poly-ICLC. *Clin. Cancer Res.* **21**, 286–294 (2015).
113. Yi, Z., Prinzing, B. L., Cao, F., Gottschalk, S. & Krenciute, G. Optimizing EphA2-CAR T Cells for the Adoptive Immunotherapy of Glioma. *Mol. Ther. - Methods Clin. Dev.* **9**, 70–80 (2018).
114. Bielamowicz, K. *et al.* Trivalent CAR T cells overcome interpatient antigenic. *Neuro. Oncol.* **20**, 506–518 (2018).
115. IF Pollack, R. J. L. B. R. H. A. P. D. N. A. C. S. D. G. M. T. W. H. O. Immune responses and outcome after vaccination with glioma-associated antigen peptides and poly-ICLC in a pilot study for pediatric recurrent low-grade gliomasdagger. *Neuro Oncol* (2016).
116. Funk, S. D. *et al.* EphA2 Activation Promotes the Endothelial Cell Inflammatory Response. *Arterioscler. Thromb. Vasc. Biol.* **32**, 686–695 (2012).
117. Sharfe, N. *et al.* EphA and ephrin-A proteins regulate integrin-mediated T lymphocyte interactions. *Mol. Immunol.* **45**, 1208–1220 (2008).
118. Aasheim, H.-C. *et al.* Ephrin-A1 binding to CD4+ T lymphocytes stimulates migration and induces tyrosine phosphorylation of PYK2. *Blood* **105**, 2869–76 (2005).
119. Hjorthaug, H. S. & Aasheim, H.-C. Ephrin-A1 stimulates migration of CD8+CCR7+ T lymphocytes. *Eur. J. Immunol.* **37**, 2326–2336 (2007).
120. Holen, H. L., Nustad, K. & Aasheim, H.-C. Activation of EphA receptors on CD4 + CD45RO + memory cells stimulates migration . *J. Leukoc. Biol.* **87**, 1059–1068 (2010).
121. Carpenter, T. C., Schroeder, W., Stenmark, K. R. & Schmidt, E. P. Eph-A2 Promotes Permeability and Inflammatory Responses to Bleomycin-Induced Lung Injury. *Am. J. Respir. Cell Mol. Biol.* **46**, 40–47 (2012).
122. Okazaki, T. *et al.* Capillary defects and exaggerated inflammatory response in the airways of EphA2-deficient mice. *Am. J. Pathol.* **174**, 2388–2399 (2009).
123. Markosyan, N. *et al.* Tumor cell-intrinsic EPHA2 suppresses antitumor immunity by regulating PTGS2 (COX-2). *J. Clin. Invest.* **129**, 3594–3609 (2019).
124. Yan, Y. *et al.* Combining Immune Checkpoint Inhibitors With Conventional Cancer Therapy. *Frontiers in immunology* **9**, 1739 (2018).
125. Karachaliou, N. *et al.* The combination of checkpoint immunotherapy and targeted therapy in cancer. *Annals of Translational Medicine* **5**, 1–10 (2017).
126. Moya-Horno, I., Viteri, S., Karachaliou, N. & Rosell, R. Combination of immunotherapy with targeted therapies in advanced non-small cell lung cancer (NSCLC). *Therapeutic Advances in Medical Oncology* **10**, (2018).
127. Qiao, M., Jiang, T., Ren, S. & Zhou, C. Combination Strategies on the Basis of Immune Checkpoint Inhibitors in Non–Small-Cell Lung Cancer: Where Do We Stand? *Clinical Lung Cancer*

19, 1–11 (2018).
128. Song, W. *et al.* Phosphorylation of PLCgamma by EphA2 receptor tyrosine kinase promotes lung tumor growth. (In revision).
129. Yang, H., Liang, S. Q., Schmid, R. A. & Peng, R. W. New horizons in KRAS-mutant lung cancer: Dawn after darkness. *Frontiers in Oncology* **9**, 953 (2019).
130. Scheffler, M. *et al.* K-ras Mutation Subtypes in NSCLC and Associated Co-occuring Mutations in Other Oncogenic Pathways. *J. Thorac. Oncol.* **14**, 606–616 (2019).
131. Pauken, K. E. & Wherry, E. J. Overcoming T cell exhaustion in infection and cancer. *Trends in Immunology* **36**, 265–276 (2015).
132. Pathria, P., Louis, T. L. & Varner, J. A. Targeting Tumor-Associated Macrophages in Cancer. *Trends in Immunology* **40**, 310–327 (2019).
133. Mantovani, A., Marchesi, F., Malesci, A., Laghi, L. & Allavena, P. Tumour-associated macrophages as treatment targets in oncology. *Nature Reviews Clinical Oncology* **14**, 399–416 (2017).
134. White, G. E., Iqbal, A. J. & Greaves, D. R. CC chemokine receptors and chronic inflammation-therapeutic opportunities and pharmacological challenges. *Pharmacological Reviews* **65**, 47–89 (2013).
135. Stuart, J. A., Harper, J. A., Brindle, K. M., Jekabsons, M. B. & Brand, M. D. Physiological Levels of Mammalian Uncoupling Protein 2 Do Not Uncouple Yeast Mitochondria. *J. Biol. Chem.* **276**, 18633–18639 (2001).
136. Verhagen, A. Using FLAG Epitope-Tagged Proteins for Coimmunoprecipitation of Interacting Proteins. *Cold Spring Harb. Protoc.* **2006**, pdb.prot4557-pdb.prot4557 (2006).
137. Mui, M. Z. *et al.* Identification of the Adenovirus E4orf4 Protein Binding Site on the B55α and Cdc55 Regulatory Subunits of PP2A: Implications for PP2A Function, Tumor Cell Killing and Viral Replication. *PLoS Pathog.* **9**, e1003742 (2013).
138. Saito, T., Matsuba, Y., Yamazaki, N., Hashimoto, S. & Saido, T. C. Calpain activation in Alzheimer's model mice is an artifact of APP and presenilin overexpression. *J. Neurosci.* **36**, 9933–9936 (2016).
139. Liu, L., Ito, W. & Morozov, A. Overexpression of channelrhodopsin-2 interferes with the GABAb receptor-mediated depression of GABA release from the somatostatin-containing interneurons of the prefrontal cortex. *Neurophotonics* **5**, 1 (2018).
140. Duennwald, M. L., Jagadish, S., Giorgini, F., Muchowski, P. J. & Lindquist, S. A network of protein interactions determines polyglutamine toxicity. *Proc. Natl. Acad. Sci. U. S. A.* **103**, 11051–11056 (2006).
141. Saeki, N., Nishino, S., Shimizu, T. & Ogawa, K. EphA2 promotes cell adhesion and spreading of monocyte and monocyte/macrophage cell lines on integrin ligand-coated surfaces. *Cell Adhes. Migr.* **9**, 469–482 (2015).
142. Mukai, M., Suruga, N., Saeki, N. & Ogawa, K. EphA receptors and ephrin-A ligands are upregulated by monocytic differentiation/maturation and promote cell adhesion and protrusion formation in HL60 monocytes. *BMC Cell Biol.* **18**, 28 (2017).
143. Finney, A. C. *et al.* EphA2 Expression Regulates Inflammation and Fibroproliferative Remodeling in Atherosclerosis. *Circulation* **136**, 566–582 (2017).
144. Shiuan, E. *et al.* Host deficiency in ephrin-A1 inhibits breast cancer metastasis. *F1000Research* **9**, 217 (2020).
145. Folkman, J. Angiogenesis: An organizing principle for drug discovery? *Nat. Rev. Drug Discov.* **6**, 273–286 (2007).
146. Ferrara, N., Hillan, K. J., Gerber, H. P. & Novotny, W. Discovery and development of bevacizumab, an anti-VEGF antibody for treating cancer. *Nature Reviews Drug Discovery* **3**, 391–400 (2004).
147. Zou, W. & Chen, L. Inhibitory B7-family molecules in the tumour microenvironment. *Nature Reviews Immunology* **8**, 467–477 (2008).
148. Pardoll, D. M. The blockade of immune checkpoints in cancer immunotherapy. *Nature Reviews Cancer* **12**, 252–264 (2012).
149. Fujii, H. *et al.* Eph-ephrin A system regulates murine blastocyst attachment and spreading. *Dev. Dyn.* **235**, 3250–3258 (2006).
150. Moon, J. J., Lee, S. H. & West, J. L. Synthetic biomimetic hydrogels incorporated with ephrin-A1

for therapeutic angiogenesis. *Biomacromolecules* **8**, 42–49 (2007).
151. Parri, M. *et al.* EphrinA1 activates a Src/focal adhesion kinase-mediated motility response leading to rho-dependent actino/myosin contractility. *J. Biol. Chem.* **282**, 19619–19628 (2007).
152. Woo, S., Rowan, D. J. & Gomez, T. M. Retinotopic mapping requires focal adhesion kinase-mediated regulation of growth cone adhesion. *J. Neurosci.* **29**, 13981–13991 (2009).
153. Lin, S., Gordon, K., Kaplan, N. & Getsios, S. Ligand targeting of EphA2 enhances keratinocyte adhesion and differentiation via desmoglein 1. *Mol. Biol. Cell* **21**, 3902–3914 (2010).
154. Sukka-Ganesh, B., Mohammed, K. A., Kaye, F., Goldberg, E. P. & Nasreen, N. Ephrin-A1 inhibits NSCLC tumor growth via induction of Cdx-2 a tumor suppressor gene. *BMC Cancer* **12**, 309 (2012).
155. Jellinghaus, S. *et al.* Ephrin-A1/EphA4-mediated adhesion of monocytes to endothelial cells. *Biochim. Biophys. Acta - Mol. Cell Res.* **1833**, 2201–2211 (2013).
156. Ende, G. *et al.* TNF-α-mediated adhesion of monocytes to endothelial cells—The role of ephrinA1. *J. Mol. Cell. Cardiol.* **77**, 125–135 (2014).
157. Yu, M., Wang, J., Muller, D. J. & Helenius, J. In PC3 prostate cancer cells ephrin receptors crosstalk to β1-integrins to strengthen adhesion to collagen type i. *Sci. Rep.* **5**, 1–10 (2015).
158. Lim, W., Bae, H., Bazer, F. W. & Song, G. Functional Roles of Eph A-Ephrin A1 System in Endometrial Luminal Epithelial Cells During Early Pregnancy. *J. Cell. Physiol.* **232**, 1527–1538 (2017).
159. Daoud, A., Gopal, U., Kaur, J. & Isaacs, J. S. Molecular and functional crosstalk between extracellular Hsp90 and ephrin A1 signaling. *Oncotarget* **8**, 106807–106819 (2017).
160. Kaplan, N. *et al.* Epha2/ephrin-A1 mediate corneal epithelial cell compartmentalization via ADAM10 regulation of EGFR signaling. *Investig. Ophthalmol. Vis. Sci.* **59**, 393–406 (2018).
161. Funk, S. D., Finney, A. C., Yurdagul, A., Pattillo, C. B. & Orr, A. W. EphA2 stimulates VCAM-1 expression through calcium-dependent NFAT1 activity. *Cell. Signal.* **49**, 30–38 (2018).
162. Valenzuela, J. I. & Perez, F. Localized Intercellular Transfer of Ephrin-As by Trans-endocytosis Enables Long-Term Signaling. *Dev. Cell* **52**, 104-117.e5 (2020).
163. Miao, H. *et al.* EphA2 Mediates Ligand-Dependent Inhibition and Ligand-Independent Promotion of Cell Migration and Invasion via a Reciprocal Regulatory Loop with Akt. *Cancer Cell* **16**, 9–20 (2009).
164. Brantley-Sieders, D. M. *et al.* Eph/Ephrin Profiling in Human Breast Cancer Reveals Significant Associations between Expression Level and Clinical Outcome. *PLoS One* **6**, e24426 (2011).
165. Ieguchi, K. *et al.* Ephrin-A1 expression induced by S100A8 is mediated by the toll-like receptor 4. *Biochem. Biophys. Res. Commun.* **440**, 623–629 (2013).
166. Youngblood, V. M. *et al.* The ephrin-A1/EPHA2 signaling axis regulates glutamine metabolism in HER2-positive breast cancer. *Cancer Res.* **76**, 1825–1836 (2016).
167. Efazat, G. *et al.* Ephrin B3 interacts with multiple EphA receptors and drives migration and invasion in non-small cell lung cancer. *Oncotarget* **7**, 60332–60347 (2016).
168. Chu, M. & Zhang, C. Inhibition of angiogenesis by leflunomide via targeting the soluble ephrin-A1/EphA2 system in bladder cancer. *Sci. Rep.* **8**, 1–13 (2018).
169. Zhuo, W. *et al.* Long Noncoding RNA GMAN, Up-regulated in Gastric Cancer Tissues, Is Associated With Metastasis in Patients and Promotes Translation of Ephrin A1 by Competitively Binding GMAN-AS. *Gastroenterology* **156**, 676-691.e11 (2019).
170. Lee, P. C. *et al.* C1GALT1 is associated with poor survival and promotes soluble Ephrin A1-mediated cell migration through activation of EPHA2 in gastric cancer. *Oncogene* 1–17 (2020). doi:10.1038/s41388-020-1178-7
171. Coulthard, M. G. *et al.* Eph/ephrin signaling in injury and inflammation. *American Journal of Pathology* **181**, 1493–1503 (2012).
172. Zhang, W. *et al.* A potential tumor suppressor role for Hic1 in breast cancer through transcriptional repression of ephrin-A1. *Oncogene* **29**, 2467–2476 (2010).
173. Frieden, L. A. *et al.* Regulation of heart valve morphogenesis by Eph receptor ligand, ephrin-A1. *Dev. Dyn.* **239**, 3226–3234 (2010).
174. Brantley-Sieders, D. M. *et al.* Host deficiency in Vav2/3 guanine nucleotide exchange factors impairs tumor growth, survival, and angiogenesis in vivo. *Mol. Cancer Res.* **7**, 615–623 (2009).
175. Varghese, F., Bukhari, A. B., Malhotra, R. & De, A. IHC Profiler: An Open Source Plugin for the Quantitative Evaluation and Automated Scoring of Immunohistochemistry Images of Human

Tissue Samples. *PLoS One* **9**, e96801 (2014).
176. Alonso-C, L. M. *et al.* Expression profile of Eph receptors and ephrin ligands in healthy human B lymphocytes and chronic lymphocytic leukemia B-cells. *Leuk. Res.* **33**, 395–406 (2009).
177. Wohlfahrt, J. G. *et al.* Ephrin-A1 Suppresses Th2 Cell Activation and Provides a Regulatory Link to Lung Epithelial Cells. *J. Immunol.* **172**, 843–850 (2004).
178. Sharfe, N., Freywald, A., Toro, A., Dadi, H. & Roifman, C. Ephrin stimulation modulates T?cell chemotaxis. *Eur. J. Immunol.* **32**, 3745–3755 (2002).
179. Binnewies, M. *et al.* Understanding the tumor immune microenvironment (TIME) for effective therapy. *Nat. Med.* **24**, 541–550 (2018).
180. Awad, R. M., De Vlaeminck, Y., Maebe, J., Goyvaerts, C. & Breckpot, K. Turn Back the TIMe: Targeting Tumor Infiltrating Myeloid Cells to Revert Cancer Progression. *Frontiers in immunology* **9**, 1977 (2018).
181. Potente, M., Gerhardt, H. & Carmeliet, P. Basic and therapeutic aspects of angiogenesis. *Cell* **146**, 873–887 (2011).
182. Dunaway, C. M. *et al.* Cooperative signaling between Slit2 and Ephrin-A1 regulates a balance between angiogenesis and angiostasis. *Mol. Cell. Biol.* **31**, 404–16 (2011).
183. Vaught, D., Chen, J. & Brantley-Sieders, D. M. Regulation of mammary gland branching morphogenesis by EphA2 receptor tyrosine kinase. *Mol. Biol. Cell* **20**, 2572–2581 (2009).
184. Kang, M. *et al.* Bifunctional role of ephrin A1-Eph system in stimulating cell proliferation and protecting cells from cell death through the attenuation of ER stress and inflammatory responses in bovine mammary epithelial cells. *J. Cell. Physiol.* **233**, 2560–2571 (2018).
185. Averaimo, S. *et al.* A plasma membrane microdomain compartmentalizes ephrin-generated cAMP signals to prune developing retinal axon arbors. *Nat. Commun.* **7**, 1–12 (2016).
186. Harboe, M., Torvund-Jensen, J., Kjaer-Sorensen, K. & Laursen, L. S. Ephrin-A1-EphA4 signaling negatively regulates myelination in the central nervous system. *Glia* **66**, 934–950 (2018).
187. Aoki, M., Yamashita, T. & Tohyama, M. EphA receptors direct the differentiation of mammalian neural precursor cells through a mitogen-activated protein kinase-dependent pathway. *J. Biol. Chem.* **279**, 32643–32650 (2004).
188. Doak, G. R., Schwertfeger, K. L. & Wood, D. K. Distant Relations: Macrophage Functions in the Metastatic Niche. *Trends in Cancer* **4**, 445–459 (2018).
189. Willms, E. *et al.* Cells release subpopulations of exosomes with distinct molecular and biological properties. *Sci. Rep.* **6**, 1–12 (2016).
190. Shiuan, E. F., Wang, S., Raybuck, A., Boothby, M. & Chen, J. Abstract B58: The role of EphA2 receptor tyrosine kinase in antitumor immunity mediated through programmed death ligand 2 (PD-L2) in non-small cell lung cancer (NSCLC). in *Cancer Immunology Research* **6**, B58–B58 (American Association for Cancer Research (AACR), 2018).
191. Chang, J. W. *et al.* Wild-type p53 upregulates an early onset breast cancer-associated gene GAS7 to suppress metastasis via GAS7–CYFIP1-mediated signaling pathway. *Oncogene* **37**, 4137–4150 (2018).
192. Rahman, M. *et al.* Alternative preprocessing of RNA-Sequencing data in The Cancer Genome Atlas leads to improved analysis results. *Bioinformatics* **31**, 3666–72 (2015).
193. Annunziata, C. M. *et al.* Phase 1, open-label study of MEDI-547 in patients with relapsed or refractory solid tumors. *Invest. New Drugs* **31**, 77–84 (2013).
194. Kamoun, W. S. *et al.* Antitumour activity and tolerability of an EphA2-targeted nanotherapeutic in multiple mouse models. *Nat. Biomed. Eng.* **3**, 264–280 (2019).
195. Wu, B. *et al.* Design and Characterization of Novel EphA2 Agonists for Targeted Delivery of Chemotherapy to Cancer Cells. *Chem. Biol.* **22**, 876–887 (2015).
196. Lee, J.-W. *et al.* EphA2 immunoconjugate as molecularly targeted chemotherapy for ovarian carcinoma. *J. Natl. Cancer Inst.* **101**, 1193–205 (2009).
197. Lee, J. W. *et al.* EphA2 targeted chemotherapy using an antibody drug conjugate in endometrial carcinoma. *Clin. Cancer Res.* **16**, 2562–2570 (2010).
198. Jackson, D. *et al.* A human antibody-drug conjugate targeting EphA2 inhibits tumor growth in vivo. *Cancer Res.* **68**, 9367–9374 (2008).
199. Chang, Q., Jorgensen, C., Pawson, T. & Hedley, D. W. Effects of dasatinib on EphA2 receptor tyrosine kinase activity and downstream signalling in pancreatic cancer. *Br. J. Cancer* **99**, 1074–1082 (2008).

200. Lim, C. J. *et al.* 4-Substituted quinazoline derivatives as novel EphA2 receptor tyrosine kinase inhibitors. *Bioorganic Med. Chem. Lett.* **24**, 4080–4083 (2014).
201. Kluger, H. M. *et al.* A phase 2 trial of dasatinib in advanced melanoma. *Cancer* **117**, 2202–2208 (2011).
202. Chee, C. E. *et al.* Phase II Study of Dasatinib (BMS-354825) in Patients With Metastatic Adenocarcinoma of the Pancreas. *Oncologist* **18**, 1091–1092 (2013).
203. Lassman, A. B. *et al.* Phase 2 trial of dasatinib in target-selected patients with recurrent glioblastoma (RTOG 0627). *Neuro. Oncol.* **17**, 992–8 (2015).
204. Mudd, G. E. *et al.* Identification and Optimization of EphA2-Selective Bicycles for Delivery of Cytotoxic Payloads. *J. Med. Chem.* (2020). doi:10.1021/acs.jmedchem.9b02129
205. Kamoun, W. S. *et al.* Synergy between EphA2-ILS-DTXP, a novel EphA2-targeted nanoliposomal taxane, and PD-1 inhibitors in preclinical tumor models. *Mol. Cancer Ther.* **19**, 270–281 (2020).
206. Topalian, S. L. *et al.* Safety, activity, and immune correlates of anti-PD-1 antibody in cancer. *N. Engl. J. Med.* **366**, 2443–2454 (2012).
207. Larkin, J. *et al.* Combined Nivolumab and Ipilimumab or Monotherapy in Untreated Melanoma. *N. Engl. J. Med.* **373**, 23–34 (2015).
208. Postow, M. A. *et al.* Nivolumab and Ipilimumab versus Ipilimumab in Untreated Melanoma. *N. Engl. J. Med.* **372**, 2006–2017 (2015).
209. Wu, J. & Luo, H. Recent advances on T-cell regulation by receptor tyrosine kinases. *Current Opinion in Hematology* **12**, 292–297 (2005).
210. Funk, S. D. & Orr, A. W. Ephs and ephrins resurface in inflammation, immunity, and atherosclerosis. *Pharmacological Research* **67**, 42–52 (2013).
211. Chen, J., Zhuang, G., Frieden, L. & Debinski, W. Eph receptors and ephrins in cancer: Common themes and controversies. in *Cancer Research* **68**, 10031–10033 (2008).
212. Chen, J., Song, W. & Amato, K. Eph receptor tyrosine kinases in cancer stem cells. *Cytokine and Growth Factor Reviews* **26**, 1–6 (2015).
213. Chiari, R. *et al.* Identification of a tumor-specific shared antigen derived from an Eph receptor and presented to CD4 T cells on HLA class II molecules. *Cancer Res.* **60**, 4855–4863 (2000).
214. Alves, P. M. S. *et al.* EphA2 as target of anticancer immunotherapy: identification of HLA-A*0201-restricted epitopes. *Cancer Res.* **63**, 8476–80 (2003).
215. Yamaguchi, S. *et al.* Immunotherapy of murine colon cancer using receptor tyrosine kinase EphA2-derived peptide-pulsed dendritic cell vaccines. *Cancer* **110**, 1469–1477 (2007).
216. Li, M. *et al.* Treatment of Dutch rat models of glioma using EphrinA1-PE38/GM-CSF chitosan nanoparticles by in situ activation of dendritic cells. *Tumor Biol.* **36**, 7961–7966 (2015).
217. Sharfe, N. *et al.* EphA and ephrin-A proteins regulate integrin-mediated T lymphocyte interactions. *Mol. Immunol.* **45**, 1208–1220 (2008).
218. Carpenter, T. C., Schroeder, W., Stenmark, K. R. & Schmidt, E. P. Eph-A2 promotes permeability and inflammatory responses to bleomycin-induced lung injury. *Am. J. Respir. Cell Mol. Biol.* **46**, 40–47 (2012).
219. Aasheim, H. C., Delabie, J. & Finne, E. F. Ephrin-A1 binding to CD4+ T lymphocytes stimulates migration and induces tyrosine phosphorylation of PYK2. *Blood* **105**, 2869–2876 (2005).
220. Hjorthaug, H. S. & Aasheim, H. C. Ephrin-A1 stimulates migration of CD8+CCR7+ T lymphocytes. *Eur. J. Immunol.* **37**, 2326–2336 (2007).
221. Guo, F. *et al.* CXCL12/CXCR4: A symbiotic bridge linking cancer cells and their stromal neighbors in oncogenic communication networks. *Oncogene* **35**, 816–826 (2016).
222. Pfaff, D. *et al.* Involvement of endothelial ephrin-B2 in adhesion and transmigration of EphB-receptor-expressing monocytes. *J. Cell Sci.* **121**, 3842–3850 (2008).
223. Korff, T., Braun, J., Pfaff, D., Augustin, H. G. & Hecker, M. Role of ephrinB2 expression in endothelial cells during arteriogenesis: Impact on smooth muscle cell migration and monocyte recruitment. *Blood* **112**, 73–81 (2008).
224. Sawamiphak, S. *et al.* Ephrin-B2 regulates VEGFR2 function in developmental and tumour angiogenesis. *Nature* **465**, 487–491 (2010).
225. Wang, Y. *et al.* Ephrin-B2 controls VEGF-induced angiogenesis and lymphangiogenesis. *Nature* **465**, 483–486 (2010).
226. Trinidad, E. M., Ballesteros, M., Zuloaga, J., Zapata, A. & Alonso-Colmenar, L. M. An impaired transendothelial migration potential of chronic lymphocytic leukemia (CLL) cells can be linked to

ephrin-A4 expression. *Blood* **114**, 5081–5090 (2009).
227. De Saint-Vis, B. *et al.* Human dendritic cells express neuronal Eph receptor tyrosine kinases: Role of EphA2 in regulating adhesion to fibronectin. *Blood* **102**, 4431–4440 (2003).
228. Yu, G., Luo, H., Wu, Y. & Wu, J. Ephrin B2 Induces T Cell Costimulation. *J. Immunol.* **171**, 106–114 (2003).
229. Yu, G., Luo, H., Wu, Y. & Wu, J. Mouse EphrinB3 Augments T-cell Signaling and Responses to T-cell Receptor Ligation. *J. Biol. Chem.* **278**, 47209–47216 (2003).
230. Yu, G., Luo, H., Wu, Y. & Wu, J. EphrinB1 is essential in T-cell-T-cell co-operation during T-cell activation. *J. Biol. Chem.* **279**, 55531–9 (2004).
231. Luo, H., Yu, G., Wu, Y. & Wu, J. EphB6 crosslinking results in costimulation of T cells. *J. Clin. Invest.* **110**, 1141–1150 (2002).
232. Luo, H., Yu, G., Tremblay, J. & Wu, J. EphB6-null mutation results in compromised T cell function. *J. Clin. Invest.* **114**, 1762–1773 (2004).
233. Kawano, H. *et al.* A novel feedback mechanism by Ephrin-B1/B2 in T-cell activation involves a concentration-dependent switch from costimulation to inhibition. *Eur. J. Immunol.* **42**, 1562–1572 (2012).
234. Nguyen, T. M., Arthur, A., Hayball, J. D. & Gronthos, S. EphB and Ephrin-B interactions mediate human mesenchymal stem cell suppression of activated T-cells. *Stem Cells Dev.* **22**, 2751–64 (2013).
235. JA Joyce, D. F. T cell exclusion, immune privilege, and the tumor microenvironment. *Science (80-.).* **348**, 74–80 (2015).
236. Aasheim, H. C. *et al.* A splice variant of human ephrin-A4 encodes a soluble molecule that is secreted by activated human B lymphocytes. *Blood* **95**, 221–230 (2000).
237. Choi, Y. *et al.* Discovery and structural analysis of Eph receptor tyrosine kinase inhibitors. *Bioorganic Med. Chem. Lett.* **19**, 4467–4470 (2009).
238. Shiuan, E. *et al.* Thrombocytopenia in patients with melanoma receiving immune checkpoint inhibitor therapy. *J. Immunother. Cancer* **5**, (2017).
239. Chen, L. & Han, X. Anti-PD-1/PD-L1 therapy of human cancer: Past, present, and future. *Journal of Clinical Investigation* **125**, 3384–3391 (2015).
240. Wolchok, J. D. PD-1 Blockers. *Cell* **162**, 937 (2015).
241. Garon, E. B. *et al.* Pembrolizumab for the Treatment of Non–Small-Cell Lung Cancer. *N. Engl. J. Med.* **372**, 2018–2028 (2015).
242. Robert, C. *et al.* Pembrolizumab versus Ipilimumab in Advanced Melanoma. *N. Engl. J. Med.* **372**, 2521–2532 (2015).
243. Brahmer, J. *et al.* Nivolumab versus Docetaxel in Advanced Squamous-Cell Non–Small-Cell Lung Cancer. *N. Engl. J. Med.* **373**, 123–135 (2015).
244. Francisco, L. M., Sage, P. T. & Sharpe, A. H. The PD-1 pathway in tolerance and autoimmunity. *Immunological Reviews* **236**, 219–242 (2010).
245. Le Roy, A. *et al.* Two cases of immune thrombocytopenia associated with pembrolizumab. *European Journal of Cancer* **54**, 172–174 (2016).
246. Kong, B. Y., Micklethwaite, K. P., Swaminathan, S., Kefford, R. F. & Carlino, M. S. Autoimmune hemolytic anemia induced by anti-PD-1 therapy in metastatic melanoma. *Melanoma Res.* **26**, 202–204 (2016).
247. Kanameishi, S. *et al.* Idiopathic thrombocytopenic purpura induced by nivolumab in a metastatic melanoma patient with elevated PD-1 expression on B cells. *Ann. Oncol. Off. J. Eur. Soc. Med. Oncol.* **27**, 546–7 (2016).
248. Bagley, S. J., Kosteva, J. A., Evans, T. L. & Langer, C. J. Immune thrombocytopenia exacerbated by nivolumab in a patient with non-small-cell lung cancer. *Cancer Treat. Commun.* **6**, 20–23 (2016).
249. Kopecký, J., Trojanová, P., Kubeček, O. & Kopecký, O. Treatment possibilities of ipilimumab-induced thrombocytopenia--case study and literature review. *Jpn. J. Clin. Oncol.* **45**, 381–4 (2015).
250. Sajjad, M. Z., George, T., Weber, J. S. & Sokol, L. Thrombocytopenia associated with ipilimumab therapy of advanced melanoma at a single institution. *J. Clin. Oncol.* **31**, 9072–9072 (2013).
251. Provan, D. & Newland, A. C. Current Management of Primary Immune Thrombocytopenia. *Advances in Therapy* **32**, 875–887 (2015).
252. Song, Y. *et al.* Abnormalities of the Bone Marrow Immune Microenvironment in Patients with

Prolonged Isolated Thrombocytopenia after Allogeneic Hematopoietic Stem Cell Transplantation. *Blood* **128**, 4602–4602 (2016).
253. Cines, D. B. & Bussel, J. B. How I treat idiopathic thrombocytopenic purpura (ITP). *Blood* **106**, 2244–2251 (2005).
254. Aslam, R. *et al.* Thymic retention of CD4+CD25+FoxP3+ T regulatory cells is associated with their peripheral deficiency and thrombocytopenia in a murine model of immune thrombocytopenia. *Blood* **120**, 2127–2132 (2012).
255. Zhong, J. *et al.* Lower expression of PD-1 and PD-L1 in peripheral blood from patients with chronic ITP. *Hematology* **21**, 552–557 (2016).
256. Birtas Atesoglu, E. *et al.* Soluble Programmed Death 1 (PD-1) Is Decreased in Patients With Immune Thrombocytopenia (ITP): Potential Involvement of PD-1 Pathway in ITP Immunopathogenesis. *Clin. Appl. Thromb. Hemost.* **22**, 248–51 (2016).
257. Weber, J. S., Kähler, K. C. & Hauschild, A. Management of immune-related adverse events and kinetics of response with ipilimumab. *Journal of Clinical Oncology* **30**, 2691–2697 (2012).
258. Michot, J. M. *et al.* Immune-related adverse events with immune checkpoint blockade: A comprehensive review. *European Journal of Cancer* **54**, 139–148 (2016).
259. Friedman, C. F., Proverbs-Singh, T. A. & Postow, M. A. Treatment of the Immune-Related Adverse Effects of Immune Checkpoint Inhibitors: A Review. *JAMA oncology* **2**, 1346–1353 (2016).